MEASURING TERRESTRIAL WILDLIFE EXTERNAL

RADIATION EXPOSURE UNDER FIELD CONDITIONS

Thesis submitted in partial fulfilment of the requirements of

the degree of Doctor of Philosophy

by

Phakphum Aramrun

School of Environment and Life Science

University of Salford

2018

DECLARATION

I hereby declare that except where specific reference is made to work of others, the contents of this thesis are original and have not been submitted in whole or in part for consideration for any other degree or qualification in this, or any other university. This thesis is my own work and contains nothing which is the outcome of work done in collaboration with others, except as specified in the text and acknowledgements.

ABSTRACT

This thesis presents the results of a 3-year project to develop methods for measuring external radiation exposure of free-ranging terrestrial animals under field conditions. An evaluation of available passive dosimeter technologies was undertaken and guidance developed on the selection of dosimeters for different sizes of terrestrial animals.

To test dosimeters under field conditions, a field study using reindeer in an area of Norway with elevated ^{137}Cs was initiated. The dosimeter selection guidance was used to identify four passive dosimeters (i.e. TLD, OSLD, RPLD and DIS), which should be suitable for reindeer. To protect these dosimeters during use, they were housed in an aluminium box that could be attached to a collar around the reindeer's neck. The performance of dosimeters within the box was tested in a laboratory. This testing confirmed dose linearity, angular linearity for the angles tested ($45° – 135°$) and energy linearity for radionuclides tested (^{137}Cs, ^{60}Co, ^{226}Ra). The dosimeter box did not respond to beta exposure.

The external absorbed doses of a reindeer herd (Vågå, Norway) were measured over 11 months using the dosimeter box developed. Dosimeter results were then compared with model predictions. There was a significant difference between the estimates of dosimeters, but the difference of the mean doses between maximum and minimum values was <14 %. Reindeer external doses were modelled based on GPS tracking data and data on radiation in their environment. The mean predicted doses using the GPS tracking data were not significantly different to RPLD and DIS. However, the TLD and OSLD results were 18% higher than the mean dose estimated using the reindeer GPS tracking data. Average external doses predicted across the herd area (without using GPS data) were significantly lower than doses from all dosimeter types and predicted using the GPS data because the animals favoured the more contaminated areas of the study site which were good grazing in several seasons for those reindeer.

A deer dosimetry phantom was created from red deer CT images and a human adult dosimetry phantom to estimate a whole-body dose and organ doses from external radiation exposure. The data of whole-body and organ doses from x-ray and ^{137}Cs were used to calculate conversion factors that can be used to convert from external whole-organism doses of deer species to individual organ doses from external exposure.

(This page is left blank intentionally)

ACKNOWLEDGMENTS

(This page is left blank intentionally)

CONTENTS

LIST OF FIGURES

LIST OF TABLES

LIST OF ABBREVIATIONS

$AgPO_4$	Silver activated phosphate glass
^{40}K	Potassium-40
^{137}Cs	Ceasium-137
^{226}Ra	Radium-226
^{232}Th	Thorium-232
^{238}U	Uranium-238
60Co	Cobalt-60
$^{90}Sr/^{90}Y$	Strontium-90/Yttrium-90
Al_2O_3	Aluminium trioxide
amu	Atomic mass unit
BOMAB	Bottle Manikin Absorption
Bq	Unit of activity (1 Bq = 1 decay event per second)
BSS2	Beta secondary standard
CaF_2	Calcium fluoride
$CaSO_4$	Calcium sulphate
COGER	Coordinating Group on Environmental Radioactivity
CR	Concentration Ratio
CRCE	Centre for Radiation, Chemicals and Environmental hazards
CV	Coefficient of variation
DCC	Dose conversion coefficient
DCF	Dose conversion factor (equivalent to DCC)
DIS	Direct ion storage
D_w	Dose to water

EC	European Commission
ERICA	EC EURATOM-funded project 'Environmental Risk from Ionising Contaminants: Assessment and Management' which developed the ERICA Integrated Approach
ERICA Tool	The computer model that was developed to support the application of the ERICA Integrated Approach
eV	Electronvolt
GIS	Geographic information system
GPS	Global Positioning System
Gy	Gray (Unit of absorbed dose)
HDPE	High-density polyethylene
Hp (10)	The personal (or human) dose equivalent at a body depth at 10mm
Hp (3)	The personal (or human) dose equivalent at the lens of the eye at 3 mm
IAEA	International Atomic Energy Agency
ICRP	International Commission for Radiological Protection
ICRU	International Commission on Radiation Units and Measurements
IUR	International Union of Radioecology
K_a	Air kerma
kVp	Kilovolts peak
$Li_2B_4O_7$	Lithium tetra-borate
LiF	Lithium fluoride
MCNP	Monte Carlo N-Particle code
MODARIA II	Modelling and Data for Radiological Impact Assessments programme

MOSFET	Metal Oxide Semiconductor Field Effect Transistor
NRPA	Norwegian Radiation Protection Authority
OSLD	Optical stimulated luminescent dosimeters
PHE	Public Health England
PTB	Physikalish-Technische Bundesanstalt
RAP	Reference Animal and Plant
RBI	Ruđer Bošković Institute
RESRAD-BIOTA	Computer model for implementing the USDoE graded approach
RPLD	Radiophotoluminescent dosimeters
SD	Standard deviation
SI	International System of Unit
Sv	Sievert (Unit of dose equivalent)
$T_{1/2}$	Physical/radioactive half-life
TINT	Thailand Institute of Nuclear Technology
TLD	Thermoluminescent dosimeters
UK	United Kingdom
USA	United States of America
USDoE	United States Department of Energy
USGS	United State Geological Survey
Z_{eff}	The photon effective atomic number
α	Alpha particle
β	Beta particle
γ	Gamma radiation

CHAPTER 1   INTRODUCTION

1.1   BACKGROUND TO RESEARCH

The radioactive contamination from Chernobyl nuclear accident in Ukraine, the world's worst nuclear power plant disaster occurred in 1986, has been deposited over many European countries (Smith & Beresford, 2005). This issue has created an increased risk to both terrestrial and aquatic organisms from ionising radiation in the environment. The development of methods to assess the impact of ionising radiation on animals in the environment is, therefore, needed to solve this issue. Currently, there are a number of models and approaches to estimate radiation exposure of wild animals (IAEA, 2010; Stark et al., 2015; Vives i Batlle et al., 2016) being used to make regulatory decisions that have significant economic and societal impacts internationally. These models and approaches have to be validated in terms of internal and external dose assessment for wildlife, to ensure that the uncertainties during those processes are considered and approaches are fit for purpose. Predicted internal dose rates can be compared to those estimated via measured radionuclide activity concentrations in organisms. To validate external dose rates, direct dosimetry measurements of wild organisms in the field are desirable.

Few studies, however, have attempted to assess radiation exposure directly to free-ranging terrestrial and aquatic organisms (e.g. Beresford et al., 2008d; Bonisoli-Alquati et al., 2015; Chesser et al., 2000; Hinton et al., 2015; Woodhead, 1973). This means it is difficult to confirm the doses predicted by these modelling tools (e.g. ERICA Tool), making it an issue for stakeholder acceptance of modelling based assessments. Also, there is a growing scientific and regulatory need to establish radiation dose-effect relationships for wildlife under field conditions which is a key of the assessment system for radiation protection to wildlife and this requires accurate measurement of dose. Compliance monitoring is increasingly required of nuclear facilities and the ability to obtain direct measurement of wildlife exposure in the vicinity of such facilities is currently lacking. The development of direct practical

external dose measurements and effective methods is, therefore, needed for assessing external radiation exposure of wildlife in different areas such as nuclear licensed sites and areas of accidental releases. In previous studies, passive dosimeters were mainly used by attaching those passive dosimeters to various animal species for measuring external absorbed doses in the fields as mentioned above. To the best of my knowledge, radiation effects combined with direct dose measurements using appropriate passive dosimetry technologies under field conditions for terrestrial wildlife have not been, to date, considered; evaluation of suitable passive dosimeters for wildlife dose measurements is a method to investigate this.

The focus of this research was to attach suitable passive dosimeters to terrestrial wildlife organisms under field conditions receiving long term external exposure from gamma radiation. The developed approaches were then tested in field experiments. The wildlife dose measurements in the field were compared with predictions of wildlife dosimetry models. An animal phantom was also developed to determine organ dose of an animal species contributed from external exposure of radionuclides in the environment. This is the advance understanding of radiation interaction in animal species which is also used to assess dose effects for endangered species. The focus of this work was on terrestrial large mammal species as it is one of ICRP reference animal & plant species and a reference organism for assessing radiation exposures in other wildlife dosimetry models (e.g. ERICA Tool and RESRAD-BIOTA).

1.2   AIM AND OBJECTIVES

The aim of this study is to develop appropriate methods for directly measuring external radiation exposure of free-ranging terrestrial animals using passive dosimeters.

The study has the following specific objectives:

1. To critically evaluate the effectiveness of the selected passive dosimeters for direct terrestrial wildlife dosimetry measurement under field conditions.

2. To inform selection of suitable passive dosimeters for long term large mammal dosimetry measurements under field conditions.

3. To test the use of collar-mounted dosimeters for long term measurements of external absorbed doses using free-ranging large mammals in an area contaminated by the Chernobyl accident.

4 To evaluate model performance by comparing model prediction of external doses of target organisms with direct dose measurements obtained from the field study.

5. To quantify the relationship between external radiation exposure and organ doses for a large mammal species.

CHAPTER 2   LITERATURE REVIEW

This chapter reviews literature on ionising radiation, wildlife exposure assessment, the environmental radiation protection framework, tools for assessing wildlife exposure and the associated uncertainties, previous studies of direct wildlife dose measurement using various passive dosimeters.

2.1   IONISING RADIATION

Ionising radiation is the energy emitted from unstable nuclides. It occurs from the decay of both natural and anthropogenic radioactive substances (Whicker & Schultz, 1982). It can be in the form of particles namely alpha (α) beta (β) and neutrons or as electromagnetic waves (photons; gamma rays (γ) and X-rays). Radioactivity is a radionuclide undergoing spontaneous disintegration, by emitting one or more radiation type, and either changing to another radionuclide or becoming a stable isotope. The rate of radioactive decay of a radionuclide can be explained by its half-life ($T_{1/2}$), which is the amount of time it takes for the radioactivity of a radionuclide to fall to half its value. Each radionuclide has its own half-life varying from a few seconds to many thousands of years. Examples are: ^{220}Rn ($T_{1/2}$ = 55 seconds), ^{137}Cs ($T_{1/2}$ = 30 years), ^{131}I ($T_{1/2}$ = 8 days), ^{238}U ($T_{1/2}$ = 4.5x10^9 years). Some radionuclide properties are shown in Table 2-1. The radiation energy released from a radionuclide during radioactive decay is expressed in electron volts (eV); that is the amount of energy that an electron gains when moving through an electric potential difference of one volt. The radiation emitted from radionuclides has specific energies ranging from keV to MeV (Table 2-1). The System of International units (SI system) uses Becquerel (Bq), which is 1 radioactive decay per second, to describe the amount of radioactivity of radionuclides. It can be used per unit mass or volume such as Bq kg^{-1}, Bq m^{-3} and Bq l^{-1}.

The most common types of radiation released from radioactive substances in the environment are alpha particles, beta particles and gamma rays. The properties of different types of radiation and radiation dose for the environment (to fauna and

flora) are described in various texts (Arshak & Korostynska, 2006; Kathren, 1984; Kelly & Thorne, 2003; Lilley, 2001; Whicker & Schultz, 1982) and are summarised below:

Table 2-1: Some radionuclides profile (data from (NuclearDataCenter, 2014))

Element	Example Radionuclide(s)	Half-life (years)	Radiation(s)	Energy (E, keV) E_{gamma}			E_{beta}	E_{alpha}
				E_1	E_2	E_3		
Cobalt	^{60}Co	5.27	β, γ	1173	1332	-	318	-
Strontium	^{90}Sr	29.1	β	-	-	-	546	-
Caesium	^{134}Cs	2.06	β, γ	569	605	796	2059	-
	^{137}Cs	30	β, γ	284	662	-	1176	-
Plutonium	^{238}Pu	87.7	α	-	-	-	-	5499
	^{239}Pu	2.4×10^4	α	-	-	-	-	5157
	^{240}Pu	6.5×10^3	α	-	-	-	-	5168
Americium	^{241}Am	432	α, γ	26	33	60	-	5485

Alpha (α) particles, a helium nucleus, consists of two protons and two neutrons bound together with a charge of plus two. They originate from the decay of radionuclides. The alpha particles only occur in radionuclides which have an atomic number greater than 82. The mass of alpha particles has 4 atomic mass units (amu), and their reactions are strong with matter (more than 10000 ionisation events per centimetre of travel) but they can only travel over short ranges in air about a few centimetres. Because the penetration ability of alpha particles is low, they are not a significant contributor to external exposure of wildlife. However, alpha emitting radionuclides can be especially hazardous if they are taken into the organism and are assimilated into body tissues.

Beta (β) particles are electrons ejected from the nucleus of unstable atoms. These electrons are mostly negatively (β⁻) charged but they can sometime be positively (β⁺) charged. The particles have a mass of 5.49×10^{-4} amu. Beta particles are able to penetrate through more matter than alpha particles but are less penetrating than gamma rays. The kinetic energy of beta particles is an indication of the penetrative capability in matter. They are of radiological importance for internal exposure but may be of little external concern for external exposure.

Gamma (γ) rays are electromagnetic waves or photons that are emitted from an atomic nucleus when they need to release the extra energy to drop down to ground energy states. Photons have no mass and no electrical charge. They are of greatest radiological importance for external irradiation because they are very penetrating.

2.2   RADIATION DOSE OF WILDLIFE

Absorbed dose is the quantity of ionising radiation energy that is absorbed, per unit mass, in a given organ or whole organism. The amount of absorbed dose is dependent on the type of the radiation and energy deposited within the tissue/organism as well as the density of biological tissue. The SI unit of absorbed dose is the gray (Gy) which is equivalent to one joule per kilogram (J kg^{-1}) of energy absorption.

Estimated absorbed dose, or usually whole-body dose rate (Gy h^{-1}), to wild animals is a key quantity in exposure assessment (Brown et al., 2016; Copplestone et al., 2001; ICRP, 2008) and this can be related to the likelihood of biological damage, based on compilations of published dose-effect studies (Andersson et al., 2009; Copplestone et al., 2010). Radiation exposures to animals are often assessed in terms of comparison with benchmarks for population-level effects (Copplestone et al., 2008; Howard et al., 2010; ICRP, 2008).

2.3   ASSESSMENT OF RADIATION EXPOSURE OF WILDLIFE

2.3.1 Environmental radiation protection framework

Radiation protection for the environment has seen significant development in its philosophy and practical guidance since the 1977 and 1990 International Commission for Radiological Protection (ICRP) recommendations which initially focused on the protection of human beings (ICRP, 1977, 1991). Around the turn of the century, and in the absence of international guidance, some countries began to develop environmental radiation protection approaches and associated methods for assessing the radiation exposure of wildlife. By 2003, taking into account national

developments, the ICRP suggested a framework for assessing the environmental impact of ionising radiation, based around the concept of Reference Animals & Plants (ICRP, 2003). This was designed to integrate with the approach used for the protection of human beings (ICRP, 2003; Pentreath, 2009, 2012b) as shown in Figure 2-1. By 2007, the ICRP updated its 'Recommendations' to include requirements to maintain biodiversity, ensure that all species are conserved and that the health and status of natural habitats, communities and ecosystem is protected (ICRP, 2007).
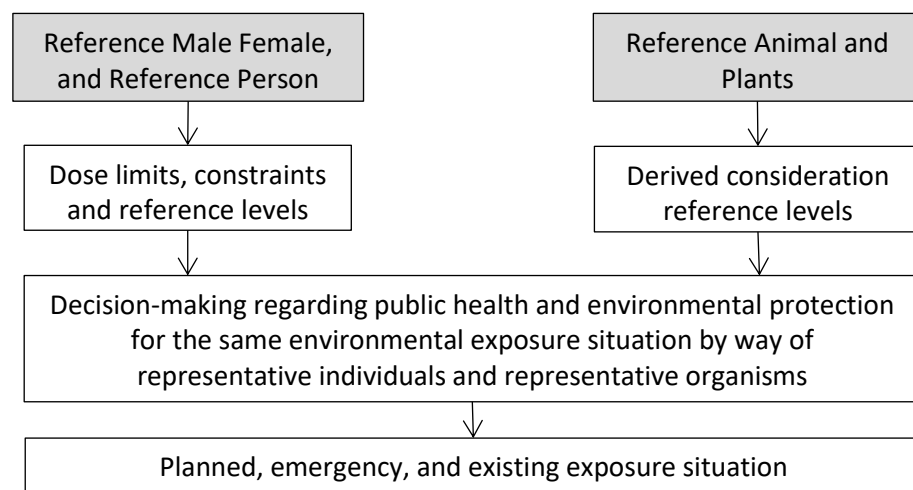
Figure 2-1: The frameworks of exposure situations developed for the protection of human and non-human biota (Pentreath, 2012b)

The ICRP Reference Animals & Plants (RAPs) framework is intended to help assess the relationships between radiation exposure and radiation dose, radiation dose and biological effect, biological effect and possible consequences for different types of biota. The RAP concept is analogous to the ICRP's 'reference man', which is used as the basis for human dose assessment and human protection to address existing, planned and emergency exposure situations (Figure 2-1) (ICRP, 2007; Pentreath, 2012b).

The framework consists of exposure pathways, dosimetry and biological effects data for a variety of lifecycle stages of 12 RAPs, which are representative of different types of fauna and flora (as shown in Figure 2-2) in generic ecosystems (freshwater, marine and terrestrial) (Copplestone, 2012; ICRP, 2008, 2009). This framework includes the identification of Derived Consideration Reference Levels (DCRLs), which are bands of dose rate within which negative effects of ionising radiation on

individuals of that type of RAP may be expected. The framework might be used in three circumstances (ICRP, 2007; Pentreath, 2012a): planned situations; normal (operational) situations; and emergency situations (Figure 2-3).

The RAP concept is similar to the Reference Organism concept used in some of the national and European assessment approaches that had been/were being developed in the late 20th/early 21st century. For example, at the European level, reference organisms formed the basis of the EC-funded FASSET framework (Larsson, 2004). This framework was subsequently incorporated into the EC-funded Environmental Risk from Ionising Contaminants: Assessment and Management (ERICA) Integrated Approach and associated computer model (Brown et al., 2008). There are thirty-nine organisms included within the ERICA Tool formed into and these are divided into three groups (freshwater, marine, and terrestrial). These organisms are intended to cover, amongst other things, European protected species. Other systems have also been developed to evaluate radiation exposures to biota with more or less organisms. For instance, RESRAD-BIOTA, a computer code developed by the U.S. Department of Energy (USDoE), has in effect four organisms: terrestrial system (animal and plant) and aquatic system (aquatic and riparian animal) (USDoE, 2004).

Reference Animals and Plants	
• **Deer** (adult)	• **Frog** (egg, tadpole, adult)
• **Rat** (adult)	• **Trout** (egg, adult)
• **Duck** (egg, adult)	• **Flatfish** (egg, adult)
• **Bee** (adult, colony)	• **Crab** (egg, larvae, adult)
• **Worm** (egg, adult)	• **Brown seaweed**
• **Pine tree**	• **Grass**

Figure 2-2: Set of Reference Animals and Plants (RAPs) and life-stages considered as presented by the ICRP (Pentreath, 2009)
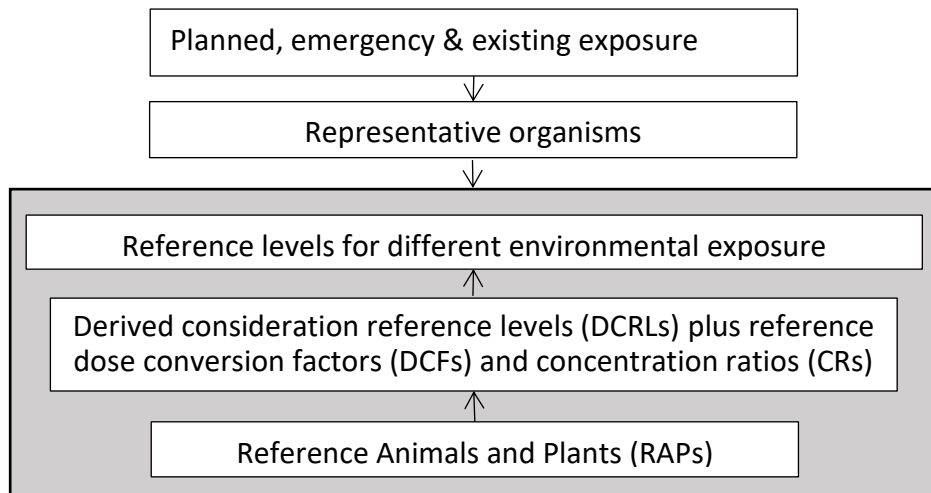
Figure 2-3: Schematic structure to the environmental radiation protection of non-human biota (Pentreath, 2012a)

There are methods to identify compliance with protection objectives provided in legislation or policy, namely measurement of radionuclide activity concentrations in media or biota. However, there are two issues to be considered (Copplestone, 2012). Firstly, wildlife species may be protected under conservation legislation so lethal sampling and analysis is problematic. Secondly, some forms of numeric criteria are required to assess the risk of the environmental impact of radioactive substances. These numeric criteria are commonly referred to as benchmarks. However, there is a lack of international consensus on the purpose of these benchmark values and what the specific values should be. Some countries have established more than one benchmark for serving different purposes. For example, The Environment Agency in England and Wales have been using 5 μGy h^{-1} as the screening value to identify sites requiring more detailed assessment (sites where calculated dose rates are less than this value are deemed to be sites where no significant impact will occur). The Environment Agency also uses a value of 40 μGy h^{-1} as an action level for radiological risk assessment. Developed between 2001 and 2003, both the screening value and action level were agreed with the statutory consultee for conservation issues, which at the time was English Nature. Other numeric values from various countries can be seen in Table 2-2. At a European level, the chronic exposure screening value adopted for use in the ERICA integrated approach is 10 μGy h^{-1} for all ecosystems (Agüero et al., 2006).

Table 2-2: Numeric values used as criteria to assess the impact of ionising radiation for wildlife in the UK, the USA and Canada (Copplestone et al., 2009)

Regulator	Numeric value
Environment Agency, England& Wales	5 µGy h^{-1} - screening value to identify sites requiring more detailed assessment. 40 µGy h^{-1} - action level as agreed with the statutory consultee for conservation issues
USDoE	10 mGy d^{-1} (∼400 µGy h^{-1}) - dose limit for native aquatic animals 1 mGy d^{-1} (∼40 µGy h^{-1}) - benchmarks for terrestrial animals 10 mGy d^{-1} (∼400 µGy h^{-1}) - benchmarks for terrestrial plants
Canada	20 µGy h^{-1} - screening dose rates for fish 220 µGy h^{-1} - screening dose rate for terrestrial and fresh water invertebrates 110 µGy h^{-1} - screening dose rate for other terrestrial and freshwater

2.3.2 Tools for radiological impact of wildlife

A generic framework for environmental radiation risk assessment on wildlife is shown in Figure 2-4 and this is the basis many of the available computer models for dose wildlife assessment (Beresford et al., 2008a; Beresford et al., 2010; Beresford et al., 2008b; Johansen et al., 2012; Vives i Batlle et al., 2007; Vives i Batlle et al., 2011); these models are often referred to as 'Tools'. The first step is to consider the scope of assessment (ecosystem, types of organisms, target radionuclides) and the media activity concentration. The external dose rate needs to be estimated from media measurement or prediction, while the internal dose rate has to use predicted or measured organism activity concentrations. The calculation of internal and external doses takes various parameters into account, including physical dimensions of the organism (geometry), residence time (time spent at sites under assessment) and habitat utilisation (time spent in different areas of the site and the extent of immersion in contaminated media). The total radiation dose is estimated as the sum of both external and internal. The impact can be predicted by comparing the estimated total dose rate with benchmark values and/or data on radiation effects (Wood, 2010).
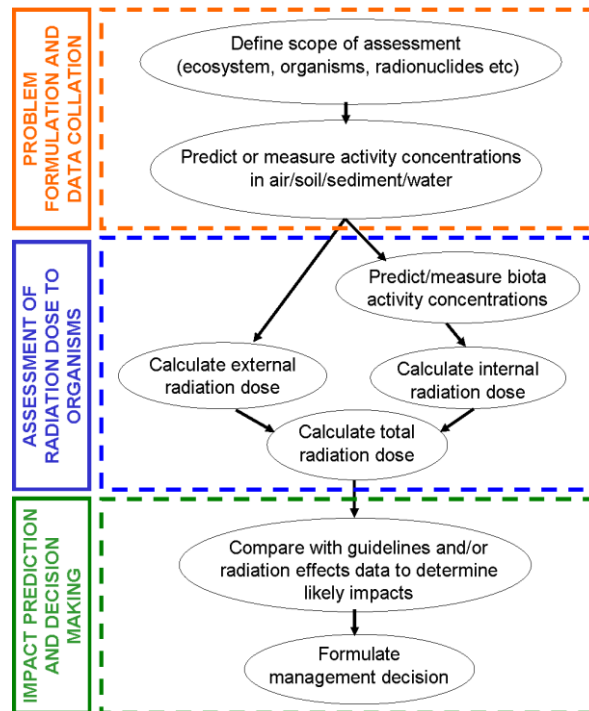
Figure 2-4: Generic frameworks for environmental ionising radiation risk assessment (Wood, 2010)

The models for assessing radiation effect to wildlife are being developed continually, and some are openly accessible. The ERICA Tool, which was mentioned in Section 2.3.1, was used to calculate dose rates within this PhD research project is the most widely used of these models (e.g. Černe et al., 2012; Kubota et al., 2015).

The equilibrium activity concentrations of radionuclides in wild animals (where they have not been measured) are calculated in the ERICA Tool, and many other models, from media activity concentrations in soil (Bq kg^{-1} dry weight), air (Bq m^{-3}) (for terrestrial wildlife) or water (Bq l^{-1}) (for aquatic wildlife). The dose rates can be calculated in the units of µGy h^{-1} in the ERICA tool when activity concentrations in media and/or biota are input. The data on the activity concentrations is used to calculate internal and external absorbed dose rates through the application of dose conversion coefficients (DCCs). The total absorbed dose rate is the sum of these internal and external dose rates.

2.3.3 Uncertainties in radiation dose assessment tools for wildlife

There are a number of models and approaches to estimate radiation exposure of wildlife (IAEA, 2010). At an international level, including through International Atomic Energy Agency (IAEA) programmes, these models have been validated and compared with one another in terms of the estimation of dose and organism activity concentrations in freshwater and terrestrial scenarios (Beresford et al., 2009; Beresford et al., 2008b).

Model outputs are, however, subject to various uncertainties. It is concluded by (Oughton et al., 2008) that technical uncertainties can occur from data or numeric uncertainties, model and scenario uncertainties. Data or numeric uncertainties can occur from the input data, parameters and values used for calculation in the models. Model and scenario uncertainties can arise from the (simplified) mathematical representation of the conceptual models and the imprecision in numerical solutions implicit in mathematical models. This also includes a lack of sufficient information about the situation (at present, in the past and in the future) and properties of the environment. It has been identified that for the radionuclides and environments selected, the parameters of models related to bioavailability and mobility of radionuclides in the environment have the most significant influence on model prediction (Avila et al., 2004)

Doses predicted by models require validation. Direct dosimetry measurements of organisms in field experiments (e.g. Beresford et al., 2008d) and laboratory based experiments (e.g. Kubota et al., 2015) can be used to provide dose measurements against which model predictions can be validated. However, there have been few published studies of radiation dosimetry measurement for a variety of wildlife and there has not been any comprehensive evaluation of the different technologies available for wildlife exposure measurement. Specific dosimetry measurement technologies have their own specific properties, which present a range of different advantages and disadvantages for their use in wildlife studies (see Section 3.3 and Section 3.4). For example, a specific dosimetry technology may be suitable for one type of animal, but not for another, due to differences in animal size, behaviour and

home range[1]. To ensure that direct measurement of wildlife exposures results in measurements with high precision and accuracy, it is necessary to conduct a comprehensive and critical evaluation of the applicability of the range of available dosimetry technologies for a diversity of wildlife applications. The details are described further in CHAPTER 3.

---

[1] Home range is defined as the area used by an animal for living, traveling and searching for food or mates.

CHAPTER 3   SELECTING PASSIVE DOSIMETRY TECHNOLOGIES FOR MEASURING THE EXTERNAL DOSE OF TERRESTRIAL WILDLIFE

The material presented in this chapter has been published as:

3.1   INTRODUCTION

The need to demonstrate the protection of wildlife from ionising radiation is an increasing requirement of national regulation (e.g. Beresford et al., 2008a; Copplestone, 2012) and is now included in international recommendations (e.g. IAEA, 2006; ICRP, 2007; ICRP, 2008). To meet these needs for radiological assessment, a number of modelling approaches have been developed to estimate absorbed doses received by wildlife (e.g. Johansen et al., 2012; Stark et al., 2015; Vives i Batlle et al., 2011; Vives i Batlle et al., 2016; Yankovich et al., 2010). Estimated dose rates are compared to benchmark (e.g. no-effect) dose rates to judge the level of risk (Andersson et al., 2009).

The assessment approaches developed have to be validated in terms of their estimates of internal and external dose to wildlife, to ensure that the uncertainties are quantified and most importantly that the approaches are demonstrated to be fit-for-purpose (i.e. suitable for use in regulatory applications). Predicted internal dose rates have been compared to those estimated via measured radionuclide activity concentrations in organisms (Beresford et al., 2010; Johansen et al., 2012; Stark et al., 2015; Wood et al., 2009; Yankovich et al., 2010). Gamma dose rate typically dominates external exposure (Vives i Batlle et al., 2007), so validating external gamma dose rate estimates using measurements from dosimeters attached to wild

organisms is desirable. However, there have been few such studies to date (e.g. Beresford et al., 2008d; Woodhead, 1973).

As well as allowing validation of dose predictions from assessment models, such dosimetry approaches would also be valuable for measuring doses to wildlife around nuclear facilities (as part of compliance monitoring programmes). In addition, poor dosimetry within field effects studies has increasingly been identified as a limitation in constructing dose-effect relationships for wildlife under field conditions (Beaugelin-Seiller et al., submitted; Beresford & Copplestone, 2011). Application of dosimeters attached to study species would help to address this issue.

It is likely that the different dosimetry technologies available will be suitable for different types of animal, due to variation in animal size, behaviour, habitat and environmental conditions. To ensure that direct measurement of wildlife exposures results in reliable estimates, a comprehensive and critical evaluation of the applicability of the available dosimetry technologies for a diversity of applications is required.

In this chapter, I focus on 'passive' dosimetry technologies and their application to terrestrial wildlife assessment. Such dosimeters can be used in either short term (e.g. days and weeks) or long term (e.g. months to years) dose measurements of terrestrial wildlife (see Section 3.4). The choice of dosimeter depends on the purpose of the study. Dosimeters can be classified as either 'passive' or 'active'. Here we define passive dosimeters as those which integrate dose over the entire exposure period and active dosimeters as those can be read at any time during use. This chapter provides guidance on the selection of appropriate passive dosimetry approaches for measuring external exposure of wildlife.

3.2 MATERIALS AND METHODS

Dosimetry technology could be used to measure radiation external exposure of target wild organisms (e.g. large mammals, small mammals and bird species) under field conditions. Previous published research on wildlife dosimetry measurement using various types of dosimeter was reviewed as described in Section 3.4. The

advantages and disadvantages of different dosimeters for different target animals were also evaluated (see Section 3.3).

Papers and books used for evaluating passive dosimeter performances were searched using Google Scholar and the University of Salford library's search and discovery system. Keywords and search terms were used to retrieve publications related to:

(i) <u>dosimeter characteristics and performance</u>: passive dosimeter; thermoluminescent dosimeter; optically stimulated luminescent dosimeter; radiophotoluminescent dosimeter; direct ion storage dosimeter; comparison on characteristics of passive dosimeter.

(ii) <u>use of dosimeters for wildlife studies</u>: external dose measurements for wildlife; terrestrial wildlife dosimetry technologies; external dose terrestrial wildlife; dose estimates small mammals or wildlife at Chernobyl; dose estimates small mammals or wildlife at Fukushima.

To ensure that all key literature was critically reviewed, further papers were retrieved using the pearl-growing strategy (Schlosser et al., 2006). Using this strategy, related publications were identified from the bibliographies, author names and keywords of the documents returned using the searches described above. The pearl-growing strategy was used until a saturation point was reached. Targeted information was also obtained from the manufacturers of passive dosimeters evaluated in the study.

Once the literature reviews were conducted, a guidance was then developed to aid suitable dosimeter selection for measuring radiation exposure on different wild animals under field conditions in various scenarios (e.g. nuclear facilities, areas impacted by nuclear accident etc.) as described in Section 3.5. Criteria considered when developing the guidance included the characteristics and properties of dosimetry technologies, the target wild animals (e.g. size, weight, behaviour and home range), parameters influencing radiation measurements under field situations (e.g. weather conditions, temperature and humanity) and spatial and temporal variations at study sites. The result would be a recommendation of suitable dosimeter selection for measuring external absorbed doses of terrestrial organisms

under field conditions (see Section 3.5.5). The recommendation in this chapter was also used to address the research objective one (see Figure 4-1).

3.3 PASSIVE DOSIMETRY TECHNOLOGIES FOR WILDLIFE DOSE MEASUREMENT

Different types of passive dosimeter could be used to estimate external doses to wild animals; these can be attached to animals and used to assess external radiation exposure under field conditions. This section describes the available technologies for measuring external gamma dose rates; advantages and disadvantages of these techniques are summarised in Table 3-1. The key characteristics considered include dose response range of the material and its fading properties (reduction in luminescence (see discussion below)). In Table 3-1, we consider two types of fading: (i) temporal fading-loss of luminescence with time, typically at ambient temperatures; and (ii) optical fading-due to exposure to light. Recently there has been the development of additional dosimeter types (e.g. thermoluminescent dosimeters: Lithium potassium borate (LKB) glasses and lithium borate (LB) glass) which have shown good performances (e.g. Hashim et al., 2014; Mhareb et al., 2015). However, as these dosimeters are not commercially available, they are not reviewed in this paper.

3.3.1 Luminescent dosimeters

The luminescent passive dosimeter materials that have previously been used for measuring exposure of wildlife are thermoluminescent dosimeters (TLD), optically stimulated luminescent dosimeters (OSLD) and radiophotoluminescent dosimeters (RPLD) (e.g. Beresford et al., 2008d; Hidehito et al., 2011; Kubota et al., 2015).

3.3.1.1 Principle and reading process

In thermoluminescent (TL) and optically stimulated luminescent (OSL) materials, free electrons are shifted from the valence band to the conduction band as a result of ionising radiation exposure, leaving free holes in the valence band (Mckinlay, 1981; Nanto et al., 2011). Once in the conduction band, these electrons are trapped by

impurities at the band gap between the valence and conduction bands until they are stimulated and emit light (luminescence) (Mckinlay, 1981). The method of stimulation of conduction band electrons depends on the luminescent material; heat is used to stimulate TL materials and light to stimulate OSL materials (Bhatt, 2011).

The response of a radiophotoluminescent (RPL) dosimeter is different. The most commonly used RPL material is silver activated phosphate glass ($AgPO_4$). When this is exposed to ionising radiation, two processes occur: (i) Ag^+ ions combine with electrons released from PO_4^- to form Ag^0; and (ii) holes (hPO_4) lose electrons which then combine with Ag^+ ions to form Ag^{2+} ions. An ultraviolet laser is then used to stimulate the material, causing luminescence (David & Shih-Ming, 2011; Nanto et al., 2011; Ranogajec-Komor, 2009).

For all types of luminescent dosimeter, the intensity of the luminescence they emit when stimulated is proportional to the radiation exposure of the material (Bhatt, 2011).

3.3.1.2 Themoluminescent dosimeter (TLD)

TLDs are generally relatively small (e.g. 4 mm diameter x 1 mm thick), of light mass (typically 20 mg) and are available in different shapes, including rods, squares or discs; the materials are also available as powders. There are many kinds of TL material currently used to make TLDs. The most commonly available commercial TLD materials are discussed below.

3.3.1.2.1 Lithium fluoride (LiF)

There are two types of LiF materials: (i) LiF:Mg,Ti (lithium fluoride doped with magnesium and titanium); and (ii) LiF:Mg,Cu,P (lithium fluoride doped with magnesium, copper and phosphorus). LiF is referred to as a 'tissue equivalent material', with an effective atomic number (Z_{eff} = 8.2) similar to that of soft tissue (Z_{eff}=7.42) (Furetta & World, 2010). When selecting dosimeter materials, it is preferable to use tissue equivalent materials so that the absorption characteristics of the material are more directly representative of those of biological tissues (Furetta et al., 2001). LiF materials may be useful for environmental purposes due to negligible influences from moisture, good sensitivity and low loss of signal with time

after materials are exposed to radiation (Kortov, 2007; Thompson et al., 1999; Xi Shen et al., 1996) but, as for all TL materials, LiF is sensitive to visible light (Duggan et al., 2000). LiF:Mg,Cu,P is easier to analyse than LiF:Mg,Ti because the glow curve (the intensity of TL emitted as a function of temperature) peaks are simpler (Thompson et al., 1999). However, as with all TLD materials, it is not possible to re-read the dosimeters multiple times because the reading process removes the signal.

3.3.1.2.2 Aluminium trioxide (Al_2O_3)

Aluminium trioxide has a sensitivity similar to that of LiF:Mg,Cu,P, but its effective atomic number (Z_{eff} = 10.2) is not a good match to that of biological tissue (Z_{eff} = 7.42). Al_2O_3 has a higher sensitivity than the other TL materials listed in , negligible temporal fading, a simple glow curve and a large dose measurement range (Kortov, 2007). However, it is highly sensitive to white light-induced fading (Sa´ez-Vergara, 2000; Thompson et al., 1999).

3.3.1.2.3 Calcium fluoride (CaF_2) and calcium sulphate ($CaSO_4$)

The Z_{eff} values of both CaF_2 and $CaSO_4$ are relatively high, 16.3 and 15.3 respectively. These materials also have complicated glow curves (Mckinlay, 1981) and relatively high temporal (Bartlett & Tanner, 2005; Kortov, 2007) and optical fading (Annalakshmi et al., 2011; Mckinlay, 1981). However, because of their high sensitivity, they have been used as environmental monitors (i.e. not attached to animals) to measure ambient dose rates from natural background radiation or planned/accidental releases of anthropogenic radionuclides (Mckinlay, 1981; Thompson et al., 1999).

3.3.1.2.4 Lithium tetra-borate ($Li_2B_4O_7$)

$Li_2B_4O_7$: Cu and $Li_2B_4O_7$: Mn have good tissue equivalence (Z_{eff}=7.4) low fading and a simple annealing procedure. However, different authors have reported sensitivities of these materials relative to LiF:Mg,Ti ranging from one tenth (Bartlett & Tanner, 2005; Mckinlay, 1981) to approximately equal (Pekpak et al., 2010). If doped with copper, silver and phosphorous ($Li_2B_4O_7$:Cu,Ag,P) a lower limit of detection can be achieved (Proki, 2002). $Li_2B_4O_7$ has low temporal fading (Bartlett & Tanner, 2005; El-Faramawy et al., 2000; Furetta et al., 2001) but its fading is increased at high

humidity (Annalakshmi et al., 2011; Takenaga et al., 1980); thermoluminescence may be induced by exposure to direct sunlight (Annalakshmi et al., 2011).

3.3.1.3 Optical Stimulated Luminescence (OSL)

Aluminium trioxide doped with carbon (Al_2O_3:C) is the main material used in OSLDs which have a higher radiation sensitivity than TLDs (Botter-Jensen et al., 1997; Thompson et al., 1999). OSLDs can be re-read multiple times because the dose accumulated in the material is not lost during readout (as is the case for TLDs). The main limitation of OSLDs is their sensitivity to optical fading (Bartlett & Tanner, 2005; Olko, 2010). OSLDs need to be mounted within appropriate holders, primarily due to their sensitivity to light and reading process. There are various sizes and shapes of holders available, ranging from 10mm x 10mm x 2 mm to 45 mm x 50 mm x 5mm (Landauer, 2015); they have relatively large sizes and masses compared to TLDs, limiting their application for some small animal types.

3.3.1.4 Radiophotoluminescence (RPL)

Radiophotoluminescence dosimeters are made from silver activated phosphate glass. As with OSLDs readings may be repeated because the dose is not lost during the readout process (Hsu et al., 2006; Lee et al., 2011). RPLDs are insensitive to ambient influences such as temperature, and have low temporal and light fading (David & Shih-Ming, 2011; Ranogajec-Komor et al., 2008). RPLDs may be relatively large (up to 1.5 mm x 12 mm) compared to TLDs. RPLDs require deployment within a holder to protect the glass elements from damage (AGC Techno Glass, 2012). This may be a disadvantage when considering the application to some smaller animal types, such as large insects. There are only a few RPLDs commercially available with relatively few commercial services offering analysis. For all the other dosimeter types discussed above there are a number of suppliers and organisations offering reading and analysis services.

3.3.2 Direct ion storage (DIS) dosimeter

Direct ion storage (DIS) dosimeters are produced as personal passive electronic dosimeters for radiation workers (e.g. https://www.mirion.com/products/instadose-

dosimetry-services/). These dosimeters can be used in either a passive or active way (Mathur, 2001; Wernli, 1996). A DIS consists of two components; an ionisation chamber and a metal oxide semiconductor field effect transistor (MOSFET), which is the "DIS memory cell" (Figure 3-1). Within a DIS, the interaction of ionising radiation with the gas in the chamber results in an electrical charge stored within the chamber that is proportional to exposure. The charge is collected by electrodes and results in a voltage drop across a capacitor. The floating gate is one of the MOSFET electrodes, which is biased to produce a high field to separate the positive and negative charges generated by incident radiation (Mathur, 2001; Sarai et al., 2004; Trousil & Spurn, 1999; Wernli, 1996). The decrease in the bias voltage of the floating gate is proportional to the dose received from the ionising radiation. The DIS can be re-read as the signal is not overwritten or deleted after reading out.

The DIS responds linearly over a wide energy range (Sarai et al., 2004). It has been reported that DIS dosimeters are sensitive to high temperatures (Mathur, 2001). For example, measured doses by the 'Instadose' DIS dosimeter were found to decrease at temperatures greater than 70 °C (Lake Mary, 2014), though this is highly unlikely to be a problem for wildlife dosimetry applications (there is no evidence for poor performance at low environmental temperatures).
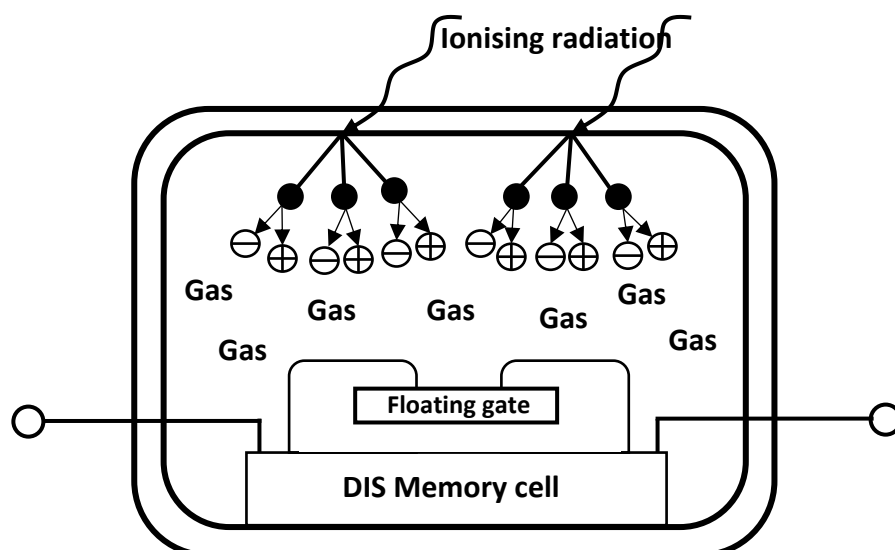
Figure 3-1: Schematic diagram of a Direct Ion Storage dosimeter (after Lake Mary, 2014; Mathur, 2001)

Table 3-1: Summary of reported performance characteristics of passive dosimeters

Dosimeter Type	Dosimeter material	Commonly available sizes	Typical mass	Effective Atomic number (Z_{eff})	Dose range	Fading		Operational energy range	Additional details
						Temporal	Optical		
TLD	LiF:Mg,Ti	4x1 mm[20]	20 mg [20]	8.2[1]	10 µGy - 10 Gy[3,11]	5 % per year[2] 5-10 % per year[3] 10 % per year stored at 18 °C and -17 °C[13]	Likely similar to LiF:Mg,Cu,P respect to white light but higher sensitivity to UV[26]	15 keV – 2.5 MeV[2,12,14]	~50% of standard deviation at 100 µGy[1]
	LiF:Mg,Cu,P				1 µGy - 20 Gy[3,11]	<5% per year[2] 3% per year[3] 10 % per year stored at 18 °C and -17 °C[13]	Up to 45% induction in thermoluminescent intensity after 2 week exposure to sun light[26]	15 keV – 2.5 MeV[2,12]	~20% of standard deviation at 10 µGy[1]
	CaF₂:Dy			16.3[1]	0.1 µGy to 10 Gy[3,11,12]	10% in 24 hours[3] 16% total in 2 weeks[3,11]	Lose signal when exposed to ambient light[12]	50 keV – 2.5 MeV[12,14]	Over-read ~ 15 times at 30 keV compared with ⁶⁰Co calibration[1, 12]
	CaF₂:Mn				0.1 µGy to 100 Gy[3,11,12]	8% in 24 hours[11] 12% total in 2 weeks[11] 15% in 3 months[3]	No observation	70 keV – 2.5 MeV[12,14]	Standard deviation at 100 µGy is 10-20%[1,28]
	CaSO₄:Dy			15.3[1]	2 µGy to 30 Gy[4,12]	5-30% in 6 months[2]	Up to 75% when exposed to direct sunlight at 40 °C for 5 hours[17]	15 keV – 2.5 MeV[2,12]	Standard deviation at 100 µGy is 10%[1]
	CaSO₄:Tm				2 µGy to 3 Gy[12]	5-30% in 6 month[2]	3-30% when exposed to direct sunlight for a few hours[12]	200 keV - 2.5 MeV[12]	Over-read ~ 11-12 times at 30 keV compared with ⁶⁰Co calibration[1, 12]
	Li₂B₄O₇:Mn			7.4[1]	100 µGy to 3 Gy[12]	~ 30% in a year[2]	80% after exposed to (fluorescent) light for 7 hours[12] .Exposure to sunlight may induce additional luminescence[17]	10 keV – 2.5 MeV[2,12]	Increase 40% fading at 95% humidity for 3 months[17]
	Li₂B₄O₇:Cu				20 µGy to 10 Gy[10,12]	About 5-30% in a year[2] c.10 % in 3 months and less than 7 % in a month[10, 16]	<10% at 1000 lux for 3-6 hours[15,18]	15 keV – 2.5 MeV[2,12]	10-25% loss of sensitivity after 2-6 months at high humidity (90%)[15]
	Al₂O₃:C			10.2[1]	0.05 µGy to 10 Gy[3]	3% per year[3] Less than 3% per year[1]	Reported to be very light sensitive [1,26]	200 keV - 2.5 MeV[12]	Over-read ~2.9 times at 30 keV compared with ⁶⁰Co[19] ~20% of standard deviation at 10 µGy[1]

Dosimeter Type	Dosimeter material	Commonly available sizes	Typical mass	Effective Atomic number (Z_{eff})	Dose range	Fading		Operational energy range	Additional details
						Temporal	Optical		
OSLD	Al_2O_3:C	From 10x10x2 mm to 45x50x5 mm[21]	5.0 g (dosimeter needs to be within the protective holder[22])	10.2[1]	10 µGy - 10 Gy[2,5]*	Little fading[2,5] 3% per year[3]	98% discharge after exposed to tungsten-halogen lamp in 45 sec., 93% for exposure to bright room light for 2 hours and 15% for 2 hours with dim room light[25] Insensitive to light unless UV light[7]	15 keV - >10 Mev[2]	~20% of standard deviation at 10 µGy[1]
RPLD	Phosphate glass	Up to 1.5x12 mm[22]	53 mg[22] (75 mg dosimeter with the standard holder or 111 mg for dosimeter with the Tin (Sn) filter holder [22])	12.04[24]	10 µGy – 10 Gy[5,6]*	Less than 5% per year[6]	No effects	High energy dependence at low energy x-ray (~350% at 30keV)[24]	High humidity may cause damage to the surface of the glass[22] Few laboratories offer commercial analyses. Uncertainty of measurement is 2.7%[29]
DIS dosimeter	Direct Io Storage MOSFET	15x54x50 mm[23]	21 g[23]	7.8[9]	10 µGy – 10 Gy[8]*	Little fading[5] Less than 2% in 90 days[10]	No effects	5 keV - 6MeV[23,27]	High temperature (>70°C) is of concern due to the dosimeters reading lower than the true dose[8] 0.8% of standard deviation at 10 µGy[8]

[1] Thompson et al. (1999), [2] Bartlett and Tanner (2005), [3] Kortov (2007), [4] Kamal et al. (2004), [5] Hidehito et al. (2011), [6] David and Shih-Ming (2011), [7] Ranogajec-Komor et al. (2008), [8] Lake Mary (2014) , [9] Mathur (2001), , [10] Furetta et al. (2001), [11] Scientific (2016), [12] Mckinlay (1981), [13] Bilski et al. (2013), [14] Antonio et al. (2010), [15] Takenaga et al. (1980), [16] El-Faramawy et al. (2000), [17] Annalakshmi et al. (2011), [18] Prokic (2001), [19] Akselrod et al. (1990), [20] https://www.phe-protectionservices.org.uk/pds/service/ [21] Landauer (2015), [22] AGC Techno Glass (2012), [23] https://mirion.app.box.com/s/719344t4988o10xms9mhmjn6ru6j1g5v [24] Knežević et al. (2013), [25] Jursinic (2007), [26] Duggan et al. (2000) [27] Chiriotti et al. (2011) [28] Weinstein and German [29] Moon et al. (2013)

* Converted from Sv to Gy assuming a weighting factor

3.4 FIELD STUDIES THAT USED DIRECT EXTERNAL DOSE MEASUREMENT FOR WILDLIFE

A variety of passive dosimetric technologies described the characteristics in Section 3.3 have been used to estimate the dose to different wild organisms under field conditions, including Thermoluminescent dosimeters (TLDs), optical stimulated luminescent dosimeters (OSLDs), and radiophotoluminescent dosimeters (RPLDs) (Beresford et al., 2008d; Chesser et al., 2000; Fuma et al., 2015; Halford & Markham, 1978; Kubota et al., 2015; Rumble & Denison, 1986; Stark & Pettersson, 2008; Woodhead, 1973). These studies are reviewed below and summarised in Table 3-2.

Plaice *(Pleuronectes platessa)* in the north-east Irish Sea around the area of the Sellafield nuclear fuel reprocessing plant had TLDs attached using a Petersen disc tag (an external tag fixed under dorsal fin of the fish with a pin) (Woodhead, 1973). The study gave good agreement (by up to a factor of 1.75) between the modelled external doses to gonads and those estimated based on the TLDs.

TLDs have also been used to measure doses to small mammals using various attachment techniques including subcutaneous implantation (Gano, 1979; Halford & Markham, 1978; Turner & Lannom, 1968), ear mounting (Rumble & Denison, 1986) and collar mounting (Chesser et al., 2000; French et al., 1966). In the Chernobyl Exclusion Zone (CEZ), TLDs fitted to collars on a range of small mammal species were found to give comparable results to measurements made with a hand-held dose rate meter at ground level (by up to a factor of 1.04) (Chesser et al., 2000). For the study of (Beresford et al., 2008d), results from the TLDs were also compared with external dose rate predictions estimated using the ERICA Tool (Brown et al., 2016; Brown et al., 2008). The model predictions were found to be acceptable (by up to a factor of 1-3 comparing the results with direct dose measurements using TLDs) given the uncertainties of the study (e.g. differences in soil types across the study sites) (Beresford et al., 2008d). Data from the study was subsequently used to compare to the predictions of a number of other assessment models (Beresford et al., 2010).

TLDs were used to assess external exposure of frogs in a wetland area contaminated with [137]Cs (Stark & Pettersson, 2008). However, TLD chips were inserted in frog phantoms rather than being attached to frogs directly. Phantoms are artificial structures created to represent the geometry and density of the organism of interest. The phantoms were placed 5 cm deep in the soil. Results of the measurement were later compared with the predictions of different dose assessment models using activity concentrations of radionuclides in soil at the sites (Stark et al., 2015) The TLD results were generally lower than the model predictions (by up to a factor of about 5). However, this was likely due to assumptions used within the modelling. The assumed depths of an organism in soil in the models are greater than that at which the phantom was placed. However, the largest contributing factor was the assumption that the soil dry matter content was 100%; a more appropriate wetland soil moisture content gave predicted dose rates in better agreement with TLD results.

Phantoms were also used to represent Chironmidae larve in a study of ^{137}Cs exposure in an artificially contaminated pond (Guthrie & Scott, 1969). The phantoms were constructed using LiF powder sealed within a cylindrical plastic tube (20mm long x 4mm outer diameter) coated with silicone rubber. The dosimeters were deployed for a period of up to one year; this early study demonstrated the potential application of passive dosimeters and phantoms to estimate exposure of wildlife.

Recently, RPLDs, OSLDs and TLDs have been used to estimate external absorbed dose rates of rodents, amphibians and barn swallow nestlings in areas of Japan contaminated by the Fukushima Dai-ichi accident (Bonisoli-Alquati et al., 2015; Fuma et al., 2015; Kubota et al., 2015). For the rodents, dosimeters were placed on the ground and underground near to animal traps being used in the study. Some dosimeters were embedded in the abdomen of non-contaminated rodent carcasses, which were then placed on the ground (Kubota et al., 2015). RPLDs were also placed in areas where adult salamanders and overwintering larvae were likely to live (i.e. in the middle of the litter layer and on the sediment of ponds) (Fuma et al., 2015). For the barn swallow nestlings, TLDs were placed in barn swallow to estimate external exposure (Bonisoli-Alquati et al., 2015). For rodent and amphibian studies,

measurements were in agreement with dose rates predicted using the ERICA Tool. To date, the barn swallow measurements have not been compared with ERICA Tool predictions.

RPLDs have also been used in field studies to determine the exposure rates for soil biota in the Chernobyl Exclusion Zone (Bonzom et al., 2016; Buisset-Goussen et al., 2014) though given the size of study organisms these were simply placed in the environment.

Table 3-2: The summary of dosimetry technologies used for the previous studies of direct dosimetry measurement to different wild species in various scenarios

Dosimetry technologies	Techniques/Applications	Study species	Study areas	References
TLDs*	TLDs attached to animals directly	Pocket mouse (*Perognathus formosus*)	Mojave Desert at the US Atomic Energy Commission's Nevada test site	French et al. (1966)
TLDs*	Subcutaneous surgical implantation	Desert lizards (*Uta stansburiana, Cnemidophorus tiger and Crotaphytus wislizeni*)	Mojave Desert at the US Atomic Energy Commission's Nevada test site	Turner and Lannom (1968)
TLDs*	TLD attachment attached with Petersen disc tags	Plaice (*Pleuronectes platessa*)	The north-east Irish Sea around the area of the Sellafield nuclear fuel reprocessing plant	Woodhead (1973)
TLDs*	Subcutaneous surgical implantation	White-footed deer mouse (*Peromyscus maniculatus*) Least chipmunk (*Eutamias minimus*) Ord's kangaroo rat (*Dipodomys ordii*)	A liquid radioactive waste disposal area at the Idaho National Engineering Laboratory Site in southeastern Idaho	Halford and Markham (1978)
TLDs*	Subcutaneous surgical implantation	Pocket mouse (*Perognathus parvus*) Deer mouse (*Peromyscus Maniculatus*) House mouse (*Mus musculus*) The western harvest mouse (*Reithrodontomys Megalotis*)	The US Department of Energy's Hanford site in Benton County, southcentral Washington (USA)	Gano (1979)
TLDs*	Ear mounted TLDs	White-footed deer mouse (*Peromyscus maniculatus*) Least chipmunk (*Eutamias minimus*) Ord's kangaroo rat (*Dipodomys ordii*)	Contaminated site in USA	Rumble and Denison (1986)
TLDs*	Collar mounted TLDs	Root vole (*Microtus oeconomus*)	Chernobyl Exclusion Zone	Chesser et al. (2000)

Table 3-2: The summary of dosimetry technologies used for the previous studies of direct dosimetry measurement to different wild species in various scenarios (cont'd)

Dosimetry technologies	Techniques/Applications	Study species	Study areas	References
TLDs*	Collar mounted TLDs	Yellow neck mouse (*Apodemus flavicollis*) Bank vole (*Myodes glareolus*) Vole species (*Microtus spp*)	Chernobyl Exclusion Zone	Beresford et al. (2008d)
TLDs*	Inserted TLDs in frog phantoms before placing in soil	Frog phantoms	A wetland area in Utnora, Sweden	Stark and Pettersson (2008)
TLDs*	Phantom comprising LiF powder in cylindrical tube coated with silicone rubber	Chironomidae larvae	^{137}Cs contaminated pond	(Guthrie & Scott, 1969)
RPLDs** and OSLDs***	Dosimeters were placed on the ground and underground RPLDs were embed in uncontaminated wild rodent carcasses which were then put on the ground	Small Japanese field mouse (*Apodemus argenteus*) Large Japanese field mouse (*Apodemus speciosus*) Japanese grass vole (*Microtus montebelli*)	A site contaminated by the Fukushima Dai-chi nuclear power plant accident	(Kubota et al., 2015)
RPLDs**	RPLDs were placed on the ground and on the sediment at the bottom of a pond	Tokoku hunobiid salamander (*Hynobius lichenatus*)	Fukushima Prefecture	(Fuma et al., 2015)
TLDs*	TLDs were attached to the inner and outer rim of bard swallow nests	Barn swallow (*Hirundo rustica*) nestlings	Fukushima Prefecture	(Bonisoli-Alquati et al., 2015)

*TLDs = Thermoluminescent dosimeters   **RPLDs = Radiophotoluminescent dosimeters

***OSLDs = Optical stimulated luminescent dosimeters

3.5 DISCUSSION

As reviewed above, there are various passive dosimeters that could be used for directly measuring the external gamma exposure of wildlife. However, there are a number of factors which need to be considered when selecting a suitable dosimetry technology (Figure 3-2).
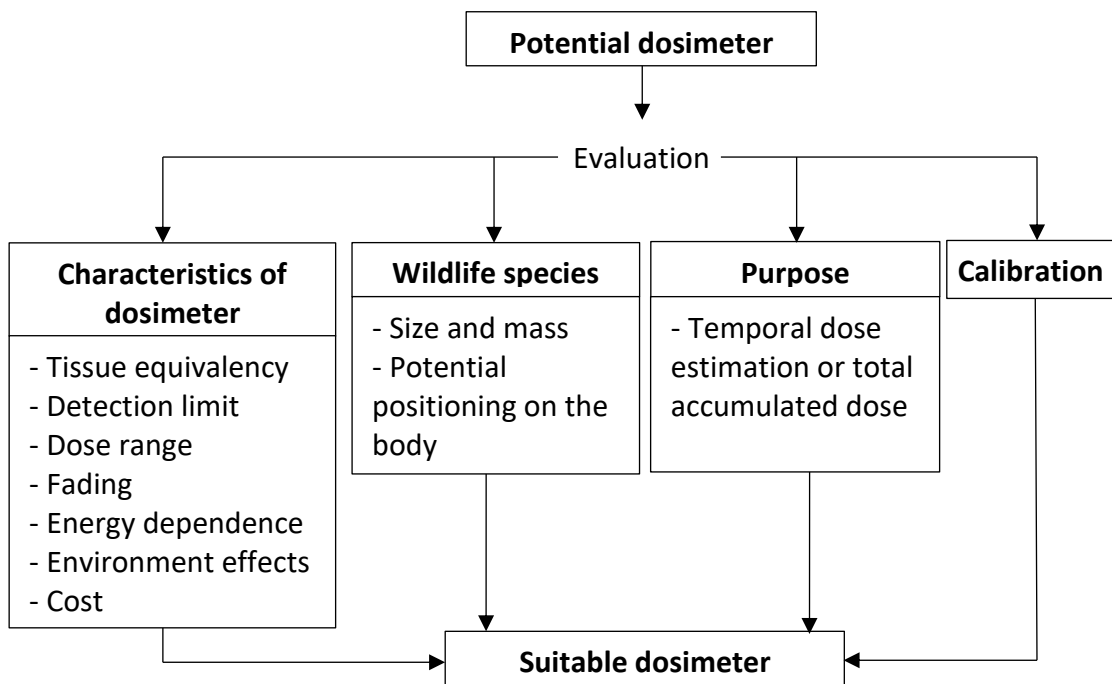
Figure 3-2: Schematic guidance of dosimetry selection for wildlife external dose measurement under field conditions

3.5.1 Dosimeter characteristics

3.5.1.1 Tissue equivalency

Ideally, the dosimeter material should have an effective atomic number as similar as possible to that of soft tissue (Z_{eff}=7.42). From this perspective, LiF TLDs and $Li_2B_4O_7$ would appear to be the best candidate dosimeters (Table 3-1). However, $Li_2B_4O_7$ has a higher detection limit than LiF and potentially higher fading rate, so LiF TLDs are likely to be the more suitable of these technologies.

3.5.1.2 Limit of detection and dose range

The limit of detection (LOD) is the lowest dose that can be detected by a given dosimetry technique. The materials with the lowest reported limit of detection are CaF_2, $CaSO_4$, Al_2O_3:C and LiF:Mg,Cu,P TLDs. The calcium based TLDs all have relatively high fading rate with most being known to suffer from optical fading. Al_2O_3:C has a relatively low fading rate but is known to be very light sensitive. Of the dosimeters considered in Table 3-1, $Li_2B_4O_7$:Mn has the highest LOD and may not therefore be suitable for some short term research applications where low dose measurements are required. However, for regulatory compliance applications, even at the lowest lower-bound Derived Consideration Reference Level (c. 4μGy h^{-1}) suggested by the International Commission for Radiological Protection (ICRP, 2008), all of the dosimeters considered provide a sufficiently low LOD; 4μGy h^{-1} is the lowest suggested benchmark that we are aware of (Howard et al., 2010).

From Table 3-1, it can be seen the highest measurable dose is of the order of 1 to 10's Gy for all dosimeter types. Therefore, the upper dose limit of all dosimeter materials is likely to be suitable for environmental purposes given dose rates likely to be encountered in the field. Even in the highest dose rate areas of the Chernobyl Exclusion Zone, it would take at least 100 days (for a subterranean organism) to reach 1 Gy of exposure (Beresford & Wood, pers. comm.). However, if dosimeters are deployed soon after an accident with a magnitude similar to Chernobyl, appropriate upper dose limits would need to be considered; exceedance of the dosimeter upper dose range could be avoided by using shorted deployment times.

3.5.1.3 Fading

For environmental use, a dosimeter material with a low temporal fading rate is required, as dosimeters will most likely be attached to animals for periods of at least weeks. The material with the lowest fading rate are LiF TLDs, Al_2O_3:C, OSLD, RPLD and DIS. On the basis of fading, Calcium based TLD would appear to be unsuitable for environmental use.

To varying degrees all TLD materials are affected by exposure to light. DIS and RPLD are unaffected by light. Al_2O_3:C TLDs are especially sensitive to light exposure and as

this compound is also the dosimeter material in OSLDs these dosimeters are also light sensitive (Duggan et al., 2000; Jursinic, 2007; Ranogajec-Komor et al., 2008; Thompson et al., 1999). However, the effect of optical fading can be reduced by covering the dosimeter to minimise exposure to light.

3.5.1.4 Operating energy range

It is necessary to ensure that the operational energy range of the dosimeters encompasses the energies of the radionuclides of interest. For the majority of dosimeter materials specified in Table 3-1, the operational energy range encompasses many of the likely radionuclides of likely interest in environmental assessments. However, some dosimeters may not be suitable for higher energy radionuclides.

3.5.1.5 Environmental conditions

There are reports that RPLDs and $Li_2B_4O_7$:Cu are affected by high levels of humidity likely to be found in some environments (>80%) (AGC Techno Glass, 2012; Annalakshmi et al., 2011; Takenaga et al., 1980). DIS are known to be affected by high temperatures, but, the temperatures at which there is any impact on recorded doses are above those normally encountered in the environment (> 70 ^{o}C). It may be possible that environmental factors (e.g. very low temperatures) have other impacts on the DIS unit (e.g. reduction in battery life).

3.5.1.6 Cost

TLDs have a relatively low cost (currently about £5/chip; Personal Dosimetry Service, Public Health England), but can only be read once whereas other dosimeters (i.e. OSLD & RPLD) are more expensive (currently £20/chip; Thailand Institute Nuclear Technology and Chiyoda Technol Corporation). DIS (Instadose) currently has a relatively high price (£126/chip/year; CHP dosimetry, USA). Additional costs may be incurred for some dosimeter types if they are lost or returned damaged.

3.5.2 Target wild organism and practical considerations

A number of dosimeter types have been used to estimate external doses of wildlife directly in the field (Table 3-2). However, to our knowledge, only TLDs (LiF material)

have been attached to free-living animals to evaluate gamma doses for both aquatic and terrestrial wildlife (Beresford et al., 2008d; Chesser et al., 2000; French et al., 1966; Rumble & Denison, 1986; Woodhead, 1973).

TLDs, OSLDs and RPLDs have all been used to estimate external exposure of animals by placing them directly in the environment or in/on phantoms (Fuma et al., 2015; Kubota et al., 2015). However, this does not account for how animals may move around a heterogeneously contaminated environment and hence may not give a true representation of dose received (Stark et al., 2017; Stark & Pettersson, 2008).

Mounting OSLDs onto small species of mammal and amphibian may be possible, but more difficult than TLDs and RPLDs because of their larger size and mass of the dosimeter and holder. However, OSLD could be an option for dose measurement for larger mammals of a few 100's of grams or more, with the advantage that they can be reread (which TLDs cannot) if required.

Previous studies have used a variety of techniques of attaching the dosimeter to animals (see Table 3-2). The size and mass of the dosimeter will impact on the ability to use it for the diverse range of wildlife which may be of interest (e.g. bee species, fish or large mammal). It has been suggested that devices to be mounted onto an animal should not exceed 5% of the mammal's body mass or 2-3 % of a bird's body mass (Ministry of Environment & Lands and Parks Resources Inventory Branch for the Terrestrial Ecosystems Task Fource Resources Inventory Committee, 1998; Sirtrack Limitted, 2016; The American Society of Mammologists, 1987). This mass limit is for all equipment mounted on the organism, including for instance a collar and if applicable GPS device as well as the dosimeter. Where a collar is not suitable (e.g. for small species such as bees) harnesses or surgical grade super glue could be used to attach the dosimeters (The American Society of Mammologists, 1987). The method of attachment could be tested by conducting a controlled test with captive animals before mounting on wild individuals to make sure that they are able to move freely and that the dosimeter stays on the animal. The methods of dosimeter attachment proposed above should be deemed ethically acceptable as they are currently used to attach other devices (e.g. GPS or radiotrackers).

Animal behaviour is another consideration of dosimeter selection. For instance, riparian animals may mainly live in the terrestrial ecosystem but will also use the aquatic environment, whilst other species may live partially underground. Other behaviours, such as rutting by deer, may also influence the choice of how, or where, a dosimeter should be mounted and consequently the choice of the dosimeter to use.

3.5.3 Purpose

The dosimeter types considered would enable an estimation of total integrated external dose over the duration of their attachment to study animals. However, there may be instances where temporal measurements are required. For instance, the aim of using a dosimeter may be to understand how an animal interacts with the environment, especially where contamination is highly heterogeneous (Hinton et al., 2013).

Collar attached active dosimeters and GPS devices have recently been developed and used to quantify external exposure of a large mammal species, wild boar (Hinton et al., 2015). These allow the location of the animal to be recorded at the same time as temporal dose rate being recorded.

The Instadose⁺ (DIS) (https://www.mirion.com/products/instadose-plus/) is an example of a dosimeter that could also be used to quantify the variation in external exposure of an animal as it moves through a contaminated environment. When such a device is mounted with a GPS, it would allow investigation of spatial and temporal variability. The size and mass of dosimeters such as the Instadose mean that they could only be used with medium or large animals. These dosimeters would require a robust enclosure for protection. Such enclosures may also protect dosimeters from environmental factors. However, the size and mass of the enclosure needs to be appropriate for the animal.

In some cases, exposure to beta radiation may influence the estimation of total integrated external gamma dose (e.g. this was the case for ^{90}Sr in the Chernobyl Exclusion Zone study of (Beresford et al., 2008d)). For larger animals, it may be possible to protect the dosimeter from beta exposure (e.g. by surrounding it in

Perspex). However, if dosimeters could not be protected by a beta shield correction factors could be established by placing paired dosimeters, one shielded from beta and one not, in different exposure situations at the site (see Beresford et al., 2008d).

3.5.4 Calibration

Once a suitable technology and method of attachment to the animal has been selected, there will be a need to calibrate the dosimeter taking into account the organism's size and the location and method of attachment. Most dosimeter readings will be reported in Sv as Hp(10), where Hp(10) is the personal (or human) dose equivalent at a body depth at 10mm (ICRP, 1996, 2010). Therefore, it is necessary to determine a conversion from Hp(10) to whole-body absorbed dose for the relevant species. It may also be necessary to consider appropriate exposure scenarios such as how the dosimeter may respond when the animal is standing up versus lying down or if the animal is burrowing. This would require the use of appropriate phantoms and controlled exposure facilities, such as those used for calibration of dosimeters for humans (ICRP, 1996). Variation in size between individuals belonging to the same species will have negligible influence on the absorbed dose (Vives i Batlle et al., 2007; Vives i Batlle et al., 2011) and hence interpretation of the results from attached dosimeters.

3.5.5 Conclusions and recommendations

There are a number of different types of dosimeter that could be used for wildlife dose measurements under field conditions. However, dosimeter properties, study animals and experimental areas need to be taken in to account to ensure that a suitable dosimeter is chosen for the target animal and study purpose.

On the basis of the discussion above, we suggest that calcium based and $Li_2B_4O_7$ TLDs are not good candidates for environmental application to estimate doses to wild animals.

LiF based and Al_2O_3:C TLDs, appear good candidates based on their limit of detection, comparatively low fading and small size. LiF based TLDs have been used successfully in a number of field studies (Table 3-2). Al_2O_3:C has potentially low limits

of detection though it is especially sensitive to light (suitable light-proof housing may negate this disadvantage); to our knowledge, no field studies have been conducted using this dosimeter material.

OLSDs and RPLDs are also likely suitable for the applications as discussed in this chapter, however, their larger size mean that they are less suitable than TLDs for some small animals.

The application of DIS is most suitable when information on temporal variation in dose is required. However, their size means that they may not be suitable for small species.

Dosimeter calibration should be considered before using dosimeters in field studies to account for variables such as method of dosimeter attachment to the animal and the likely environmental dose range. The dose recorded by a passive dosimeter attached to an animal may include a contribution from radionuclides incorporated in the animal's body; to our knowledge field applications of passive dosimeters have not, to date, considered this issue; phantoms could be used to investigate this.

The advice presented in this chapter should be useful in guiding field dose-effect studies and regulatory compliance monitoring.

3.6 SUMMARY

This chapter present the critical review on selection of a suitable passive dosimeter for wildlife dose measurement under field conditions. Previous studies of measuring external absorbed doses of wild organisms using various passive dosimeters were evaluated on advantages and disadvantages of individual technologies and measuring techniques. These were challenges of establishing a guidance and criteria about suitable dosimeter selection for using with wildlife species in different ecological wildlife applications. The properties of passive dosimeters, target animal, purpose and calibration are the main criteria of initial consideration on wildlife dosimetry applications using a suitable passive detector. The DIS (Instadose+) dosimeter is a passive detector that can be used to solve spatial and temporal variation when it is used in combination with a radio tracking device. LiF based and

Al$_2$O$_3$:C TLDs, appear good candidates. LiF based TLDs have been used successfully in a number of field studies. OLSDs and RPLDs are also likely good options for the applications of large mammal species as discussed in this chapter.

However, these suitable dosimeters are required to test with a target organism in the field. Before employing selected dosimeter to target animal species in field, a robust method needs to be established and to be tested with the selected dosimeters in laboratory conditions. The passive dosimeters were therefore tested their performances in a laboratory using a developed method for discovering the accurate external absorbed doses of large mammal species in the field. The details are described further in CHAPTER 5.

CHAPTER 4   METHODOLOGY

This chapter presents an overview of the experimental methods used within this PhD to address the research objectives (see Figure 4-1). Separate sections of this chapter describe the experimental methods used to:

- determine dosimeter performance (Section 4.1);
- test dosimeters under field conditions and evaluate dose assessment model predictions (Section 4.2); and
- determine external dose contributions to organ absorbed doses in deer (Section 4.3).

Further details of the methods used are presented in the relevant research chapters (CHAPTER 5 to CHAPTER 7).

Aim
Development of appropriate methods for directly measuring external radiation exposure of free-ranging terrestrial animals using passive dosimeters

Objective 1
To evaluate the effectiveness of the selected passive dosimeters for wildlife dose measurements

Objective 2
To inform passive dosimeter selection for long term large mammals measurements under field conditions

Objective 3
To test the use of collar-mounted dosimeters for long term measurements of external doses of the species in a contaminated area

Objective 4
To evaluate model performances by comparing model prediction with direct dose measurements

Objective 5
To quantify the relationship between external exposure and organ dose for a large mammal species

Research chapter 1
Selecting passive dosimeters for wildlife external dose measurement
(See CHAPTER 3)

Research chapter 2
Characterisation of passive dosimeters in enclosure for wildlife dose measurements
(See CHAPTER 5)

Research chapter 3
Measuring the radiation exposure of reindeer in Norway under field conditions
(See CHAPTER 6)

Research chapter 4
A novel method to determine deer organ dose from external exposure
(See CHAPTER 7)

Figure 4-1: The relationship among the aim, objectives and stages of methodology

4.1 CHARACTERISING DOSIMETERS

4.2.1 Design method for long term terrestrial wildlife dose measurements

Using the dosimeter selection guidance (Section 3.5), which was developed from the critical review described in Section 3.1 above, four dosimeter types were selected for measuring external absorbed dose of large mammal species (Figure 4-2). The dosimeters selected were TLD (LiF:Mg, Cu, P), OSLD (Al_2O_3:C), RPLD in waterproof plastic capsules (GD-352M) and direct ion storage (DIS) (Instadose+).

To allow these dosimeters to be fitted to a large mammal for an extended period (i.e. for a number of months), it was necessary to develop an appropriate housing and attachment mechanism. An IP68[2] aluminium enclosure was chosen as the container to fit in four dosimetry techniques because it provides durability, a waterproof enclosure and shielding of beta radiation. These are important things to be taken into account because the dosimeter enclosures have to contend with extreme weather (e.g. heavy snow, rain and very low temperatures), large mammal behaviours and radionuclides emitting beta radiation. The dimensions of the aluminium box were 60 mm. x 55 mm. x 31 mm and the four dosimetry technologies could be mounted securely within the box in a consistent geometric relationship (see Section 5.2.1). The box lids were secured with four stainless steel fixing screws (one at each corner). The gap between the boxes and the lids was sealed by a neoprene rubber gasket to make it waterproof.

---

[2] IP68 enclosures are dust, dirt and sand resistance and can withstand submersion in 1.5m of water for up to 30 minutes. This level of protection was deemed to be sufficient for large mammals inhabiting a terrestrial environment.

Figure 4-2: Dosimetry technologies used for measuring external doses of large mammals

It was essential to ensure that the mounting of dosimeter boxes on Global Positioning System (GPS) collars for large mammals (Figure 4-3) would not significantly affect the weight balance of the collar or the daily life of large mammals (e.g deer). Aluminium plates were fabricated (55 x 90 x 2 mm) for use as a connector between the collar and the dosimeter box. The aluminium plates were drilled to create four mounting points so that the dosimeter box could be secured to the collar with nuts and bolts. Custom made plate washers (20 x 30 x 1.5 mm), with a 10-mm gap between 2 holes, were prepared to minimise any risk of tearing of the collars and tightly fitted between the dosimeter box and the collar. A dosimeter box mounted on an aluminium plate was attached to a collar in the laboratory at Salford to ensure that the mounting was durable (Figure 4-4). The attachment procedure was repeated many times to ensure that it could be done rapidly (i.e. within 3-5 minutes which were the times for replacing batteries of GPS devices attached on the reindeer collars). The waterproof performance of the aluminium boxes was also validated by immersion in water for at least 48 hours; all boxes were found to perform as expected.

Figure 4-3: A GPS collar for large mammals

Figure 4-4: Testing mounting of the dosimeter box on a large mammal GPS collar

The performance of the dosimeters within the box was studied using a series of experiments undertaken at the Public Health England (PHE) calibration laboratory (see Section 5.2.2). Dosimeters in the box were calibrated using caesium- 137 (^{137}Cs), Radium-226 (^{226}Ra) and Cobalt-60 (^{60}Co) sources. These radioactive sources were representative of anthropogenic and natural radionuclides that may be present in the environment and allowed calibration across a range of gamma energies. The calibration collar was mounted on a cylindrical head phantom (used in medical dosimetry) as this most closely represented the dimensions and density of a large mammal neck (Figure 4-5). Experiments were performed to determine dose linearity, angular dependence, energy dependence, beta response and the contribution of internal contamination within a large mammal's body to the measurement recorded by the dosimeters (CHAPTER 5 Section 5.3).
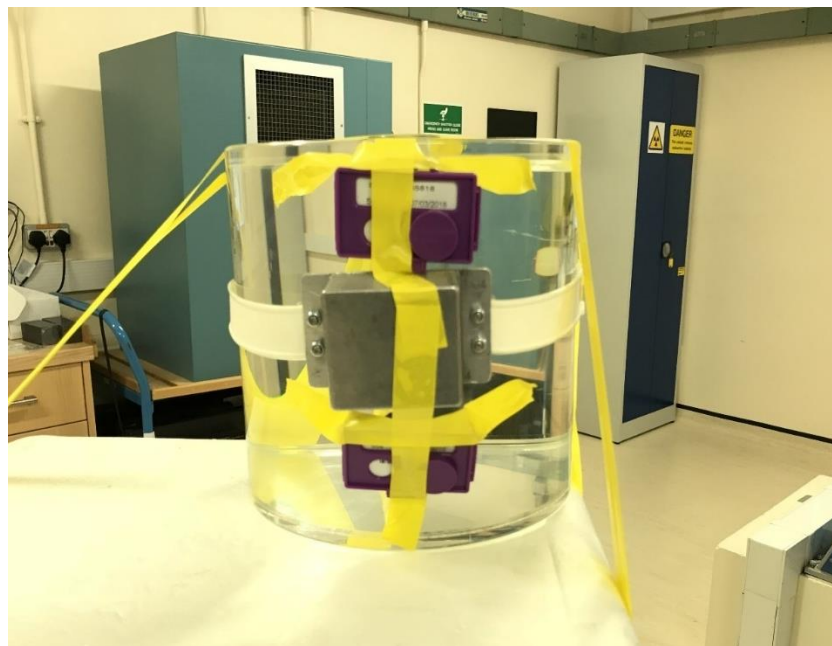
Figure 4-5: Attaching the dosimeter box on a collar to the cylindrical head phantom representing the neck of a large mammal

4.2 FIELD EXPERIMENT

4.2.1 Norwegian reindeer external dose measurement

A study site (Vågå, Norway) was selected for field testing of dosimeter boxes. Norwegian reindeer was the target species chosen for the experiment. This element of the research was conducted in collaboration with the Norwegian Radiation Protection Authority (NRPA) and Vågå reindeer herders. The NRPA have a long-standing relationship with these reindeer herders through an ongoing research programme to study the movement of reindeer through areas of Norway that received contamination from the Chernobyl accident. Twenty-one reindeer from a Vågå herd have been fitted with collars onto which GPS units have been mounted (Table 4-1). These allow the NRPA and the herders to track the movement of the Vågå herd reindeer in real-time (Figure 4-6). For the herders, this helps with herd management. For the NRPA, this allows identification of reindeer which have been grazing in the more contaminated areas. These reindeer are then live-monitored by the NRPA to determine the activity concentration of ^{137}Cs in their meat and ensure that contaminated meat is not entering the human food chain.
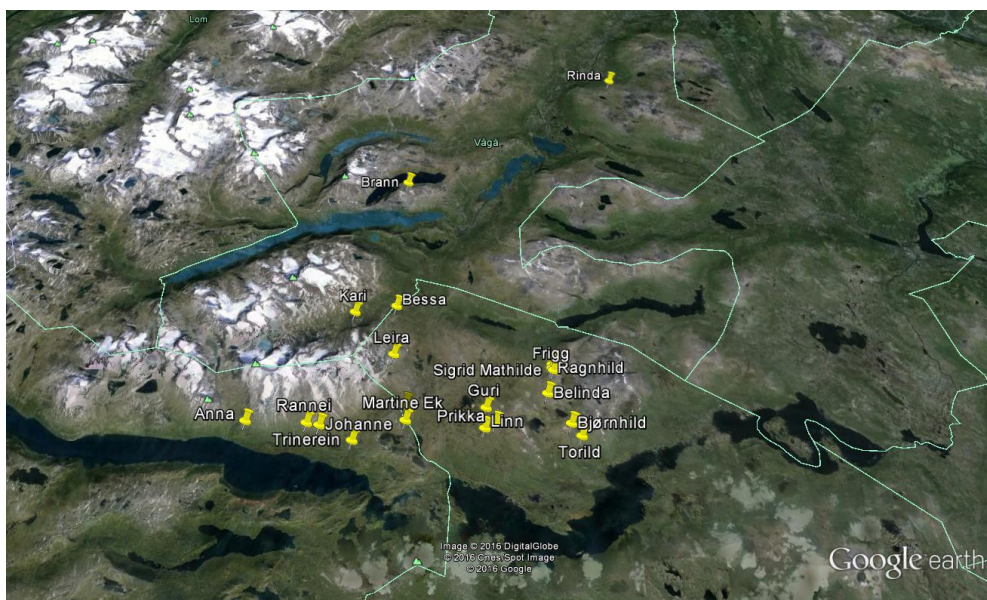
Figure 4-6: Locations of the reindeer in Vågå can be obtained from their GPS collars and displayed in Google Earth

Table 4-1: Details of the reindeer fitted collars mounted GPS and dosimeter boxes

Name	Sex	Ear tag number	GPS number	Dosimeter box number
Linn	Female	07-122	61758	1
Frida	Female	M322	81371	2
Ragnhild	Female	006	96405	3
Trinerein	Female	L002	103800	4
Bessa	Female	P408	112071	5
Prikka	Female	E026	61617	6
Sigrid Mathilde	Female	272	97995	7
Rinda	Female	L474	56315	8
Krone	Female	292	103613	9
BjØrnhild	Female	M176	112562	10
Guri	Female	016	112426	11
Frigg	Female	048	80276	12
Martine EK	Female	188	61305	13
Kari	Female	L336	96472	14
Anna	Female	No ear tag	89165	15
Leira	Female	510	56315	No dosimeter box*
Belinda	Female	126	61535	No dosimeter box*
Johanne	Female	6281	61740	No dosimeter box*
Rannei	Female	5232/08-180	88037	No dosimeter box*
Tea	Female	M356	103263	No dosimeter box*
Torild	Female	08-L132	103382	No dosimeter box*

*The collared reindeer without dosimeter boxes because those reindeer were firstly fitted the collars on their neck after the dosimeter boxes were prepared

4.2.2 Preparing dosimeters for field applications

TLDs, OSLDs and RPLDs were annealed and supplied for use by Public Health England (PHE), Thailand Institute Nuclear Technology (TINT) and Ruđer Bošković Institute (RBI) respectively. For DIS (Instadose+) dosimeters were set to log dose measurements every 4 hours 48-minute periods (i.e. five measurement periods each day) by the manufacturer (Mirion Technologies) before deployment in the field. The dose measurements recorded by the Instadose+ are stored on-board. When the dosimeter was retrieved, it communicated with the Mirion web server and the dose measurements were reported.

For the dosimeter boxes to be used in Norway, the individual components were transported separately and the boxes assembled on arrival in Norway. The

dosimeters were carried in hand luggage and declared at airport security checkpoints so that the dosimeters were not passed through X-ray machines. This was done to avoid the dosimeters recording additional radiation dose from the x-ray machines prior to their deployment at sites in Norway. Three sets of dosimeters have been being used to control transit doses between Manchester and study site in Vågå and also control background doses of Norway. The transit doses were subtracted from all dosimeters used in Norway.

Eighteen sets of dosimeters in aluminium boxes were used in total:

- Fifteen dosimeter boxes were mounted on reindeer GPS collars and used for measuring the external radiation dose to reindeer.
- Three dosimeter boxes were used to measure transit doses between UK and Norway. These were retained in a shielded room at the NRPA head office in Oslo, Norway. One box contains an operational Instadose+ and the other two boxes contain 'dummy' Instadose+ units because the number of units that Mirion Technologues was able to provide (at no cost to the project) was limited.

The use of these dosimeters within different parts of the experiment is summarised in Figure 4-7. The dosimeter box numbers and serial numbers of dosimeters fitted in an individual box were recorded on a record form to ensure that final dosimeter results were clearly attributable to specific experimental elements.
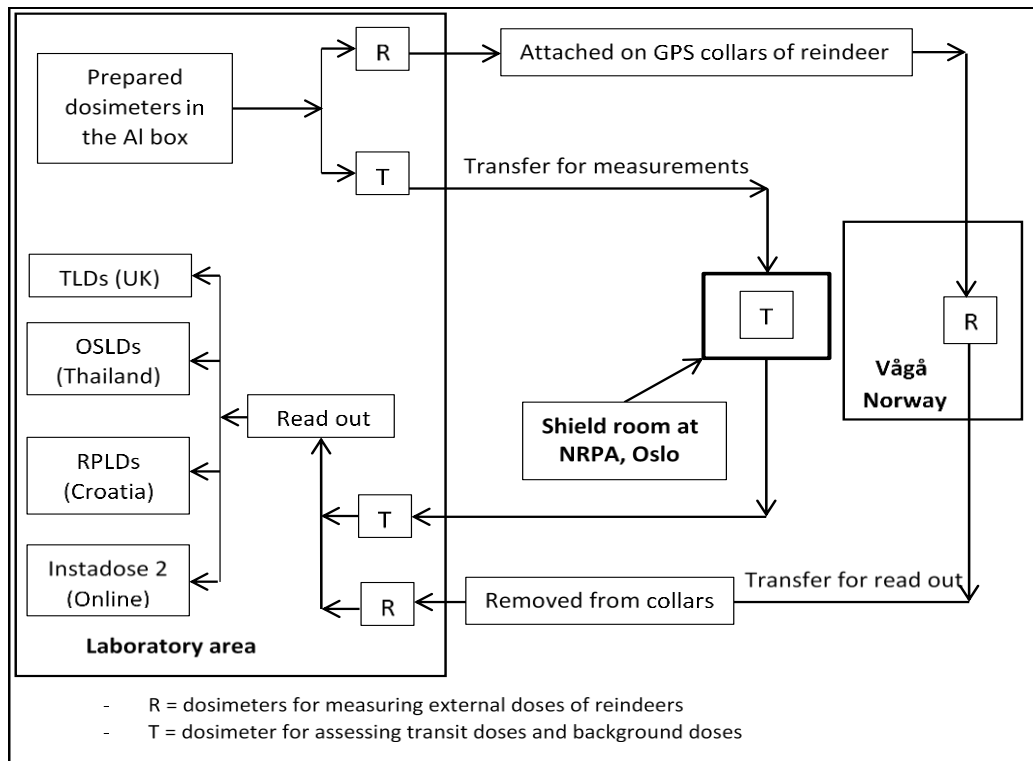
Figure 4-7: The schematic layout of external doses measurements using four dosimetry technologies for this study

4.2.3 Fitting dosimeter boxes on GPS collars

The reindeer herd is driven from their habitats to the slaughtering area two times per year, once in late summer and once in winter (Figure 4-8). The collars were fitted during the winter herding activity (January 2016). The reindeer were divided into small groups by herders on snowmobiles and herders controlling dogs. Once a small group of reindeer was in the final enclosure, they were screened by herders for slaughtering or released back into the environment (Figure 4-9).

Reindeer with GPS collars were moved to another enclosure for live monitoring of internal radiocaesium activity concentrations using a Sodium Iodine (NaI) active detector (Figure 4-10). The reindeer were manually secured throughout the live monitoring process and during this time the GPS collars were detached for replacing batteries and attaching dosimeter boxes.

Figure 4-8: The Vågå reindeer herd driven by herders from their habitats to slaughtering area

Figure 4-9: Some of the reindeer herd in screening enclosure for slaughtering, releasing to the environment and monitoring ^{137}Cs activity concentration

Figure 4-10: NRPA staff using an active detector to measure the internal ^{137}Cs activity concentration in GPS collared reindeer

The activities in the field experiment can be seen from Figure 4-11 to Figure 4-15. Ethical approval (from the Science & Technology Research Ethics Panel, University of Salford) and informed consent (from the Vågå herders) were obtained prior to starting work at the site to ensure that the experiment complied with University of Salford ethical research procedures.

Figure 4-11: Detaching the GPS collar of a reindeer for attaching the dosimeter box and replacing batteries

Figure 4-12: The reindeers held by herders during fitting the dosimeter boxes on the collars

Figure 4-13: Making holds on collar before fitting dosimeter box

Figure 4-14: Dosimeter box mounted on the collar preparing to reattach to a reindeer

Figure 4-15: A reindeer mounted a GPS device and a dosimeter box before released to the environment

4.2.4 Dosimeters reading out

Dosimeters were taken out from the aluminium boxes at the end of the experiment. Dosimeters were declared to security at airport check points to avoid x-ray scanning during transport back to the UK.

The luminescence dosimeters were sent to one of three laboratories:

- TLDs were sent to Public Health England, Oxford, the UK
- OSLDs were sent to Thailand Institute Nuclear Technology, Nakorn Nayok, Thailand
- RPLDs were sent to Ruđer Bošković Institute, Zagreb, Croatia

The total external doses accumulated were provided after reading out of the dosimeters by the respective laboratories. For the Instadose+, the dosimeters were linked to the webserver of Mirion technologies via its website (https://instadose.com/Default.aspx) to obtain the doses stored in the devices

throughout the measurement period. The dose data were downloaded along with the exact date and time of each measurement.

4.2.5 Comparison of model and field experiment

The reindeer in the study site have internally incorporated ^{137}Cs which will contribute to the external doses recorded by four dosimeter types. This contribution needed to be calculated (See Section 6.2.5) and subtracted from the total external doses to ensure that the actual external doses were estimated from radionuclide in the environment.

Measured doses recorded by dosimeters could then be compared with those predicted using the ERICA Tool using two assessment approaches:

- Approach 1: The external absorbed dose was predicted using the average ^{137}Cs activity deposition and activity concentration of natural radionuclides (i.e. ^{40}K, ^{232}Th and ^{238}U) in soil over the herd areas (see Section 6.2.6). The estimated activity concentrations in soil of the radionuclides were input into the Tier 2 of the ERICA Tool using the tool large mammal geometry to predict external absorbed dose rates of the reindeer herd. The total mean external absorbed dose of the herd from the radionuclides were finally estimated over the length of time over which the direct dose measurements were conducted (i.e. 11 months).

- Approach 2: The GPS tracking data of collared reindeer were input into a GIS to estimate the time weighted mean ^{137}Cs activity depositions and activity concentration of natural radionuclides in soil for each reindeer (see Section 6.2.7). These data were then used to predict the average external absorbed dose of each individual reindeer over eleven months using the beta-gamma DCC for large mammal from the ERICA Tool.

To ensure that the measured doses could be directly compared with dose predicted using the two approaches described above, the cosmic radiation contribution needed to be included in the model predictions (i.e. two approaches). The external exposure due to cosmic radiation was estimated using the herd average altitude for

Approach 1 and the altitude of each GPS-tracked reindeer for Approach 2. These values were then input into the equation for estimating mean annual absorbed dose of the reindeer herd and also individual collared reindeer due to cosmic radiation (see Section 6.2.6).

The results from models for the collared reindeer and the reindeer herd were compared with the actual estimated doses of the collared reindeer from four types of passive dosimeters as presented in Section 6.3.2.

4.3 DEER PHANTOM STUDY

Organ dose estimates from external exposure of radionuclides in the environment were determined. A deer phantom was created from the female red deer CT images using a human phantom at the University of Salford (see Section 7.2.1). The locations of important organs (i.e. thyroid, lung, heart, liver, spleen, kidneys, ovaries and uterus) were mapped from the red deer CT images Figure 4-16 to the human phantom for creating the deer phantom using the ratios between the sectional human phantom and the cross-sectional deer organ images. As the two-red deer scanned were females, predicted doses to testes was assumed that they were located in the same place as human testes. The ratios were also used with the organ positions to determine predrilled organ holes in the phantom slices as locations of the internal deer organs for placing TLDs and subsequently determining organ doses.
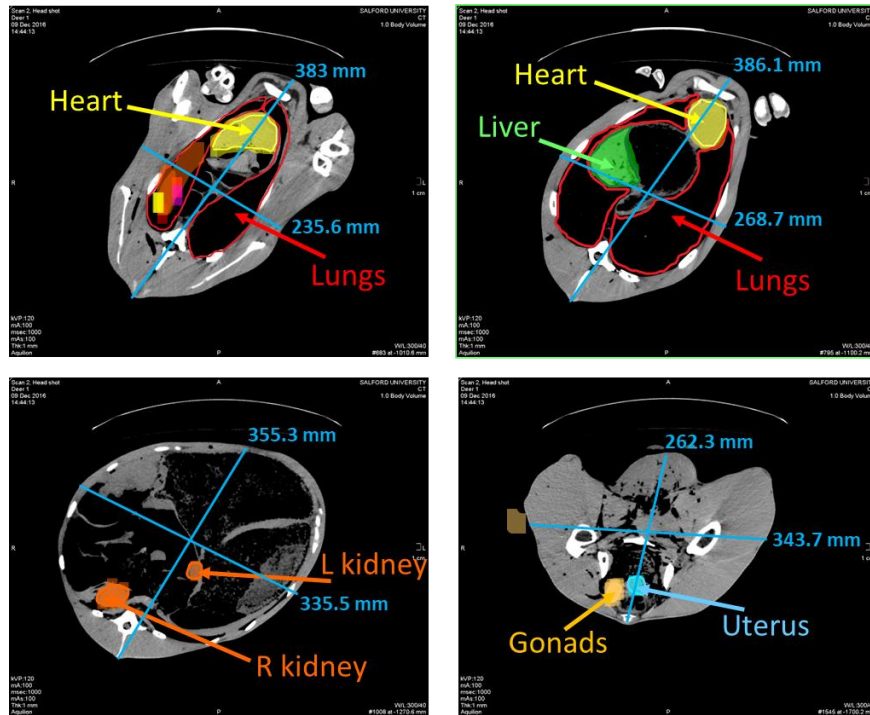
Figure 4-16: Example of cross-sectional deer organ mapping using sagittal CT scan images

The deer phantom was then loaded with TLDs and used to measure organ doses (see Section 7.2.2). The whole-body absorbed doses of the phantom were also measured using TLDs housed in an aluminium box and fitted to an animal collar which was attached on the side of the neck of the phantom. The phantom loaded TLDs into the organs and fitted TLDs in an aluminium box at the neck (

Figure 4-17) was exposed to x-ray at 50 kVp (100 mAs) and 100 kVp (100 mAs) at the University of Salford radiography laboratory (see Section 7.2.3). The phantom was also exposed to gamma radiation of ^{137}Cs at the PHE calibration laboratory (see Section 7.2.4). The TLDs irradiated to x-ray and gamma radiation were read at the University of Salford dosimetry laboratory to obtain mean external absorbed doses of whole body and each organ of the phantom. The comparison of the whole-body dose and organ doses provided conversion factors for individual organs to quantify their external doses when the whole-body dose is recorded by dosimeters fitted on the neck or from modelled estimates.

Figure 4-17: Applied deer phantom loaded TLDs in and attached dosimeter box at the neck of the phantom for irradiated to x-ray (50 kVp (100 mAs) and 100 kVp (100 mAs)) and gamma radiation (^{137}Cs, 662 keV)

CHAPTER 5   CHARACTERISATION OF PASSIVE DOSIMETERS ASSEMBLED IN A ROBUST ENCLOSURE FOR MEASURING EXTERNAL RADIATION ABSORBED DOSE OF LARGE MAMMAL SPECIES

The material presented in this chapter has been submitted for publication in the Journal of Radiological Protection:

Aramrun et al., submitted. Characterisation of passive dosimeters assembled in a robust enclosure for measuring external radiation absorbed dose to large mammal species. Journal of Radiological Protection.

5.1   INTRODUCTION

Direct external dose measurement of terrestrial wildlife using passive dosimeters is a method to record external accumulated doses and validate the predicted external dose rates of wildlife dosimetry models (CHAPTER 4; Aramrun et al., 2018). Practical direct dosimetry measurement is an effective method and necessary for accurately measuring external exposure of target terrestrial wildlife under field conditions; either contaminated areas or compliance monitoring areas. There were several studies to measure the external ionising radiation doses of terrestrial animal species using thermoluminescent dosimeters (TLDs), optically stimulated luminescence dosimeters (OSLDs) and radio-photoluminescence dosimeters (RPLDs) by directly attached passive dosimeters on animals or phantoms (e.g. small mammals, amphibian and birds) (e.g. Beresford et al., 2008d; Bonisoli-Alquati et al., 2015; Stark & Pettersson, 2008) or dosimeters placed in animal habitats (e.g. Fuma et al., 2015; Kubota et al., 2015).

However, there has as yet been no reported study on external dosimetry measurements using passive dosimeters under field application for large terrestrial mammal species (e.g. deer). Direct attachment of dosimeters to large mammal

species for measuring external absorbed doses is a challenge because their behaviours and environmental conditions may cause damage or loss to the dosimeters in the field. A dosimeter may need to be packed in a robust housing (e.g. aluminium box) before attaching in an appropriate position on a large mammal species to protect the dosimeter from any damage. Different passive dosimeter types may also be assembled together in a robust enclosure to compare those dosimeter performances and seek suitable dosimeters for accurately assessing external absorbed doses of large mammal species.

Passive dosimeters are normally used for measuring doses in the field of radiation protection, environmental monitoring and in medicine (e.g. Bartlett & Tanner, 2005; McKeever et al., 1995; Nanto et al., 2011; Ranogajec-Komor, 2008). Those passive dosimeters are normally reported in the unit of Sievert (Sv) as the personal dose equivalent at a body depth of 10 mm ($H_p(10)$) representing to whole body personal dose equivalent. The personal passive dosimeters need to be considered in a radiation quantity when they are used for wildlife radiation dose measurements (Brown et al., 2016; Copplestone et al., 2001; ICRP, 2008). This is because the quantity of wildlife dose assessments is expressed as absorbed dose (Gy) or whole body absorbed dose rate (Gy h^{-1}). Before using passive dosimeters for wildlife dose measurements, their performance needs to be tested in the laboratory conditions which are similar to the field experiments to ensure that factors associated with each dosimeter's response (e.g. linearity of measured dose to air kerma, energy dependence, angular dependence and types of radiation) are taken into account.

However, when the dosimeter performances are tested in laboratory to determine dose responses with reference doses, the air kerma, radiation energy deposited or absorbed in a unit mass of air (Gy), is the radiation quantity that need to be used for the measurements of laboratory experiments using conversion coefficients. Conversion coefficients are used to convert between personal dose equivalent $H_p(10)$ and air kerma (e.g. Petoussi-Henss et al., 2010) and between air kerma and whole body absorbed dose of animals (e.g. Ulanovsky & Pröhl, 2008, 2012) using appropriate parameters where the dosimeters are used (e.g. phantom or animal shapes (e.g. cylinder or ellipsoid), tissue materials to compare with air, angles and

57

energy sources). In this chapter, I present the responses of four types of dosimeters which are TLD, OSLD, RPLD and direct ion storage (DIS) when they are assembled in an aluminium (Al) enclosure called in this study as the 'dosimeter box'.

5.2 MATERIALS AND METHODS

5.2.1 Design of passive dosimeters in an aluminium box

The following dosemeters were placed in the aluminium dosimeter box:

- thermoluminescent dosimeter (TLD) (LiF:Mg,Cu,P; standard Harshaw[TM] type, generally used for personal monitoring and supplied by Public Health England (PHE), Oxford, UK),
- optical stimulated luminescent dosimeter (OSLD) (Al_2O_3:C; Nagase Landauer, Ibaraki, Japan),
- radio-photoluminescent dosimeter type GD-352M (RPLD) in waterproof plastic capsules (GD-352M; AGC Techno Glass Corporation, Shizuoka, Japan, (AGC Techno Glass, 2012))
- direct ion storage (DIS) dosimeter (Instadose+; Mirion Technologies, California, USA) were chosen for this study.

The characteristics of the individual dosimeters can additionally be found in (AGC Techno Glass, 2012; Aramrun et al., 2018; Gilvin et al., 2007). These dosimeters were assembled within an aluminium box (IP68 Deltron, 480 Series Diecast Aluminium Boxes) as shown in Figure 5-1. A bare TLD plate was placed in the bottom of the dosimeter box and then the Instadose+ was put on top of the TLD. The OSLD and RPLD (in a waterproof holder) were placed as a top layer above the TLD and Instadose+. Pieces of foam were used to fill any voids to make sure that the dosimeters fitted tightly in the box and that the geometric relationship between the dosimeters was maintained. Two 5 g bags of silica gel were inserted in each box to absorb any build-up of moisture which may affect dosimeter performance.
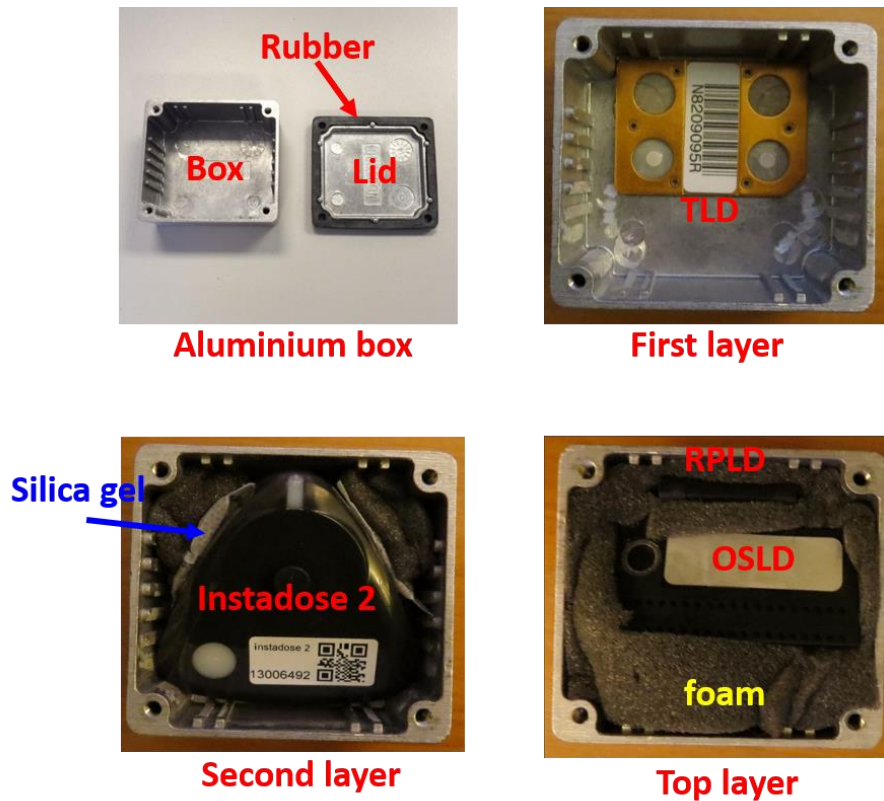
Figure 5-1: Arrangement of the four dosimeters in the dosimeter box

5.2.2 Laboratory Irradiation of dosimeter box

A cylindrical Oramed type phantom (Bordy et al., 2011) was used in this study. The phantom is a water-filled, 20 cm diameter, right circular cylinder of a height of 20 cm, with poly-methylmethacrylate (PMMA) walls of a thickness of 0.3 cm and 1.0 cm thickness top and bottom. The phantom simulates the neck of a large mammal species such as deer on which the dosimeter box will be attached during the field study (for example see CHAPTER 6). The dosimeter box is attached to a rubber collar for attaching around a large mammal species neck. For the laboratory tests, the box was attached using the same collar around the cylinder of the phantom simulating its position around the large mammal species neck. The angles between the dosimeter box on the phantom and a radiation source were defined as ±45°, ±90° and ±135° which were considered for investigating angular dependence (Figure 5-2). This is based on the assumption that the dosimeter box is attached on the side of each animal's neck. The animals tested in the field study were from a commercially husbanded herd of reindeer that were given large bells to wear around their necks

by the herders (see Section 4.2 and Section 6.2.3a.i.6.2.3). The bells were attached securely facing the ground, and there was no room at that location for the dosimeter box to be positioned. In the field (near the Arctic Circle), the box is therefore at an angle of +45 degrees to the assumed main ionising radiation source, the contaminated ground.
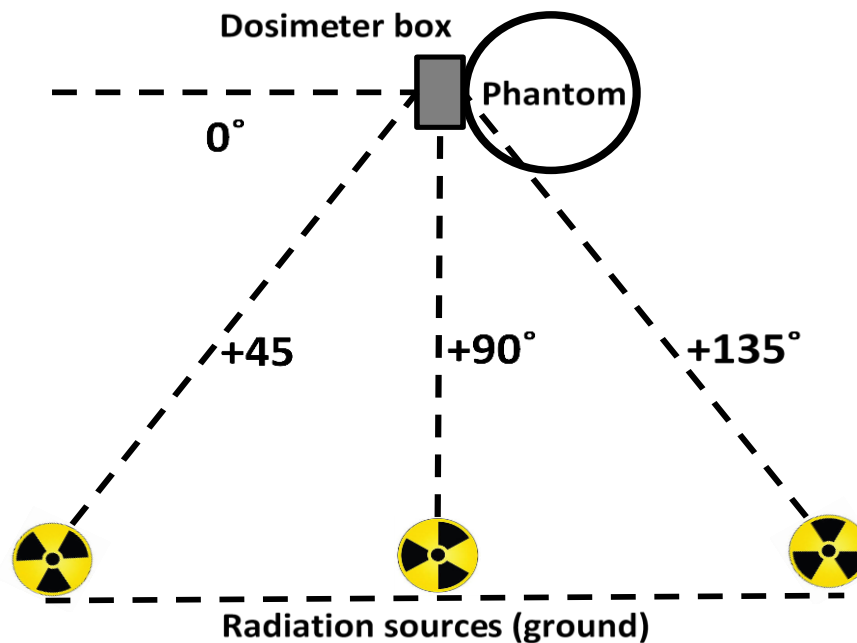
Figure 5-2: The diagram showing the direction between the dosimeter box and the laboratory radiation source at +45, +90 and +135 degrees

Irradiation of the dosimeter box was undertaken in one of the gamma or beta dose rate irradiation facilities at the Centre for Radiation, Chemicals and Environmental hazards (CRCE), Public Health England (PHE). The air kerma dose rates in the CRCE gamma irradiation facilities are directly traceable to the National Physical Laboratory (NPL), UK. The dosimeter boxes on collars were irradiated using four radioactive sources (Table 5-1):

- ^{137}Cs is representative of anthropogenic radionuclides and for this work has been defined as the target gamma source;
- ^{226}Ra is representative of natural background radiation;
- ^{60}Co is representative of high energy naturally occurring radionuclides (e.g. ^{40}K);

- $^{90}Sr/^{90}Y$ is representative of pure beta radionuclides.

The gamma radionuclides are significant contributors to the total dose measured by the dosimeter boxes used in the field. $^{90}Sr/^{90}Y$ is representative of high energy beta radiation (which might be able to penetrate the dosimeter box, unlike lower energy beta radiation). When high energy beta particles are involved, there is also the possibility that bremsstrahlung radiation could be detected.

The dosimeter box was separately irradiated with ^{137}Cs, ^{226}Ra and ^{60}Co gamma sources at +45° because this angle was defined as the dominant direction from which the dosimeter box will receive external exposure from the ground in the environment during the field study, due to the habits and movements of the reindeer. Caesium-137 was used to irradiate the dosimeter box separately with reference air kerma values of 0.3, 0.7 and 1 mGy respectively for the field at the reference point, to investigate the dose linearity of the dosimeters positioned in the dosimeter box. These doses were chosen because they are in a range of annual doses typically received by terrestrial wildlife (Beresford et al., 2008c) and of natural background in the environment (Oatway et al., 2010). The dosimeter box was also exposed to a ^{137}Cs source, with reference air kerma of 0.7 mGy at +90° and +135°, and ^{60}Co with a reference air kerma of 0.7 mGy at +135° in order to consider the direction dependence of the dose responses for the four dosimeter types positioned in the dosimeter box. The influence of beta radiation on dosimeters positioned in the aluminium dosimeter box was also tested in this study by irradiation with a $^{90}Sr/^{90}Y$ source with a reference absorbed dose (to water) of 3 mGy at 2 angles; 0° and +90°) in order to verify that the dosimeter box would be able to shield the dosimeters from beta radiation in the environment.

Table 5-1: The details of the irradiation of the dosimeter box using a variety of radioactive sources

Irradiation*	Type of Ionising Radiation	Source (Mean energy)	Quantity	Angle of exposure** (Degree)	Dose (mGy)
1	Photon	Cs-137 (662 keV)	Air kerma, K_a	+45	0.3
2	Photon	Cs-137 (662 keV)	Air kerma, K_a	+45	0.7
3	Photon	Cs-137 (662 keV)	Air kerma, K_a	+45	1.00
4	Photon	Cs-137 (662 keV)	Air kerma, K_a	+90	0.7
5	Photon	Cs-137 (662 keV)	Air kerma, K_a	+135	0.7
6	Photon	Co-60 (1170/1330 KeV)	Air kerma, K_a	+45	0.7
7	Photon	Co-60 (1170/1330 KeV)	Air kerma, K_a	+135	0.7
8	Photon	Ra-226***	Air kerma, K_a	+45	0.7
9	Beta	Sr-90/Y-90 (0.546 MeV/2.28 MeV)	Dose to water, D_w	-90	3.00
10	Beta	Sr-90/Y-90 (0.546 MeV/2.28 MeV)	Dose to water, D_w	0	3.00

* Each irradiation was repeated 3 times

** The phantom was turned anticlockwise for positive angles, and turned clockwise is negative angle

***[226]Ra emits a variety of gamma energies (Chisté et al., 2007)

5.2.3 Attaching dosimeter box on active phantom

A cylindrical phantom, containing gel with homogenously dispersed ^{137}Cs within, was used to assess any external absorbed dose to the four dosimeters within the aluminium dosimeter box from activity concentration within the phantom. The phantom is made of 6 mm thick high-density polyethylene (HDPE), and its dimensions are 150 mm diameter, 40 cm long, with a fill cap in the middle. The phantom is the upper leg part of a Bottle Manikin Absorption (BOMAB) phantom representing an average adult human (Youngman, 2003). The phantom contains ^{137}Cs activity concentration of 60 kilo Becquerel (kBq) on 6th November 2017 (± 10%) in approximately tissue-equivalent set gel. The dosimeter box on a collar was attached to the outside of the phantom for 52 days and 1 hours (1249 hours) (Figure 5-3) and kept in a ground-floor storeroom adjacent to the exterior of the building annex far from any known sources at CRCE PHE for the 52 days. Four TLD dosimeters (LiF:Mg, Cu, P; Public Health England (PHE), Oxford, UK), in their usual plastic

holders containing build-up, were also attached around the phantom, with the front build-up facing the phantom, for comparison of dose results with all the dosimeters placed within the dosimeter box as shown in Figure 5-3. In addition, the mean absorbed dose of dosimeters in the dosimeter box calculated from the H_p (10) body dose was used for calculating absorbed dose rate. The volume, gel density and ^{137}Cs activity concentration of the phantom were also used to calculate activity concentration per mass (Bq^{-1} kg). These data were then used for calculation of the absorbed dose rate per activity concentration of ^{137}Cs at 1 Bq in mass of gel (μGy h^{-1} Bq^{-1} kg).
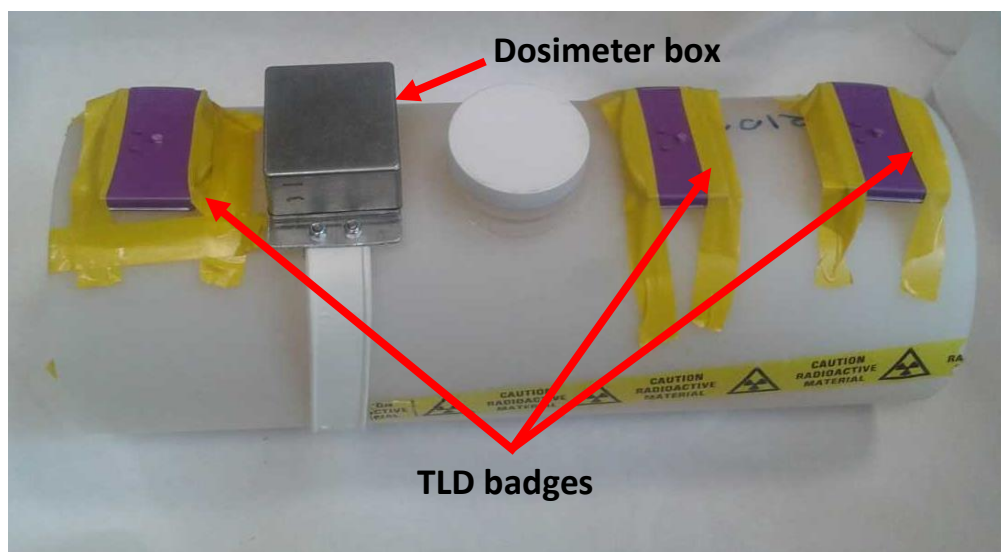
Figure 5-3: The attachment of dosimeter box and TLD badges on the active cylindrical phantom

5.2.4 Calculation of conversion coefficient

Occupational exposures of people are determined in terms of personal dose equivalent, $H_p(10, \square)$, in units of Sieverts (Sv), which is the dose at a depth of 10 mm in soft tissue below a specified point on the body, from radiation incident from angle $\square$ (ICRP, 1996, 2010; ICRU, 1993). The dosimeters are usually calibrated by exposing them to reference radiation fields, for which the air kerma, K_a, can be determined using reference ionization chambers with traceability to a primary standards laboratory. The air kerma is converted to personal dose equivalent using published ISO (ISO, 1999) or ICRU (ICRU, 1998) $H_p(10, \square)/K_a$ conversion coefficients (Sv/Gy).

However, for some of the angles and sources used here, the conversion coefficients have not been published. Conversion coefficients from air kerma, K_a to personal dose equivalent $H_p(10, \Omega)$ for the laboratory radiation sources to the cylindrical Oramed-type phantom were simulated using the Monte Carlo N-Particle (MCNP6) code (Pelowitz, 2013).

The geometry of cylindrical phantom used for the experiment in Section 5.2.2 was input into the MCNP model and was defined using two materials; air and soft tissue (Hydrogen, Carbon, Nitrogen and Oxygen) (ICRU, 1998). The radiation sources ^{137}Cs, ^{60}Co and ^{226}Ra were created in the model as isotropic plane sources placed at 2 m distance from the Oramed type phantom. The models were simulated to emit radiation from each source at different angles to the front centre of the Oramed type phantom. A depth of 10 mm, with a circular diameter of 10 mm was defined as the reference point for calculation. The results of MCNP simulations were air kerma per source particle and tissue kerma per source particle, in the units of (Gy). Tissue kerma was being used as an estimate of absorbed dose or dose equivalent, because it could be assumed that secondary charged particle equilibrium was being achieved at a depth of 10 mm. Both values were divided by the value of fluence 'free in air' from those sources in units of cm^{-2} to obtain air kerma per fluence and absorbed dose per fluence respectively in units of Gy cm^2. Finally, the absorbed dose per air kerma could be calculated as the ratio of these two quantities. The different types of sources, mean energy and angles of exposure used for the model are shown in Table 5-1.

5.3   RESULTS AND DISCUSSSION

5.3.1 Conversion coefficient

Air kerma per fluence and absorbed dose per fluence for ^{137}Cs, ^{60}Co and ^{226}Ra for the angles given in Table 1 were simulated using the MCNP code. The ratios between absorbed dose per fluence and air kerma per fluence (i.e. the absorbed dose per air kerma conversion coefficients in the unit of Gy Gy^{-1}) of individual radioactive emissions for the specific angles were then calculated as shown in Table 5-2. These

conversion coefficients can be used as estimates of the $H_p(10,\alpha)$ per air kerma

conversion coefficient at angle α, which has units of Sv Gy^{-1} because of the

unrestricted linear energy transfer ($Q(L)$) for photons has a value of 1 for all energies

(ICRP, 1991; ICRU, 1998). The modelled conversion coefficients were then used to

convert from the personal dose equivalents $H_p(10)$ of dosimeters irradiated by ^{137}Cs,

[60]Co and [226]Ra at specific angles to air kerma in Gy for this study.

Conversion coefficients have been published in ICRU (1998) for [137]Cs (1.20 at 0°, 1.16

at 45° and 0.91 at 90°) and [60]Co (1.16 at 0°, 1.15 at 45° and 0.95 at 90°) or ISO (1999)

for [137]Cs (1.21 at 0°, 1.22 at 45°) and [60]Co (1.15 at 0°, 1.16 at 45°). However, there

are no data available for conversion coefficients from air kerma, K_a to personal dose

equivalent $H_p(10)$ for radiation sources for the cylindrical phantom used for this

study. A comparison of the modelled data and published conversion coefficients was

made to validate the MCNP model used, even though they are different types of

phantom. It is found that there is good consistency between the modelled

conversion coefficient with the ICRP and the ISO conversion coefficients for [137]Cs

(i.e. at 0°, 45° and 90°) and [60]Co (i.e. at 0°, 45° and 90°). This gives confidence to the

calculation using MCNP for the cylindrical phantom for other radiation sources at

specific angles which have not been published.

Table 5-2: Conversion coefficient from air kerma to personal dose equivalent $H_p(10)$
for cylindrical phantom, as calculated using MCNP

Radiation quantity	$H_p(10)$ personal dose equivalent to air kerma in Sv Gy^{-1} for angle of incident radiation			
	0˚ ±SD	45˚ ±SD	90˚ ±SD	135˚ ±SD
[137]Cs	1.18 ±0.00	1.17 ±0.06	1.03 ±0.13	0.57 ±0.03
[60]Co	1.10 ±0.02	1.14 ±0.03	1.04 ±0.31	0.67 ±0.02
[226]Ra	n/a	1.14 ±0.01	n/a	n/a

5.3.2 Dose responses of dosimeter types

The dose response of TLDs, OSLDs, RPLDs and DISs within the aluminium box irradiated at 45° with a ^{137}Cs source between 0.30 and 1.00 mGy is presented in Figure 5-4 (a)-(d). Four dosimeter types showed linear dose response in the investigated dose range. The coefficient of variation (CV) of mean measured dose of all dosimeter types were between 1% and 22%.
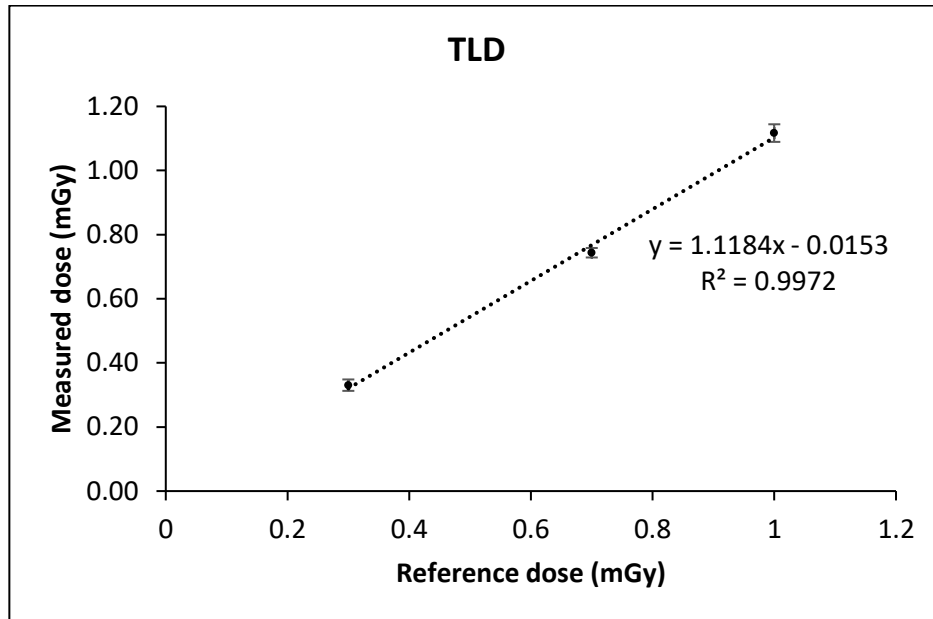
Figure 5-4 (a): Dose linearity of TLD to ^{137}Cs gamma radiation at 45 degrees
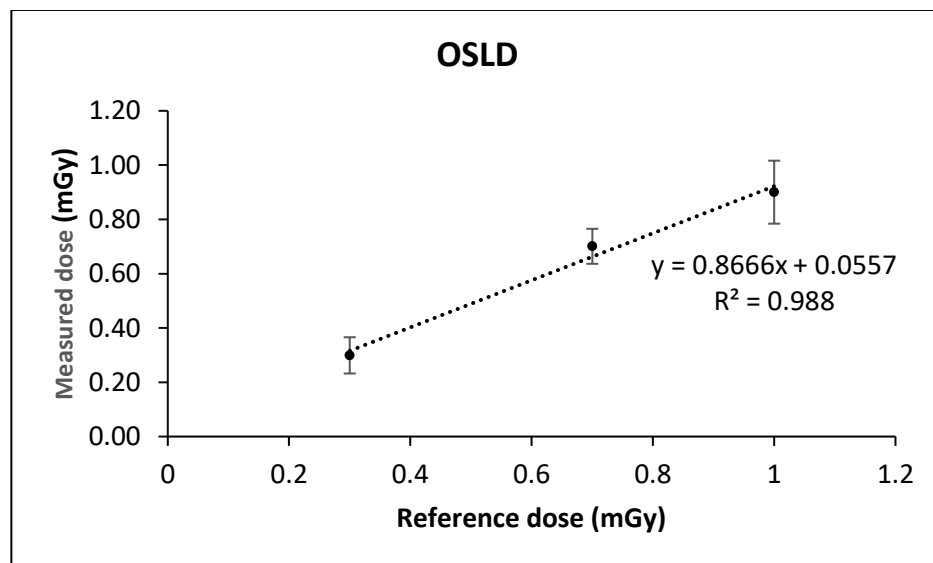
Figure 5-4 (b): Dose linearity of OSLD to ^{137}Cs gamma radiation at 45 degrees
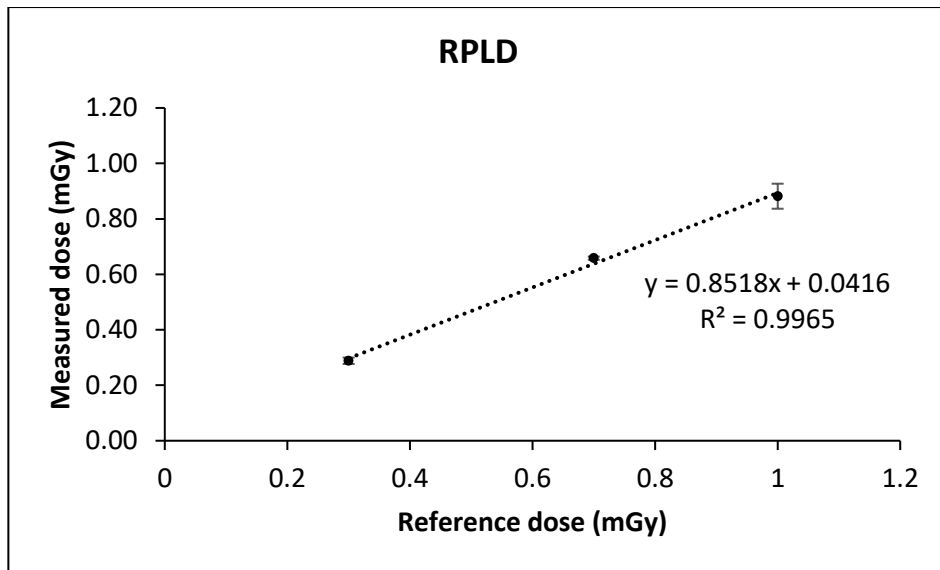
Figure 5-4 (c): Dose linearity of RPLD to ^{137}Cs gamma radiation at 45 degrees
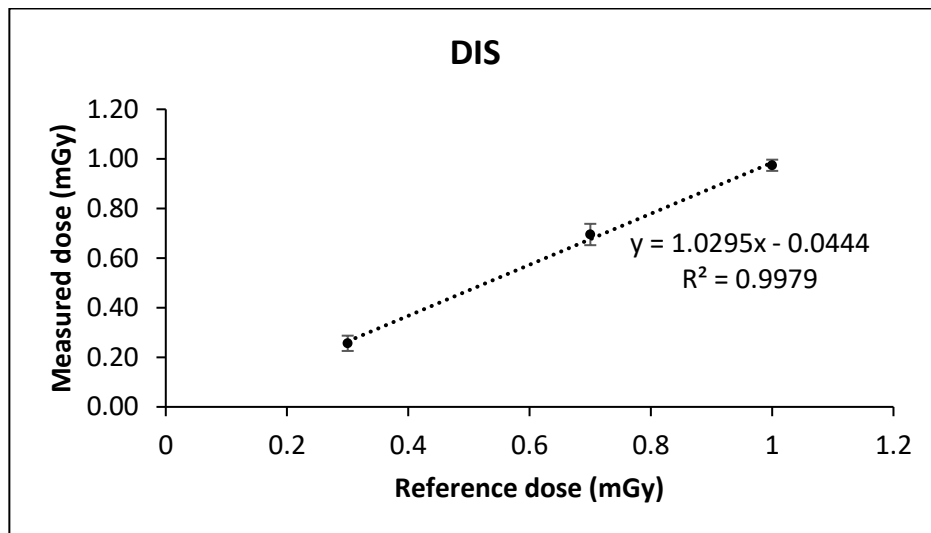
Figure 5-4 (d): Dose linearity of DIS to ^{137}Cs gamma radiation at 45 degrees

Relative energy dependence of response of the four dosimeter types in the aluminium box irradiated using [137]Cs ^{60}Co and [226]Ra with a dose of 0.7 mGy at 45° were compared and shown in Figure 5-5. The relative response ($R_{E,A}$), for the specific mean energy (E) and specific angle (A) is calculated (after ISO, 1999):

$$R_{E,A} = \frac{(D_{measured,E,A}/(H_p(10)/K_a))}{D_{reference,E,A}}$$

Where $D_{measured,E,A}$ is the personal dose equivalent $H_p(10)$ for a certain mean photon energy and angle in Sv, $H_p(10)/K_a$ is the reciprocal of the conversion coefficient from

air kerma to $H_p(10)$ from Table 5-2 and $D_{referenceE,A}$ is reference dose (0.7mGy) kerma free in air for the specified mean photon energy and angle.

The results for the four dosimeter types showed flat energy response for three energies of the radionuclides used in this study. The relative response of the dosimeter types was between 0.9 and 1.1 which is ±10%, and a CV value of measured doses was less than 9%.
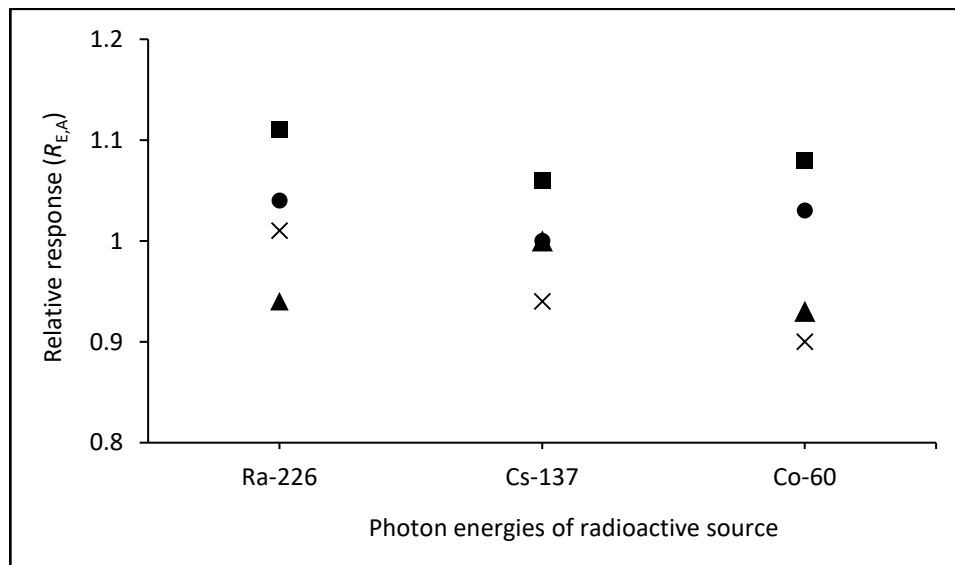
Figure 5-5: Energy dependence of TLD (■), DIS (●), OSLD (▲) and RPLD (X) in air relative to ^{226}Ra, ^{137}Cs and ^{60}Co (n=3, n=1 for RPLD of ^{60}Co at 45° and ^{226}Ra at 45°)

The comparison of angular response for the dosimeters for using ^{137}Cs (45˚, 90˚ and 135˚) and for ^{60}Co (45˚ and 135˚) are presented as Figure 5-6 (a)-(b). It is found that there was little angular dependence for the different dosimeter within the dosimeter box for the angles and radiation sources tested, with results within ±10%. The angular responses of OSLD to ^{137}Cs irradiation (at 90˚ and 135˚ relative to 45˚) and the TLD to ^{60}Co irradiation at 135˚ (relative to 45˚) were about 20%. Due to the limited number of available RPLDs, the RPLDs were only tested at a few mean energies and angles.

The results for the four dosimeter types in the dosimeter box irradiated with ^{90}Sr/^{90}Y with an absorbed dose of 3 mGy (0˚ and 90˚) showed that doses for all dosimeters were reported at background. This demonstrated that beta radiation does not

penetrate the dosimeter box sufficiently to produce a discernible dose on the enclosed dosimeters.
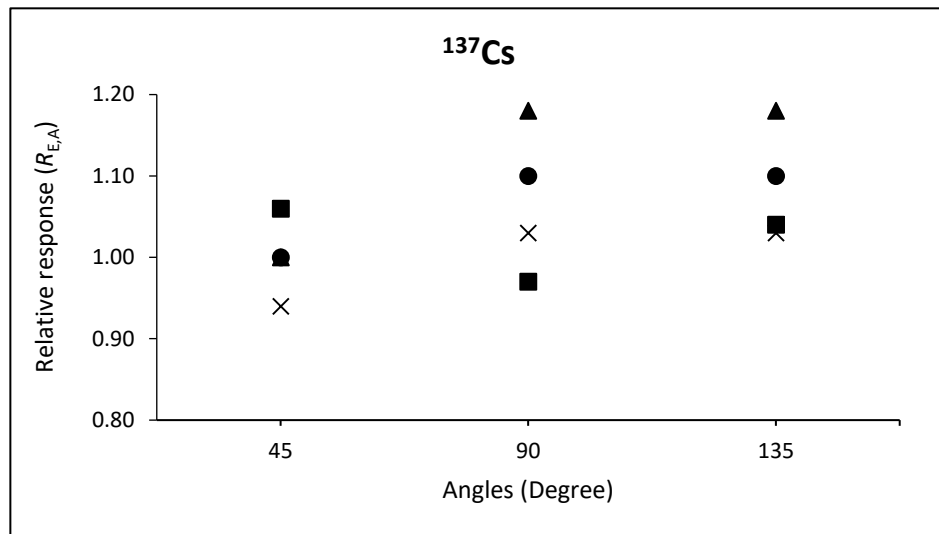
Figure 5-6 (a): Angular dependence of TLD (■), DIS (●), OSLD (▲) and RPLD (X) in air relative to ^{137}Cs
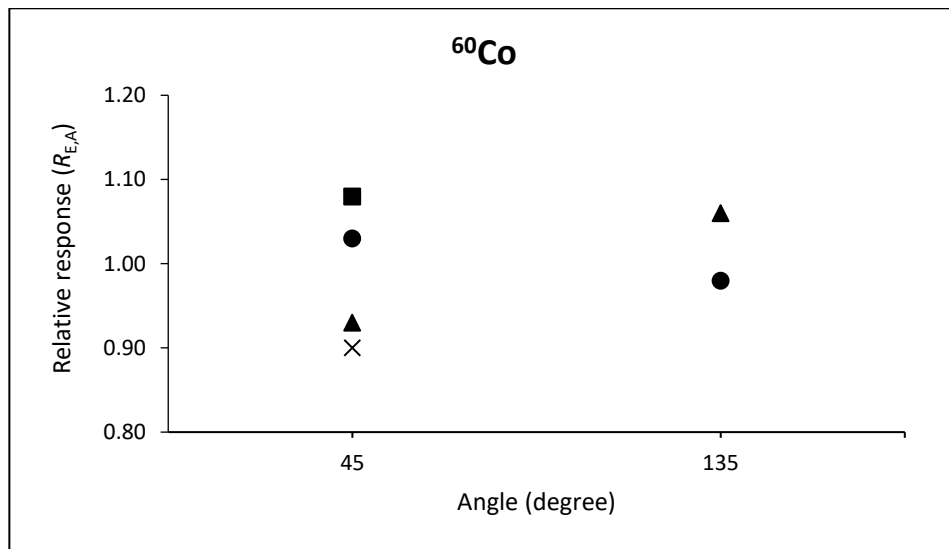
Figure 5-6 (b): Angular dependence of TLD (■), DIS (●), OSLD (▲) and RPLD (X) in air relative to ^{60}Co

5.3.3 External dose contribution from internal activity concentration of active phantom

The doses from the dosimeters inside the dosimeter box are presented in Table 5-3. The measured doses were between 0.34 and 0.42 mGy with a mean dose was 0.37

mGy (CV value of 9.7%). This compares well with the mean absorbed dose for the TLD badges placed outside and directly touching the phantom (see Figure 3). Four dosimeter types reported slightly lower external absorbed doses than the mean TLD badges on outside the phantom which were between 0.06 and 0.10 mGy. This is the indication that the results for all dosimeter types are reasonably consistent.

Table 5-3: The doses reported by the four dosimeter types within the dosimeter box from ^{137}Cs activity within the BOMAB leg phantom

Source	External absorbed dose of dosimeter types* (mGy)				
	TLD	DIS	OSLD	RPLD	Mean TLD badges on outside of phantom
[137]Cs contaminated in phantom	0.35	0.42	0.36	0.34	0.48

* Converted from Sv to Gy assuming a weighting factor of 1 (ICRU, 1993)

From this study, it has been found that the activity concentration of tissue-equivalent gel in the BOMAB upper leg phantom, containing [137]Cs 60 kBq, contributes a mean absorbed dose rate at the phantom surface of 0.29 μGy h[-1] measured by dosimeters in the aluminium box and 0.38 μGy h[-1] measured by TLD badges for 52 days and 1 hour (1249 hours). In addition, the dose rate per activity concentration of ^{137}Cs at 1 Bq in mass of gel (μGy h[-1] Bq[-1] kg) calculated from details of the active phantom and the dosimeter types was 0.028 nGy h[-1] as shown in Table 5-4. These are valuable data to estimate absorbed dose rates of large mammal species from radioactivity within the target animals from dosimeters placed in dosimetry boxes on collars around the necks of those animals.

Table 5-4: Dose rate per ^{137}Cs activity concentration at 1 Bq in mass of BOMAB active phantom

Gel of phantom			Activity concentration of gel (kBq)		Mean dose rate of dosimeters at phantom surface (μGy h[-1])	dose rate per activity concentration of ^{137}Cs at 1 Bq kg^{-1} in mass of gel (nGy h[-1] 1 Bq[-1] kg)
Volume (cm³)	Gel density (kg m^{-3})	Mass (kg)	Whole phantom	Phantom per kg		
5800	1000	5.8	60	10	0.29	0.028

5.4 CONCLUSION

Passive dosimeters can be used to directly measure absorbed doses of large mammal species in field applications. It is concluded that TLD, DIS, OSLD or RPLD can be used to measure external dose to large mammal species by placement in an aluminium box (the dosimeter box) before fitting on those species. The dosimeter box has dose linearity in the dose range between 0.3 and 1.0 mGy and significant flat angle dependence of response for the angles tested. The energy response for the dosimeters tested in the dosimeter box is also significantly flat for the radionuclides tested. The radionuclides tested in this study are those likely to occur in the environment (naturally occurring for ^{226}Ra, and from anthropogenic sources such as fallout or accidental release for ^{137}Cs and ^{60}Co). The angles tested also represent the range from which gamma radiation is likely to be incident on the dosimeter box, namely from the ground whilst the large animal is standing or grazing. The dosimeters in the aluminium box did not respond to beta radiation from outside of the box, so the shielding provided is larger than the ranges of the beta particles and no measurable bremsstrahlung was reaching the dosimeters. Doses were recorded for dosimeters within the dosimeter box when placed on the outside of a BOMAB upper leg phantom containing 60 kBq of ^{137}Cs. For field studies, doses contributed by internal activity concentration from within the large mammal therefore need to be taken into account.

The conversion coefficients calculated in this study can be used to convert from the personal dose equivalents $H_p(10)$ in Sv for dosimeters irradiated by ^{137}Cs, ^{60}Co and ^{226}Ra at specific degrees to air kerma in Gy if the dosimeter box is attached on the neck of large mammal species such as deer.

CHAPTER 6 mMEASURING THE RADIATION EXPOSURE OF NORWEGIAN REINDEER UNDER FIELD CONDITIONS

6.1 INTRODUCTION

Models and approaches have been developed to predict radiation exposure of wildlife for regulatory assessments (e.g. Johansen et al., 2012; Stark et al., 2015; Vives i Batlle et al., 2011; Vives i Batlle et al., 2016; Yankovich et al., 2010). Direct dosimetry measurements, using dosimeters attached to wildlife in the field, can be used to validate model predictions of external gamma dose rates. However, there have been few attempts to validate model predictions in this way (Beresford et al., 2008d), even though such validation would likely improve stakeholder confidence in modelling-based assessments.

Various dosimetry measurement technologies have the potential to be used in wildlife studies (Aramrun et al., 2018), but the deployment methodologies (e.g. collar mounting for large mammals) and dosimeter performances need to be tested under field conditions. Once the performance of different technologies for wildlife applications has been, their application will provide opportunities for testing of assessment model dose-predictions and enable field research on dose-effect relationships to be informed by accurate dose measurements.

Norway was one of European countries most affected by radioactive contamination from the 1986 Chernobyl accident, especially in the central Norway. Reindeer (*Rangifer tarandus tarandus*) populations in these areas have continuingly high levels of Ceasium-137 (^{137}Cs) in their tissues (Jakobsen, 2014). However, despite studies on potential biological effects of the fallout on the reindeer (e.g. Røed & Jacobsen, 1995), a total dose estimate for the reindeer including external exposure measurements have never been made. Gamma emitting from ^{137}Cs, natural radionuclides (e.g. potassium-40 (^{40}K)) and cosmic radiation are likely to be the main contributors of external doses to reindeer in Norway.

The ERICA (Environment Risk from Ionising Contaminants-Assessment and Management) Tool is a computerised model for estimating the exposure of wildlife to ionising radiation (Brown et al., 2016; Brown et al., 2008). It is now widely used to predict radiation exposure for wildlife in various situations (e.g. Brown et al., 2016; Černe et al., 2012; Kubota et al., 2015). The basic ERICA concept to calculate dose to wildlife can be divided into two steps: (i) the calculation of activity concentrations in animals (if not known) from environmental media (i.e. transfer) and (ii) the estimation of the dose rate to animals (i.e. dosimetry) (Brown et al., 2008). To give confidence in regulatory assessments, predictions of external absorbed dose rates of wildlife using the ERICA Tool and other assessment models need to be validated by direct measurement in field studies; to date this has only been conducted for small mammals like rodents in a study within the Chernobyl Exclusion Zone (Beresford et al., 2010; Beresford et al., 2008d).

Simple assumptions are generally made in assessments regarding animal movement, for instance, mean activity concentrations over an assumed home range may be used to estimate external (and internal) doses (e.g. Beresford et al., 2005) There is a need to test if this assumption is fit for purpose within framework of regulatory assessment. To test the assumption, it would be useful to have animals fitted with Global Positioning System (GPS) tracking units and dosimeters, together with a radionuclide (anthropogenic and natural) contamination surface and data on any other radiation types (e.g. cosmogenic) for the study area.

In this Chapter, I describe a study conducted to measure the external absorbed doses of reindeer from a herd in Oppland county (Norway) using four types of passive dosimeters (thermoluminescent dosimeter (TLD), optical stimulated luminescent dosimeter (OSLD), radiophotoluminescent dosimeter (RPLD) and direct ion storage (DIS) dosimeter). I estimate total external absorbed doses of reindeer using these four different dosimeter types and also absorbed doses from model predictions. I compare the total measured absorbed doses from each dosimeter type and model predictions.

6.2 MATERIALS AND METHODS

6.2.1 Study site

The study site was in Vågå, Oppland County in south central Norway; the site is part of a reindeer monitoring project (Skuterud et al., 2016). Oppland county is one of the areas of Norway with comparatively high levels of ^{137}Cs in soil as a consequence of deposition from the 1986 Chernobyl accident (Backe et al., 1986) (see Figure 6-1). The study area is grazed by a herd of semi-domesticated reindeer, owned by a non-Sami reindeer company, and the herd ranges over an area of approximately 1360 km^2 (Skuterud et al., 2005; Skuterud et al., 2016). The caesium deposition over approximately 50% of the study area was greater than 15 kBq m^{-2}; maximum concentrations of 50 to 70 kBq m^{-2} occurred in an area of approximately 100 km^2 (Baranwal et al., 2011). Since 2011 the Vågå herders have fitted fifteen reindeer with collars onto which Global Positioning System (GPS) units (Telespor AS, Tromsø, Norway) are attached. These GPS units report online, and are practical tools for the herders to follow the movements of their animals. The Norwegian Radiation Protection Authority (NRPA) has been provided access to the data from this system, and the movements of the herd are used together with an aerial survey of the ^{137}Cs deposition in the area to estimate ^{137}Cs activity concentrations in plants and lichens over the pasture land based on the ^{137}Cs deposition values and concentration of plant and lichen species in the area (Skuterud et al., 2016).

Monthly average temperatures recorded at a weather station located at the eastern edge of the study area range from approximately -14°C to 12°C with minimum and maximum daily temperatures of -40°C to 25°C. Monthly precipitation ranges from 0 to 77 mm.
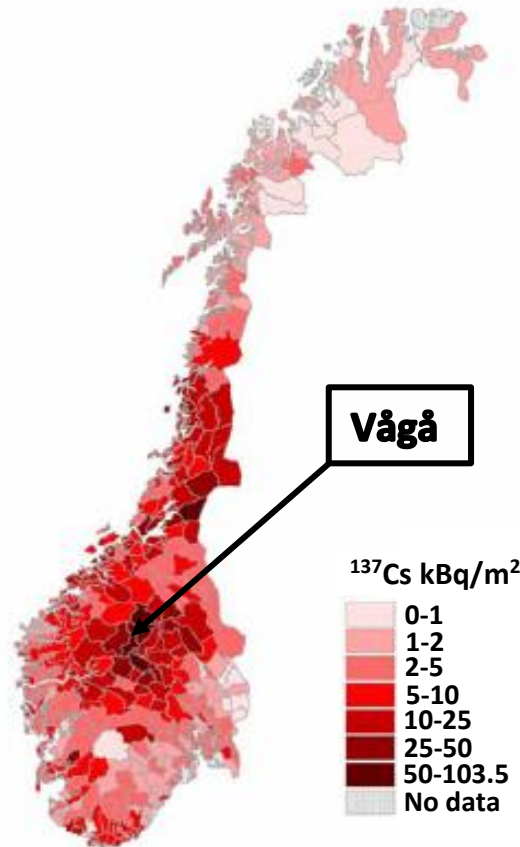
Figure 6-1: Average radioactive ^{137}Cs activity deposition in Norwegian soil in 1986 (Nowegian Radiation Protection Authority, 2006)

6.2.2 Dosimeters for external dose measurement of reindeer

Four types of dosimeter were chosen for this study based on the our earlier assessment of potential dosimeters for field application (CHAPTER 4; Aramrun et al., 2018): thermoluminescent dosimeter (TLD) (LiF:Mg,Cu,P; standard Harshaw[TM] type, (Gilvin et al., 2007) generally used for personal monitoring and supplied by Public Health England (PHE), Oxford, UK); optical stimulated luminescent dosimeter (OSLD) (Al_2O_3:C; Nagase Laddauer, Ibaraki, Japan); radiophotoluminescent dosimeter (RPLD) in waterproof plastic capsules (GD-352M; AGC Techno Glass Corporation, Shizuoka, Japan); direct ion storage (DIS) dosimeter (Instadose+; Mirion Technologies, California, USA). The dosimeters would have to contend with extreme weather (e.g. snow, rain and low temperatures), reindeer behaviour and radionuclides emitting beta radiation (in addition to the gamma radiation I wanted to estimate) and hence required appropriate housing. An aluminium box (IP68 Deltron, 480 Series Diecast

Aluminium Boxes) was chosen to house the four dosimeters because it was durable, waterproof and provided shielding of beta radiation. The four dosimeters were mounted securely within the box in a consistent geometric relationship (Section 5.2.1). All dosimeter types in the aluminium box were calibrated with ^{137}Cs, ^{60}Co and ^{226}Ra sources to test the linearity of energy responses (over the range of doses estimated in the field for 11 months using data of ^{137}Cs depositions and natural radionuclide activity concentrations from Baranwal et al. (2011)), angular dependence at relatively different angles and flat energy response between ^{137}Cs and ^{60}Co. It was confirmed that energy responses, angular dependence and flat energy response do not affect the doses estimated by the four dosimeter types when exposed to radiation under laboratory conditions (Section 5.2.2).

TLDs, OSLDs and RPLDs recorded accumulated external dose over the study period. The Instadose+ dosimeters were set to record and store doses over 4 hours 48-minute periods (i.e. five measurement periods each day) by the manufacturer (Mirion Technologies). The dose measurements recorded by the Instadose+ were stored by the unit. The DIS unit also recorded total doses over the period of the deployment, which could be read once the Instadose+ was recovered.

The individual components were transported from the UK, and the boxes assembled on arrival in Norway. The dosimeters were carried in hand luggage and declared at airport security checkpoints so that they were not passed through X-ray machines. Three sets of dosimeters were used as controls to measure transit doses to and from Norway. The transit doses were subtracted from results of the dosimeters used in Norway.

6.2.3 Mounting the dosimeter box on the reindeer GPS collar

The reindeer GPS collars were standard livestock collars (OS ID, Oslo, Norway) (Figure 6-2). A collar had a total weight of 490 g which comprised the collar itself, a GPS unit and counterweights. It was essential to ensure that the mounting of dosimeter boxes on the collars would not significantly affect the weight balance of the collar or the daily life of the reindeer. The dosimeter box was fitted onto the side of the collar opposite to the buckle (Figure 6-2); mounting at this point minimised

deformation of the collar curvature as this is the flattest part of the reindeer neck. The total mass of the dosimeter box was approximately 150 g, which the Vågå herders were confident that it would not affect the shape or balance of the collar.

A dosimeter box mounted on a collar was calibrated at the Public Health England (PHE) calibration facilities. Experiments were performed to establish the influence of various factors on the dosimeter response including energy, absolute dose, dosimeter orientation relative to source and contribution of radionuclides in deer body to the dosimeters (CHAPTER 5).

Figure 6-2: A dosimeter box attached onto a reindeer GPS collar and counterweights

6.2.4 Field application of the dosimeters

The herd, which is about 2000 animals, was gathered in January 2016 so that some reindeer could be slaughtered for human consumption. The fifteen reindeer with GPS collars were measured to determine ^{137}Cs activity concentration using a NaI live-monitor (Skuterud, 2012, 2017). When a collar was removed from a reindeer for battery replacement, the dosimeter box was mounted on it before the collar was refitted to the reindeer.

Dosimeter boxes were mounted on the GPS collars of fifteen reindeers. A dosimeter box was mounted on a collar within 3-4 minutes to avoid unnecessary stress to the reindeer. A video of fitting dosimeter boxes onto collars is available at https://youtu.be/gyW7ty_Zxns.

Dosimeter boxes were recovered when the animals were regathered in December 2016. The animals were again live-monitored in December 2016 and the dosimeters then removed from the boxes. During transport back to the UK, dosimeters were again declared at the airport security check points to avoid them being X-rayed. The luminescent dosimeters and the control dosimeters were sent to one of three laboratories for analyses: TLDs to PHE (UK); OSLDs to Thailand Institute Nuclear Technology (TINT) (Thailand); RPLDs to the Ruđer Bošković Institute (RBI) (Croatia). For the Instadose+, the dosimeters were sent to Mirion technologies to obtain the doses stored on the devices throughout the measurement period.

6.2.5 Contribution to the dosimeter reading from internal contamination of reindeer

It is suggested that internally incorporated ^{137}Cs of large mammal species need to be considered when dosimeters are fitted on those animals (e.g. on their necks) for direct external dose measurements in the field (CHAPTER 5 Section 5.4). This is because the internally incorporated ^{137}Cs will contribute to the dose recorded by the dosimeters which is 0.028 nGy h^{-1} per Bq kg^{-1}. Therefore, we estimated this contribution for reindeer in this study using a coefficient (i.e. 0.028 nGy h^{-1} per Bq kg^{-1}) relating dose recorded by externally attached dosimeters to the internal activity concentration in a phantom, containing ^{137}Cs, representing a large mammal determined in controlled laboratory studies (Section 5.2.3) and the results of the live-monitoring described above. For each reindeer the average estimate from the January and December 2016 live-monitoring were used for this calculation.

6.2.6 Prediction of average external absorbed dose for the reindeer herd

For the purposes of estimating external dose rates a 'herd area' was defined, this was the 1360 km^2 bounded by the known grazing area of the reindeer as determined by the GPS co-ordinates for the collared animals. The average ^{137}Cs activity deposition, potassium (K) in % by weight, uranium (U) and thorium (Th) in ppm concentrations (Baranwal et al., 2011) over the herd area were calculated by a GIS (ARCGIS Version 10.3) and converted to average activity concentrations in Bq kg^{-1} of [137]Cs (assuming a soil depth of 6 cm and a soil density at 1600 kg/m^3 for ^{137}Cs), [40]K (using 313 bq kg^{-1} per 1% of [40]K), Uranium-238 ([238]U) (using 0.081 ppm per 1 bq kg^{-1}) and Thorium-232 ([232]Th) (using 0.246 ppm per 1 bq kg^{-1}). The activity concentrations of [238]U, [232]Th and [40]K were required to estimate external absorbed dose of reindeer from natural radionuclides in soil. The estimated activity concentrations in soil were input into Tier 2 of the ERICA Tool using the tools large mammal geometry (a deer) to predict external absorbed dose rates of the reindeer herd assuming the herd roamed equally everywhere in the study site. Uranuium-238 and [232]Th series radionuclides with physical half-lives greater than ten days were assumed to be in equilibrium with the series parent (e.g. [226]Ra was assumed to have the same soil activity concentration as [238]U); daughter radionuclides with a half-life of less than ten days are included in their immediate parents for dose conversion coefficient (Brown et al., 2008). The total mean external absorbed dose of the reindeer herd from ^{137}Cs and natural radionuclides was estimated over 11 months (the length of time over which dosimeters were deployed).

Cosmic radiation will also likely contribute to the dose recorded by the dosimeters. The mean altitude in the study site (data from the U.S. Geological Survey (USGS), https://earthexplorer.usgs.gov/) was calculated using the GIS and input into Equation 1 to estimate mean annual absorbed dose of the reindeer herd due to cosmic radiation ($\dot{E}_1(z)$) (Cinelli et al., 2017):

$$\dot{E}_1(z) = \dot{E}_1(0)[0.21e^{-1.649z} + 0.79e^{0.4528z}] \qquad (1)$$

Where z is the altitude in km; $\dot{E}_1(0)$ is annual dose at sea level, 240 µGy (converted from Sv to Gy assuming a weighting factor of 1). The calculated absorbed doses from cosmic radiation were correct from an annual dose to an 11-month dose and included in total predicted doses of the reindeer.

6.2.7 Estimation of external absorbed dose of individual reindeer using GPS tracking data

The GPS tracking data of the 12 reindeer between 11th January 2016 and 11th December 2016 were input to a GIS to estimate the time weighted mean ^{137}Cs activity deposition and ^{40}K, ^{238}U and ^{232}Th concentrations in soil for each individual collared reindeer. These activity concentrations were then used to estimate the average external absorbed doses of individual reindeer by applying the external beta-gamma dose conversion coefficients for the large mammal geometry extracted from the ERICA Tool.

Cosmic radiation exposures at ground level of individual reindeer were also estimated using the GPS tracking data and Equation 1; the mean altitude estimated for each reindeer was used in this calculation.

6.2.8 Statistical analyses

The external absorbed doses of individual collared reindeer estimated by different passive dosimeter types and model prediction using GPS tracking data were compared using a repeated one-way ANOVA in SPSS v23. Prior to analysis, normality of the data was tested with Kolmogorov-Smirnov tests. One-tailed t-tests were conducted to determine the comparison between the external doses of the collared reindeer (estimated by dosimeter types and the GPD tracking data) and the mean external dose of the reindeer herd. This is because the repeated one-way ANOVA could not be used to analyse the comparison between the mean external dose of the reindeer herd (i.e. one data) and the external doses of collared reindeer (i.e. twelve data for each dosimeter types and GPS tracking approaches) due to different number of data.

6.3 RESULTS

6.3.1 Physical condition of dosimeters after collection

In December 2016, after a study period of 11 months, 12 dosimeter boxes of the 15 fitted were recovered which was 80 % of recovery rate. The dosimeters were all in good physical condition and there was no water or dust ingress into the boxes. Two reindeer that had been fitted with dosimeters were within the gathered group, but had lost their collars. The remaining collared reindeer was not within the herd that was gathered in December 2016.

6.3.2 External absorbed doses measured in the field

The estimated external absorbed doses of the twelve reindeer from the four different dosimeters are shown in Table 6-1. The external absorbed doses (Gy) was assumed to be the same as the dose equivalent for the whole body as reported for the dosimeters (Sv); this was justified on the basis of the conversion coefficient of ^{137}Cs at 45˚ from personal dose equivalent Hp (10) to air kerma, k_a in Gy Sv^{-1} as described in Section 5.2.4 and from air kerma, k_a to average absorbed dose described by Ulanovsky (2014). The accumulated doses recorded across all dosimeter types ranged from 480 to 825 µGy (Table 6-1). The values presented in Table 6-1 are corrected for contributions from the transit dose of each dosimeter types (i.e. an estimated dose from an original place when dosimeters are prepared to a final place when dosimeters are reading out using controlled dosimeters) and internally incorporated ^{137}Cs to give the absorbed doses to the reindeer for external sources (APPENDIX 1 Table A-1). For individual reindeer, the maximum difference between the estimates using different dosimeters was a factor of 1.3 with a coefficient of variation of the four dosimeter measurements less than 15%.
For the Instadose+, data were only available for nine reindeer as three of the units failed. For all nine-remaining unit, the batteries expired before the Instadose+ were collected and hence a full-time series of data was not recorded. It is likely that the batteries expired due to the cold weather. However, it was possible to recover a

total integrated dose from the nine dosimeters as this is recorded by the Instadose units without the requirement for a battery; these data are presented in Table 6-1.

Table 6-1: Estimated external absorbed doses for Norwegian reindeer over 11 months using different dosimeter types (note the dosimeter result presented has been correct for transit dose and the contribution of internally incorporated ^{137}Cs to the dosimeter reading)

Reindeer Name	TLD (μGy)	OSL (μGy)	RPLD (μGy)	DIS (μGy)	Mean	SD	%CV
Linn	760	820	600	651	708	100	14.2%
Ragnhild	735	825	615	625	700	99	14.2%
Trinerein	707	717	607	567	650	74	11.4%
Prikka	666	546	556	536	576	61	10.5%
Sigrid Mathilda	685	595	715	n/a	665*	62*	9.4%*
Rinda	620	630	480	n/a	576*	84*	14.6%*
Krone	710	670	580	530	622	82	13.2%
Guri	798	798	618	n/a	738*	104*	14.1%*
Frigg	736	816	686	716	739	56	7.5%
Martine EK	713	723	593	733	690	66	9.5%
Kari	726	806	716	740	747	41	5.4%
Torild	671	651	641	611	643	25	3.9%

n/a – not available   *The summary values were calculated from TLD, OSLD and RPLD only

6.3.3 Mean predicted external absorbed dose for the reindeer herd

The mean predicted external absorbed doses for the Vågå reindeer herd from ^{137}Cs, [40]K, [238]U and [232]Th were calculated over an 11-month period using average activity soil concentrations over the whole grazing area as calculated using a GIS and the subsequent external dose rate predicted by the ERICA Tool. The total estimated mean external absorbed dose of the reindeer herd based on these radionuclides and cosmic radiation was 471 μGy with standard deviation (SD) of 104 (Table 6-2): the mean predicted external absorbed doses of radionuclides for the reindeer herd were also presented in APPENDIX 1. The mean total external absorbed doses of the reindeer over 11 months from the ^{137}Cs and natural radionuclides in soil was estimated to be 174 μGy, with ^{137}Cs contributing most to this. The mean annual cosmic radiation in the reindeer herd habitat was estimated to be 297 μGy (SD=40)

which is about 50% of the total absorbed dose; this is relatively higher than those of the dose predicted from the ^{137}Cs and natural radionuclides in soil as the altitude above sea level of the site is ~ 1100 meters.

Table 6-2: Predicted mean absorbed doses for the herd over eleven months from external sources

Radionuclide	External dose over 11 months (µGy)	SD
^{137}Cs	103	93
^{40}K	47	19
^{232}Th	9	6
^{238}U	15	9
Cosmic radiation	297	40
Total mean external absorbed dose	**471**	**104**

6.3.4 External absorbed doses of individual reindeer from reindeer GPS tracking points

Using the reindeer GPS tracking points to estimate the external dose to each reindeer from ^{137}Cs and natural radionuclide activity concentrations in soil and cosmic radiation, the estimated external absorbed doses of the twelve reindeer over 11 months were between 554 and 601 µGy (Figure 6-3). ^{137}Cs is the dominated radionuclide in the herd area contributing to absorbed external dose of the reindeer (though cosmic radiation is the biggest single contributor). Collared reindeer mostly stayed in the area with the highest ^{137}Cs activity concentrations in soil (Figure 6-4 (a)) this resulted in the average external doses of the twelve reindeer from ^{137}Cs activity concentrations (195 µGy) in soil being about twice as high as the herd average presented in Table 6-2. For natural radionuclides (i.e. ^{40}K, ^{238}U and ^{232}Th) in soil (Figure 6-4 (b)-(d)), ^{40}K is the largest contributor to external dose (50-60 µGy). Estimated external doses of individual reindeer from all-natural radionuclides (between 73 and 83 µGy) considered here were about 12-14 % of the total estimated absorbed dose. As for the herd average, cosmic radiation is the main contributor to external absorbed dose of the collared reindeer. Figure 6-4 (e)

demonstrates that the reindeer were in the areas of high altitude (>1000 meters). The average absorbed dose of the twelve-reindeer estimated from cosmic radiation was about 310 µGy (~50% of total estimated dose) which is relatively similar to the cosmic radiation predicted for the reindeer herd habitat.
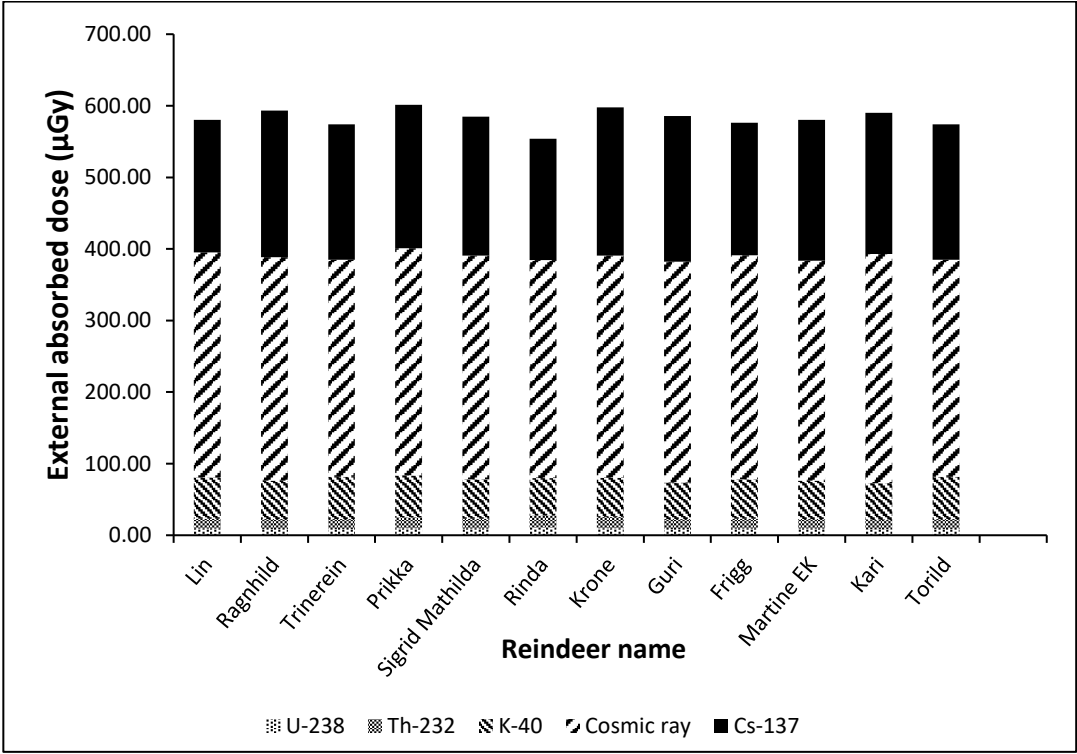
Figure 6-3: External doses of twelve Norwegian reindeers over 11 months calculated using the radionuclide activity concentrations in soil and GPS tracking units
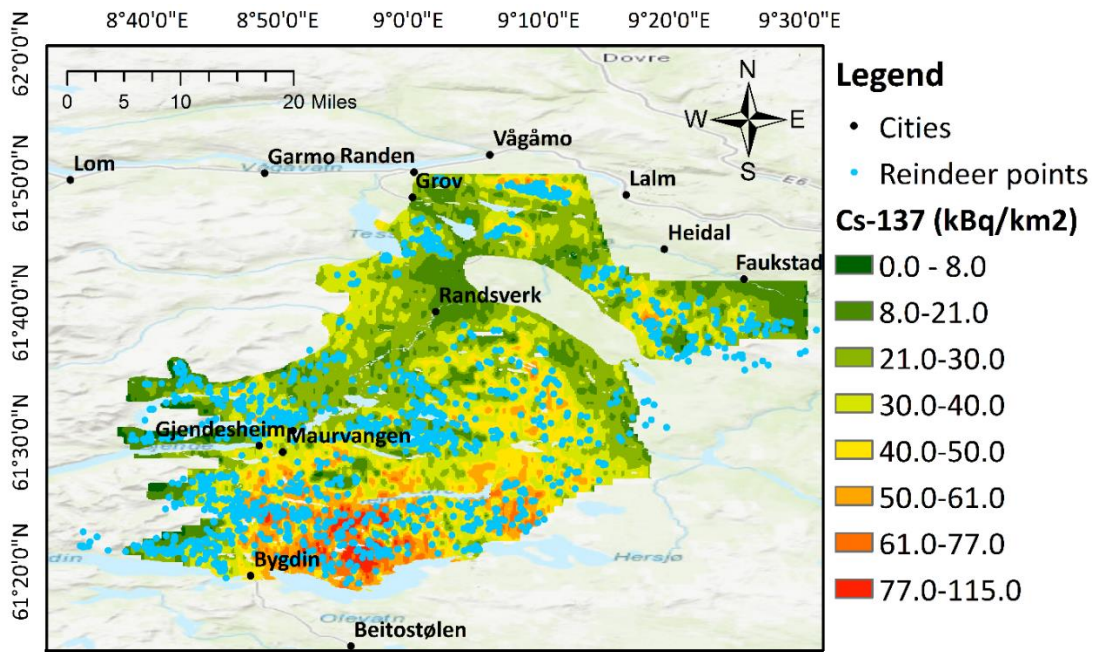
Figure 6-4 (a): GPS tracking locations over 11 months of an example (and typical) reindeer (Frigg) overlaid on ^{137}Cs activity deposition (sources of based map: the GIS base map: Esri, HERE, Delorme, Intermap, increment P Corp., GEBCO, USGS, FAO, NPS, NRCAN, GeoBase, IGN, Kadaster NL, Ordnance Survey, METI, swisstopo, MapmyIndia, OpenStreetMap contributors and the GIS Use community)
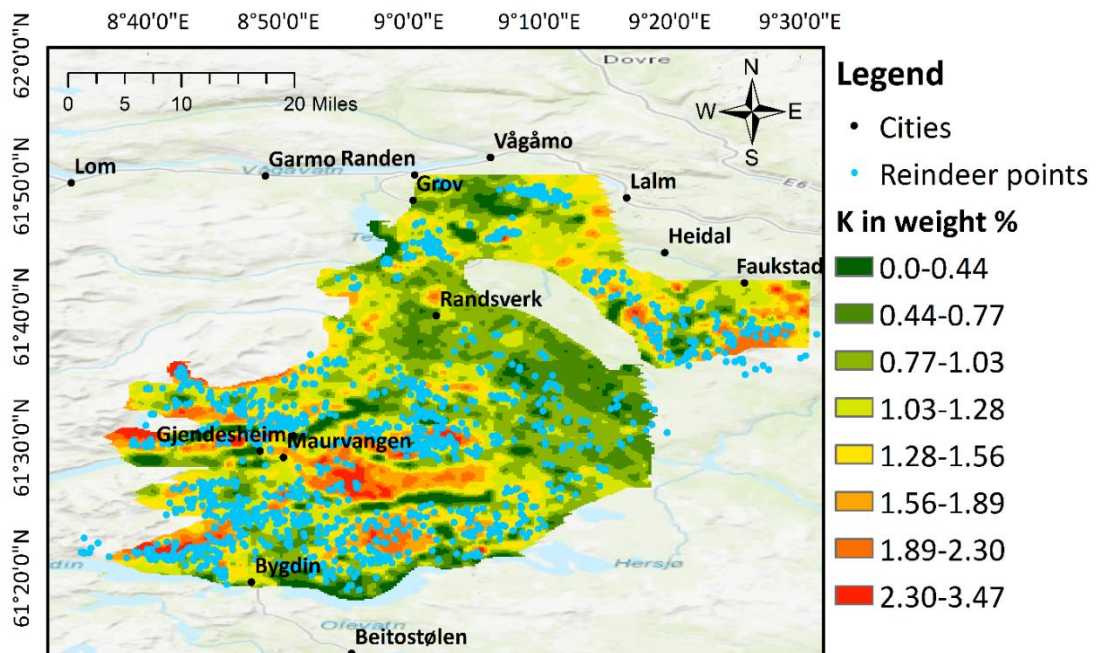
Figure 6-4 (b): GPS tracking locations over 11 months of an example (and typical) reindeer (Frigg) overlaid on soil K concentrations
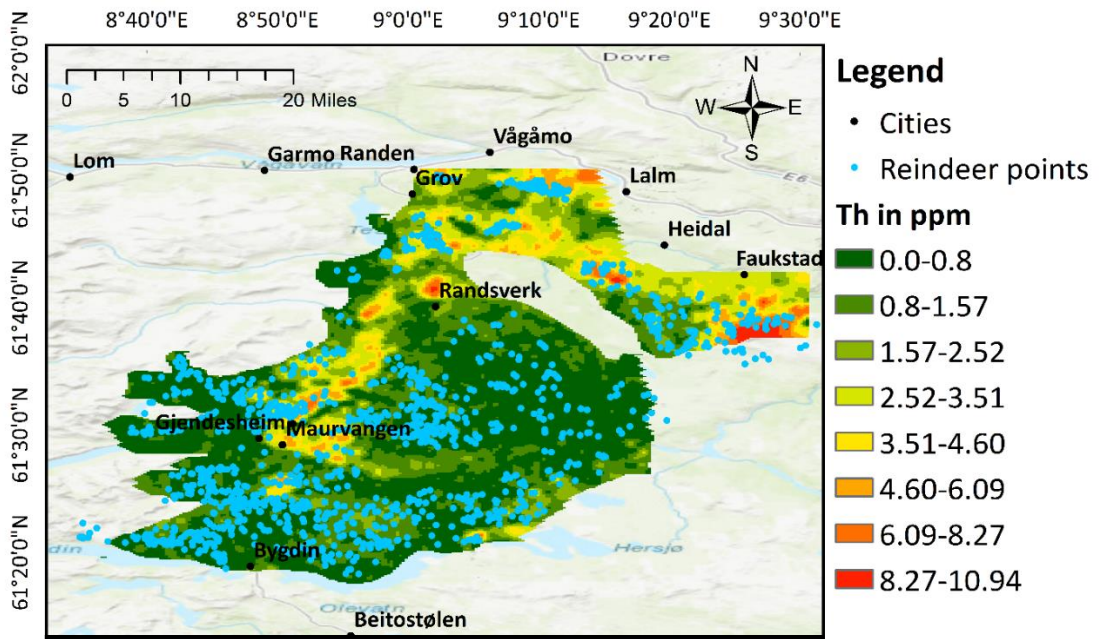
Figure 6-4 (c): GPS tracking locations over 11 months of an example (and typical) reindeer (Frigg) overlaid on soil Th concentrations
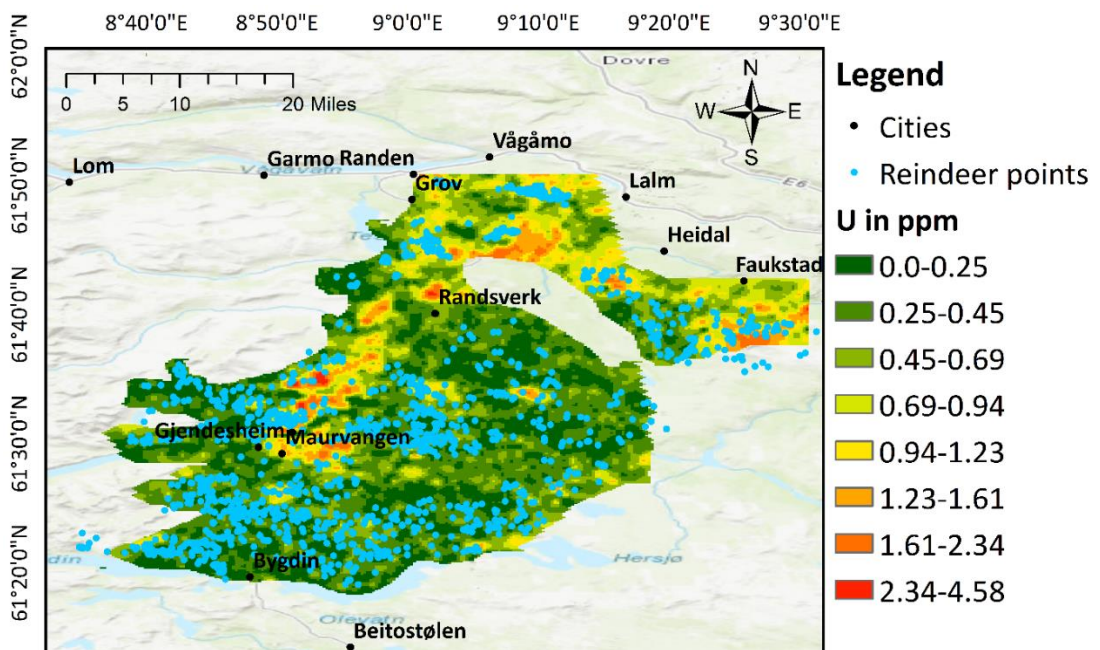
Figure 6-4 (d): GPS tracking locations over 11 months of an example (and typical) reindeer (Frigg) overlaid on soil U concentrations
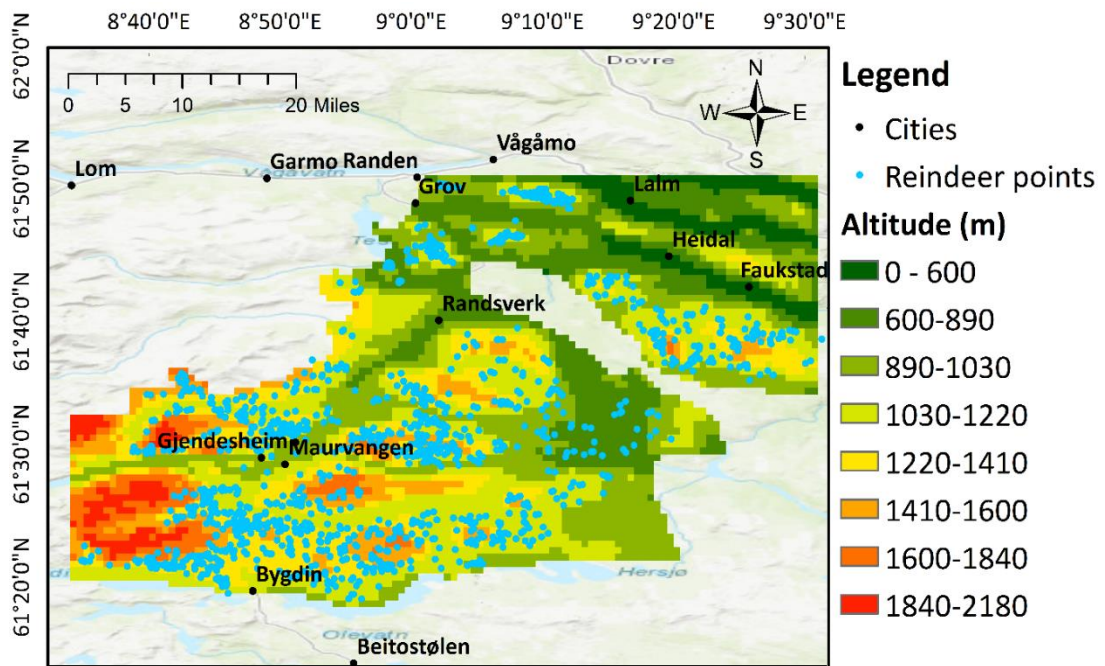
Figure 6-4 (e): GPS tracking locations over 11 months of an example (and typical) reindeer (Frigg) overlaid on altitude

6.3.5 Comparison of model predicted dose and direct dosimeter measurements

Kolmogorov-Smirnov tests showed that the data were normally distributed (P = 0.20). Repeated one-way ANOVA indicated initial significant differences in external dose measured between the different dosimeters and the GPS tracking model ($F_{1,8}$ = 1985, P < 0.001). A comparison of mean external doses estimates using the different dosimeters and the mean predicted individual dose using GPS co-ordinates are shown in Figure 6-5. The data for three reindeer (i.e. Sigrid Mathilda, Rinda and Guri) were removed prior to analysis because the DIS (Instadose+) data could not be retrieved. Bonferroni-corrected pairwise comparisons indicate that while the external dose measured by TLD did not differ significantly with OSLD (p=1.00) and DIS (P = 0.10), but higher than the external doses measured by RPLD (P < 0.05). The estimated dose from OSLD were significantly higher than doses estimated by RPLD and DIS (P < 0.05). The RPLD measurements were not significantly different from DIS measurements (P = 1.00). The GPS tracking predictions were not significantly different (P > 0.05) from the values recorded by RPLD (P=1.00) and DIS (P = 0.86) but

significantly lower than the external doses measured by TLD and OSLD (P < 0.05). One-tailed Student's t-tests showed that the external doses of all dosimeter types and the GPS tracking predictions estimated for the collared reindeer were significantly higher than average external dose predicted for the reindeer herd (Table 6-3).
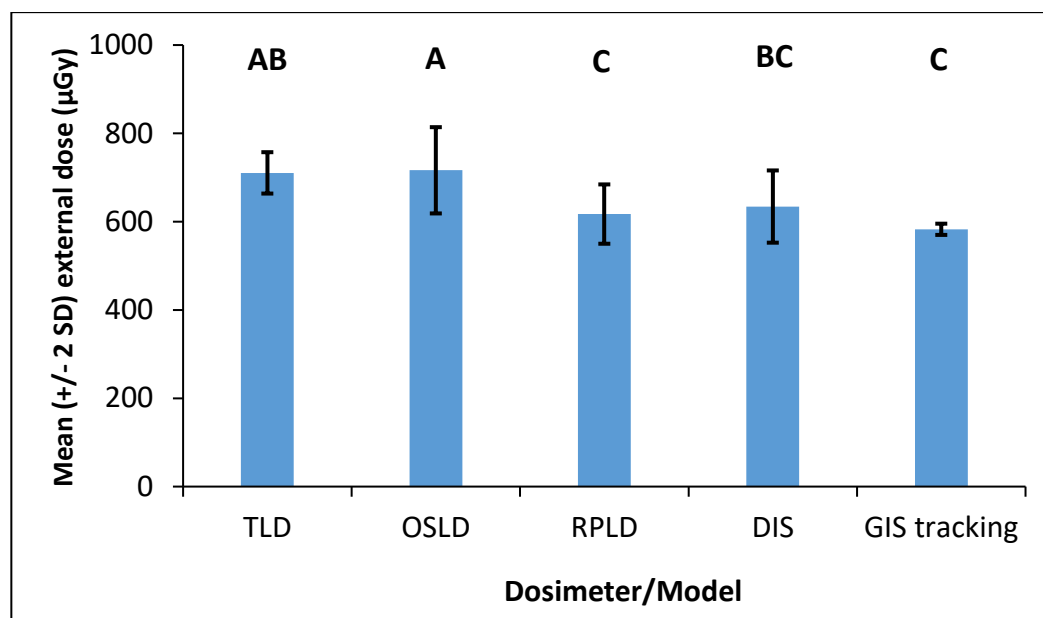
Figure 6-5: Mean (± 2 SD) external dose of nine reindeer estimated by four dosimeter types and modelled based on GPS tracking data (estimates with the same letter are not significantly different (P>0.05))

Table 6-3: Results of one-tailed t-tests comparing the average dose predicted for the reindeer herd (mean 471±104 µGy) with the external doses of reindeer measured by dosimeters or modelled using GPS tracking data

	TLD	OSLD	RPLD	DIS	GPS tracking
Dose (µGy)					
Mean	710	716	617	634	583
SD	47	98	67	82	13
Number	12	12	12	9	12
t	17.247	8.708	7.547	4.528	30.395
P (one-tailed)	< 0.001	< 0.001	<0.001	<0.001	<0.001

6.4 DISCUSSION

External absorbed dose to reindeer in Vågå were measured over 11 months using a variety of dosimeters. This is the first attempt to conduct comparatively long-term dose measurements of large mammals in the field. The method, using an aluminium enclosure housed passive dosimeters before fitting on animal collars, was successful. The passive dosimeters (i.e. TLDs, OSLDs, and RPLDs) within the aluminium box could record accumulated doses for the collared reindeer under relatively extreme (e.g. cold and snow) field conditions.

For an individual reindeer, the variation across the four different dosimeters was less than a factor of 1.3 (ratio of highest and lowest estimated doses).

Whilst there was a significant difference between the estimates of dosimeters, (i.e. TLDs versus RPLDs; OSLDs versus RPLDs and DIS) the difference of the mean doses between maximum and minimum values was <14 % which is trivial compared to other uncertainties in environmental radiological assessments (e.g. Beresford et al., 2008a). Therefore, it is likely that all four dosimeters will give similar results of integrated dose for relatively long-term (i.e. 1 year) dose measurements of large mammal species under field conditions (excepting the issues of extreme cold on the Instadose+ performance). The smaller dosimeters (i.e. TLD, RPLD and OSLD) could also be used with smaller animals providing suitable housing and mounting could be designed (Aramrun et al., 2018).

For application to animals of different sizes consideration would need to be given using the dose conversion coefficient (DCC) for the study animals to 'correcting' the reported dose rate recorded by attached dosimeters such that they were applicable to the study organism (the external DCC increases as organism size decreases (e.g. see values presented in Vives i Batlle et al., 2007; Vives i Batlle et al., 2011)). (Ulanovsky (2014)) also presents relationships which should help in this.

In this study, the reindeer herd lived in the winter season with snow covers up to 100 cm in the study side which was about 4 months. This is a cause of gamma attenuation from radionuclide activity concentrations at ground to dosimeter boxes on collared reindeer in the winter time that causes lower dose estimates then other

seasons from the dosimeter reading (Offenbacher & Colbeck, 1991). However, the ERICA tool predicts external doses to animals without consideration of gamma attenuation in the areas having snow covers. Therefore, it is suggested that the ERICA tool underestimates external dose from both anthropogenic and natural radionuclides to the reindeer herd in this study having the snow covers in winter. To compare modelled dose estimates with dosimeter readings we could not only consider the estimated dose from the anthropogenic radionuclide (i.e. ^{137}Cs). We also had to consider the contribution of natural background radionuclides and cosmic exposure. In this mountain habitat cosmic radiation was the dominant source of exposure for the reindeer because of the altitude. At more highly contaminated sites there may not be a need to consider cosmic radiation or natural radionuclides because the proportion of external doses predicted from activity concentrations of the anthropogenic radionuclide in soil are largely higher than the cosmic radiation. For instance, Beresford et al. (2008d) found relatively good agreement between external doses estimated from TLDs attached to small 'mouse like' mammals and predicted doses based upon soil ^{137}Cs activity concentrations which ranged from *c*. 7 to 100 kBq kg^{-1} dry mass across three study sites in the Chernobyl exclusion zone. Mean estimated and measured external absorbed dose rates at these sites ranged from *c*. 2 to 70 µGy h^{-1} and hence the contribution of cosmic radiation or natural background was unimportant. However, if dosimeters were used in compliance monitoring areas or low contaminated areas giving the estimated dose from the anthropogenic radionuclides lower than the cosmic radiation in those areas, then the contributions of cosmic and background radiation would need to be considered. In interpreting the dosimeter results we also had to consider the contribution of ^{137}Cs internally incorporated in the reindeer to the reading on the dosimeters attached to their necks. The estimated contribution of internally incorporated ^{137}Cs to the dosimeter reading (e.g. 157±27 µGy for the herd average estimate) was similar to the external dose estimated from all of the soil radionuclides considered. Therefore, in any future studies it would be important to estimate the contribution of internally incorporated ^{137}Cs to the dosimeter results to be able to best interpret them. The coefficient we used to relate internal ^{137}Cs contamination to the contribution to the dosimeter reading (i.e. 0.028 nGy per Bq kg^{-1}; CHAPTER 5) would

be applicable to other mammal of a similar size (e.g. wild boar or wolves). However, it could not be used for smaller animals for which the contribution of internal contamination to the dosimeter would be less. For the contribution of internally incorporated ^{40}K, it was presented by Beresford et al. (2008c) that the mean ^{40}K activity concentration in all mammals was about 100 bq kg^{-1} which is less contribution to dosimeters fitted on animal body. The ^{40}K also have high energy which is less contribution to dosimeters or biological tissues comparing with ^{137}Cs. Therefore, the ^{40}K is not necessary to consider for the contribution of internally incorporated radionuclides to dosimeters attached on animals.

When considering the modelled ^{137}Cs external dose estimates, those calculated using the GPS tracking locations for the reindeer were approximately twice the ^{137}Cs dose estimated as the herd average, assuming the reindeer grazed equally over the area. This was because the reindeer favoured the more contaminated areas (i.e. the geographical central areas) which were good grazing in several seasons for those reindeer, which highlights the benefit of understanding where in a study/assessment area animal actually spend their time. A typical assessment would adopt the approach used here to determine the herd average external absorbed dose rate and hence in this example would underestimate exposure of reindeer. For smaller mammals (mice and vole species), (Beresford et al. (2008d)) previously found that using an average of the assumed home range gave reasonable agreement with estimates from attached TLDs which cannot be applied to consider for this study. The results of this study have shown that average external dose predictions to animals using their home range may not appropriate in some circumstances where those animals spend their time in specific areas.

There is considerable debate about the interpretation of studies considering the effects of radiation on wildlife (e.g. Beresford et al., in press 2018). One criticism of a number of field studies considering effects is the lack of proper dose estimates. Here we have demonstrated that the use of appropriate dosimeters attached to animals will likely give reasonable estimates of absorbed external dose rates and help resolve this debate.

CHAPTER 7   A NOVEL METHOD TO DETERMINE DEER ORGAN DOSE FROM ^{137}CS EXTERNAL EXPOSURE

7.1   INTRODUCTION

A framework for radiological environmental protection based on the concept of twelve reference animals and plants (RAPs) has been proposed by *International Commission on Radiological Protection* (*ICRP*) to ensure that all species are conserved and that the health and status of natural habitats, communities and ecosystem is protected (ICRP, 2003, 2007). Twelve RAPs have had their radiation exposures estimated using simplistic models and representations of their geometries (ICRP, 2008). This concept is also implemented in other computer models for wildlife radiation dose assessment, such as the ERICA Tool (Brown et al., 2016). The predicted doses from these models are calculated as organism whole-body doses. Generally they assume ellipsoid geometries and a uniform distribution of radionuclides in the organism and relevant environment media (e.g. soil or water) (Stark et al., 2017).

An alternative model for a number of RAPs has been developed to estimate doses to different organs and tissues by creating voxel phantoms of animal species from computerized tomography (CT) images (e.g. Caffrey et al., 2016; Caffrey & Higley, 2013; Kinase, 2008; Stabin et al., 2006). The voxel models can identify uncertainties of dose predictions from computer models using ellipsoid geometries (Ruedig et al., 2015) and may also have value in interpreting field studies. The development of animal phantoms, made from tissue equivalent materials for laboratory experiments, is another technique that can be used to estimate organ dose of animals. The organ dose estimates using a physical phantom-based animal phantom can be also used to compare to predictions of voxel phantom studies. Whilst Reference Deer has been suggested as one of the ICRP (2008) RAPs, to our knowledge, there is currently no organ phantom for a large wild mammal species.

The aim of this chapter was to develop and use a novel physical method to determine deer organ doses focussing on external radiation sources.

7.2 MATERIALS AND METHODS

This section describes the method used to determine the organ doses of deer exposed to external radiation. This involved: (i) using computed tomography (CT) scanning to map important internal deer organs; (ii) using the CT images to adapt a tissue equivalent phantom developed for humans to represent the positioning of internal deer organs; (iii) exposing the phantom to different external radiation sources to be able to relate organ dose to whole-body dose.

7.2.1 Determination of deer anatomy

Two female adult red deer *(Cervus elaphus)* shot as part of a routine forestry management at a site in north-west England were obtained on the day they were culled; no ethical issues were raised as their sacrifice was part of normal routine game management policy. Their live-weights were approximately 90 kg. To map important organs (thyroid, lung, heart, liver, spleen, kidneys, ovaries and uterus) the red deer were scanned using computed tomography at 120 kVp and Automatic Tube Current Modulation (Toshiba Aquilion 16 MDCT scanner, Minato-ku, Japan) at the University of Salford. The animals were secured on the scanning table in the supine position. Image data was reconstructed in the axial, coronal and sagittal planes in order to obtain detailed anatomy. CT images were generated at 1 cm intervals. Interpretation of these images and identification of the organs was conducted by an experienced consultant radiologist; annotated images from one of the deer are presented in Figure 7-1.
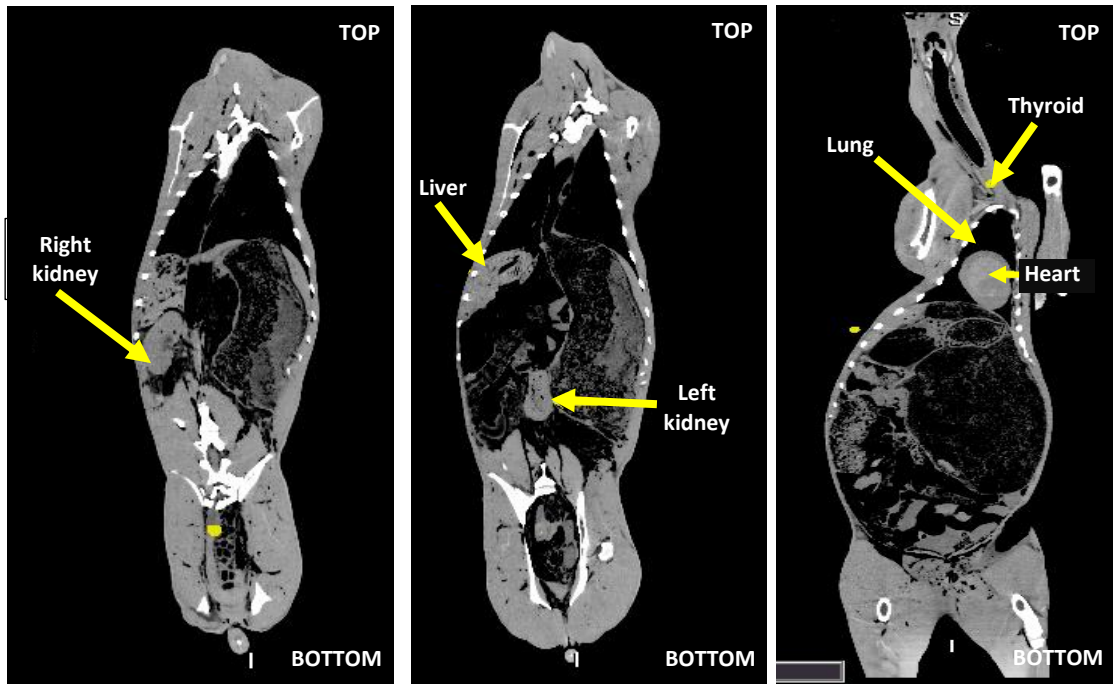
Figure 7-1: Adult female red deer *(Cervus elaphus)* anatomy shown on sagittal CT scan slices

7.2.2 Adaptation of human organ dosimetry map to create a deer organ map

Human dosimetry phantoms are provided with organ maps which indicate where organs are located; holes in the phantom can be used to suitably locate thermoluminescent dosimeters (TLDs) in order to determine organ dose.

Phantoms for large wild mammals with tissue equivalent materials are not commercially available for use in radiation dosimetry experiments. High budgets would likely be required to construct a bespoke deer phantom. Therefore, a human organ dosimetry map phantom (CIRS adult ATOM dosimetry phantom model 701 (CIRS Inc, Norfolk, Virginia, USA)) was adapted to create a deer organ map because the human dosimetry phantom has similar size, physical properties and anatomical regions to red deer, as determined by the CT images. The ATOM phantom, which consists of a trunk and head with no arms or legs, is 98 cm high and has a mass of 73 kg; the cross-sectional dimensions of the phantom are 23cm x 32 cm. It consists of tissue-equivalent epoxy resins divided into 39 slices each of 25 mm thickness. When the human organ map is applied, the phantom consists of 22 organs, including eyes,

94

brain, thyroid, heart, thymus, lungs, liver, gall bladder, spleen, esophagus, stomach, pancreas, kidneys, adrenals, intestine, ovaries, uterus, urinary bladder, testes, prostate, breasts and active bone marrow. On the human organ map, there are 268 predrilled holes for TLDs located in the simulated 22 organs.

The sectional human phantom and the cross-sectional deer organ images were compared to quantify body ratios (from front to back (depth) and from side to side (width)) and organ positions at every 10 mm. The ratios and the organ positions were used to determine organ holes in the phantom slices as locations of the internal deer organs for placing TLDs and subsequently determining organ doses. The holes for deer internal organs were selected from the internal organ holes of the human phantom using the ratios described above to estimate the hole locations. As the two-red deer scanned were females, to model dose to testes it was assumed that they were located in the same place as human testes.

7.2.3 X-ray exposure

Using the deer organ map, the phantom was loaded with TLDS-100H (LiF:Mg,Cu,P) dosimeters (Thermo Scientific, USA) and used to measure organ doses. Seventy-two TLD-100H's were loaded into sectional deer organ phantom (see details in Table 7-1) from the top position (thyroid) to the bottom position (testes) as shown in Figure 7-2.

External whole organism absorbed doses was also measured using TLD-100H housed in an aluminium box and fixed to an animal collar which was mounted on side of the neck of the phantom. I had previously used this method of attaching dosimeters in a field study investigating reindeer (Section 0).

Table 7-1: Location and number of TLDs-100H in deer phantom organs

Number	Organ	Number of TLDs	Phantom slide number
1	Thyroid	2	11
2	Lung	19	12, 14, 16, 18, 20
3	Heart	2	17
4	Liver	25	20, 21, 22, 23, 24
5	Spleen	5	22, 23
6	Kidney	5	25, 26
7	Uterus	6	38, 39
8	Ovaries	2	38
9	Testes	3	37

Once the TLDs had been loaded into the predrilled holes, using the deer organ map, and the aluminium box with TLDs fitted to the phantom, the phantom was exposed to x-rays. A Wolverson Arcoma Arco Ceil general x-ray machine (Wolverson X-Ray Ltd, Willenhall, West Midlands, UK), with a Varian X-ray tube (Varian medical systems, Salt Lake City, UT, USA) was used. The x-ray tube has a Tungsten-Rhenium anode with an angle of 12º, and an inherent filtration of 3.0 mm aluminium equivalent (for 75 kVp); no added filtration was used. A source to phantom distance of 200 cm was used with the front/chest of the phantom facing the source (this exposure orientation best mimics exposure of animals in the field from contaminated soil). Exposures were made at 50 kVp (100 mAs) and 110 kVp (100 mAs); exposures were repeated three times to reduce random error. All error values presented in this paper are standard deviations (SD). X-ray collimation and the distance between the phantom and the X-ray tube remained constant for each exposure. These exposures would result in a dose to the phantom of approximately 180 µGy (50 kVp) and 950 µGy (100 kVp) as estimated by a detector (RaySafe X2 (Unfors RaySafe AB, Sweden) strapped to the front of the phantom during irradiation. To put the energies of the x-rays exposures into context with the subsequent exposure to gamma radiation then, kilovolts peak (kVp) denotes the most energetic x-rays emitted, so the maximum x-ray energy for 110 kVp is 110 keV.
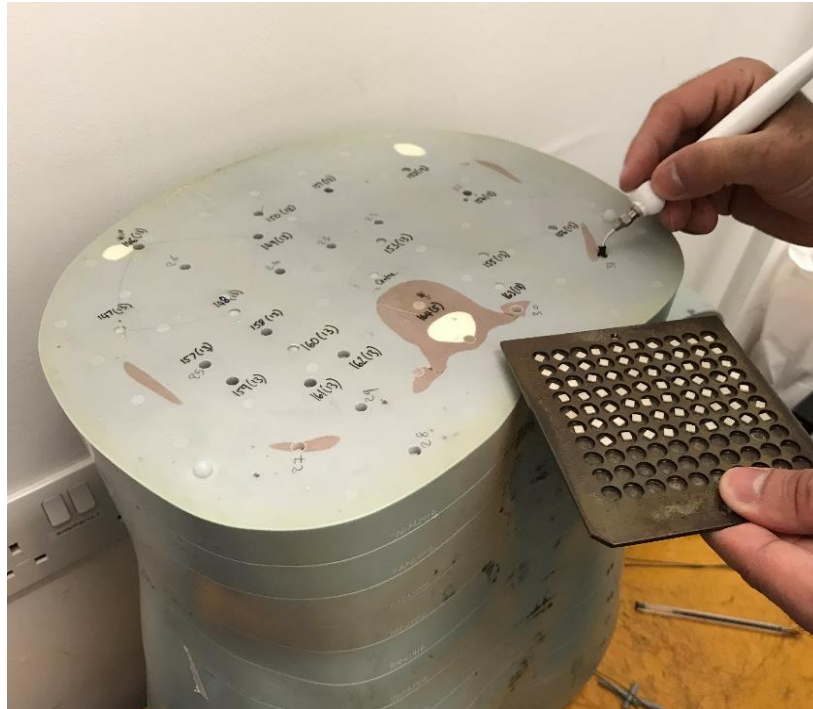
Figure 7-2: Demonstration of how TLDs are loaded into predrilled holes which represent locations of deer organs

7.2.4 Exposure to a ^{137}Cs source

Subsequent to exposure to X-rays the phantom was exposed to a ^{137}Cs source. Caesium-137 is environmentally relevant and was the focus of an earlier study to determine external exposure of a deer species in the field (CHAPTER 6). Because of the relative attenuation/adsorption differences between the energies from the x-ray machine and ^{137}Cs (662 keV) this second exposure was necessary to provide an estimate of deer organ doses due to ^{137}Cs. The experimental set up was the same as used for the x-ray machine. Again, the phantom was exposed three times to minimise random error with an air kerma doses of 950 µGy. The ^{137}Cs source was located at the Public Health England (PHE) calibration facilities.

The normality of data obtained from both exposures was tested using the Shapiro-Wilk test. Correlations were performed using Pearson's correlation coefficient (r) (IBM SPSS Statistics 23) between the x-ray (both x-ray energies) and the ^{137}Cs organ doses and also doses from the different exposures to the TLDs in the aluminium box.

7.2.5 Estimation of whole body absorbed dose

The TLD-100H dosimeters read in terms of air kerma (Gy) were converted to whole body absorbed dose (Gy) using conversion coefficients calculated using the Monte Carlo N-Particle (MCNP5) code (Pelowitz, 2013). An ellipsoid shape used as simplistic large mammal shapes for wildlife dosimetry models (e.g. ICRP, ERICA) was input into the MCNP model and was defined using two materials; air and soft tissue (Hydrogen, Carbon, Nitrogen and Oxygen) (ICRU, 1998). The weight of the ellipsoid phantom was 100 kg which is similar with the female standard weight of red deer (Lowe, 2014). The x-ray source (i.e. 50 kVp and 110 kVp) and the ^{137}Cs source were created in the model as the isotropic volumetric sources having their sizes larger than the phantom and 10 cm thicknesses. The sources were placed at 60 cm distance from the phantom. The models were simulated to emit radiation from each source to the whole ellipsoid phantom. The results of MCNP simulations were air kerma per source particle and tissue kerma per source particle of the ellipsoid phantom for the x-ray at 50 kVp and 110 kVp and the ^{137}Cs source, in the units of (Gy). The ratios of these two quantities were used as conversion coefficients to convert from air kerma to whole body absorbed doses for the deer phantom in this study once the TLD-100H dosimeters in the aluminium box from each exposure were read.

7.3   RESULTS

7.3.1 Deer organ map phantom

From the CT scans showed, unsurprisingly, differences in body shape to the available human phantom, with the deer being longer than the human phantom. The deer body was also consistently larger from front to back (depth) than the human phantom by up to a factor of two (in the body area where lungs are located). From side to side (width) the comparatives sizes differed, the top of the phantom was slight larger than the deer (this area contains the thyroid, lung, heart and part of the liver). The lower portion of the phantom, containing the remaining organs considered here, was smaller than deer. The thyroid, lungs, heart, liver, spleen and

kidneys of the red deer and the human phantom had similar positions although not necessarily sizes. Because of the greater length of the deer body, organs in the lower regions (i.e. gonads and uterus) had to be relocated relative to other organs and placed at the lower extremity of the phantom. Whilst located in generally similar positions, because of the greater depth of the deer body compared to the human phantom, some organs (e.g. the lung, kidney and spleen) were partially located outside of the phantom geometry. Therefore, only the proportion of these organs within the human phantom geometry could be modelled using representative holes for each organ.

7.3.2 Deer organ doses from x-ray

TLDs in each organ exposed to x-rays were averaged to give a single organ dose and along with data from whole body absorbed dose. The results are presented in Figure 7-3 (a) (50 kVp) and Figure 7-3 (b) (110 kVp). At 50 kVp (100 mAs), deer organ doses varied between 3 µGy and 93 µGy; deer organ doses varied between 125 µGy and 857 µGy for 110 kVp (100 mAs). The whole-body absorbed doses converted from air kerma read from TLD-100H in aluminium box using conversion coefficients (i.e. 50 kVp = 0.18 and 110 kVp =0.40) were 13 µGy for 50 kVp and 311 µGy for 110 kVp. The least exposed organs were the kidney and spleen for both x-ray energies with ovaries, testes and thyroid being the most exposed. However, the difference between organs was greater for the 50 kVp exposure. This is because the greater penetrating power of the 110 kVp exposure meant that the kidney and spleen (the organs most distant from the exposure source) were comparatively more highly irradiated. Also, the whole-bode doses for the 50 kVp and the 100 kVp exposure were lower than most organ doses except the organs at the posterior of the phantom (i.e. spleen and kidney). However, the difference between whole-body dose and organ doses for the 110 kVp exposure decreased when comparing with the 50 kVp x-ray.
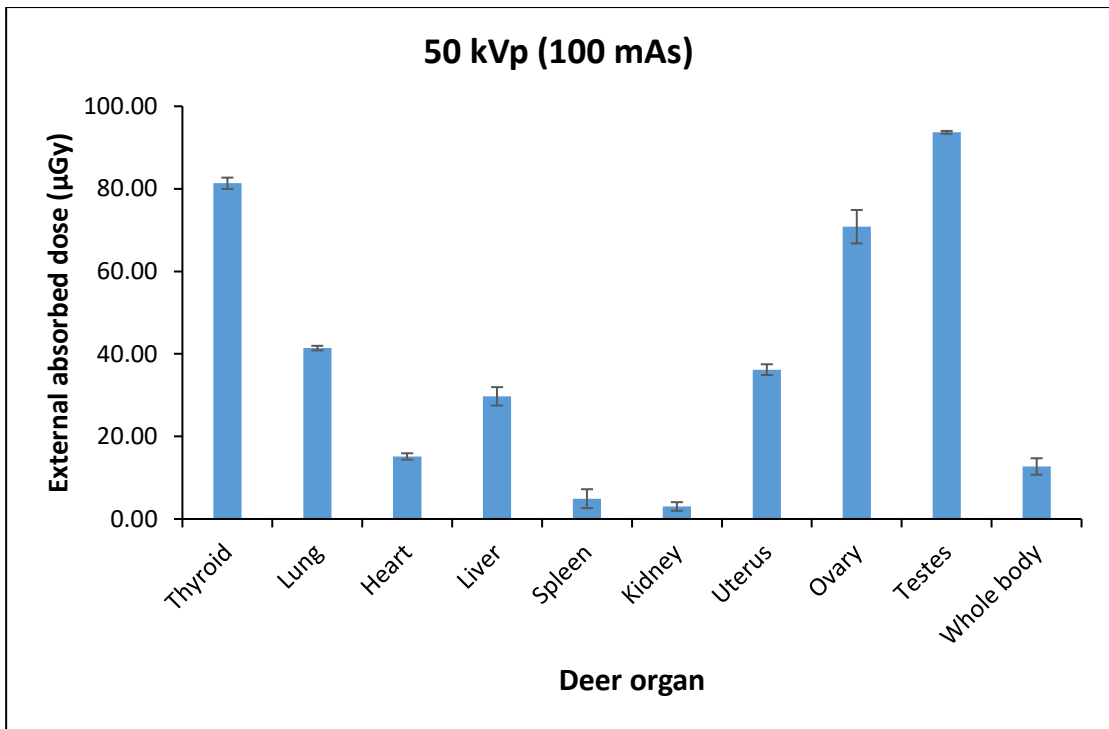
Figure 7-3 (a): Average dose to each deer organ from 50 kVp (100 mAs) x-rays
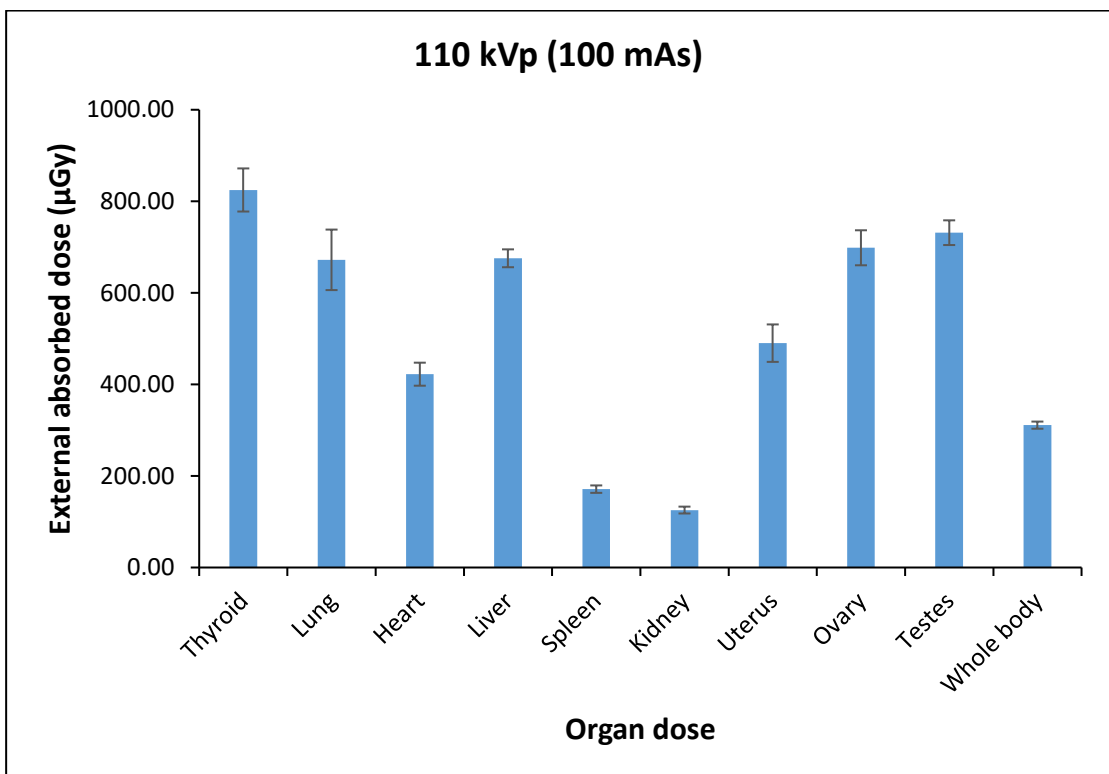
Figure 7-3 (b): Average dose to each deer organ from 110 kVp (100 mAs) x-rays

7.3.3 Average deer organ doses due to [137]Cs

For ^{137}Cs, deer organ doses varied between 222 µGy (kidneys) and 677 µGy (ovaries) (Figure 7-4). The organs positioned towards the front of the deer phantom (i.e. thyroid, ovaries and testes) received similar doses between 613 µGy and 642 µGy. The whole-body dose converted from air kerma using the conversion efficient for [137]Cs (i.e 0.6) was 404 µGy which was similar with the organ doses of heart (425 µGy) and liver (456). As for exposure to x-rays, the whole-body dose of ^{137}Cs exposure was also lower than most organ doses except kidneys and spleen which were the organs receiving the lowest doses. However, the difference of whole-body dose and organ doses was lower than the 50 kVp and 110 kVp sources. The proportion of organ doses received from external exposure tended to be higher than the 50 kVp and 110 kVp x-ray exposures because of the higher energy and higher penetration.
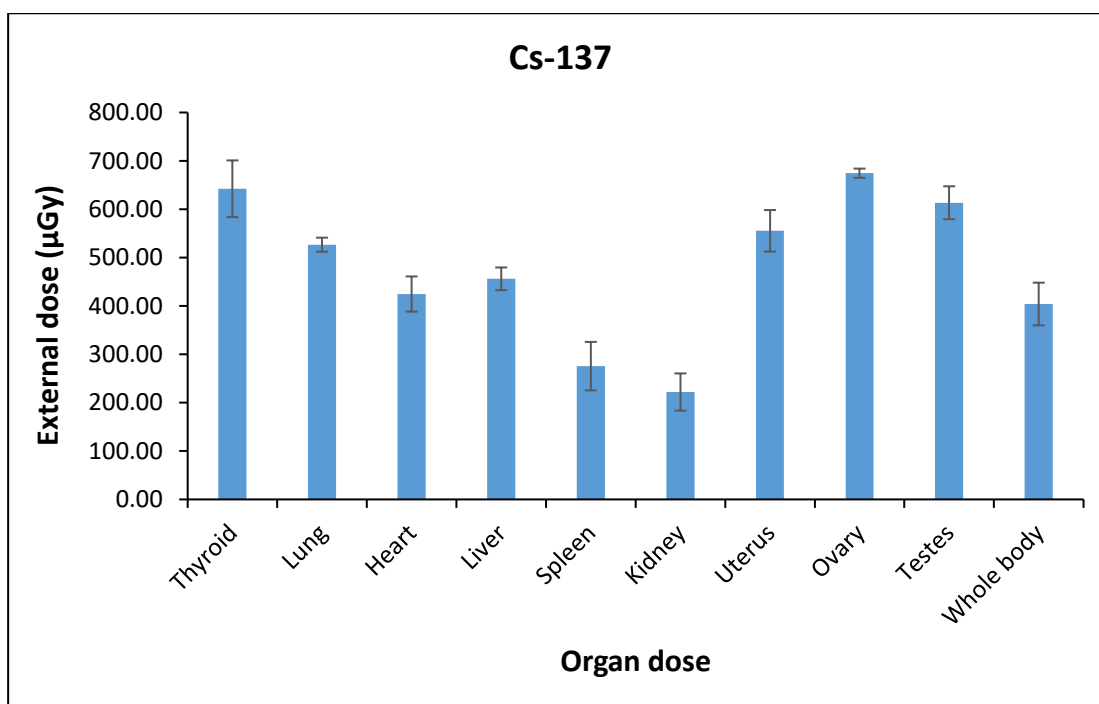
Figure 7-4: Dose to deer organs from exposure ^{137}Cs at 950 µGy

7.3.4 Conversion factors for calculating deer organ doses

Estimations of deer organ doses from 50 kVp and 110 kVp x-rays and ^{137}Cs were compared with whole-body doses as converted from air kerma of the TLD in the aluminium box attached to the neck of the phantom using conversion coefficients;

the aluminium box fitted with dosimeters had previously been used to estimate the external exposure of free-ranging reindeer (CHAPTER 6). The ratios between estimated whole-body dose and each organ dose for each energy represent conversion factors which could be used to estimate organ doses of similarly sized mammal species from modelled or measured (i.e. through attached dosimeters) external whole-body dose (Table 7-2). Generally estimated organ doses of spleen and kidney located furthest from the source of exposure were lower than the estimated whole-body dose for 50 kVp and 110 kVp x-ray and ^{137}Cs and hence the conversion factors are virtually <1. The conversion factors of organs (i.e. thyroid, ovary and testes) for 50 kVp exposure positioning nearest to the source were abundantly higher than those of conversion factors of organs for 110 kVp and ^{137}Cs exposures. The difference of conversion factor values for three energy exposures decreased for the organs in deeper positions from the phantom surface. It is noticed that the conversion factors of heart located in the middle of the phantom showed similar values (i.e. 1.05-1.36) for three energy sources. However, the conversion factors of organ doses (i.e. spleen and kidney) positioning furthest to the sources showed significantly higher values for the higher energy sources.

Table 7-2: Conversion factor for deer organ doses relative to estimated whole-body external dose for 50 kVp and 110 kVp x-rays and [137]Cs

Organ	Conversion factors of organ doses relative to estimated whole-body dose		
	50 kVp (100 mAs)	110 kVp (100 mAs)	[137]Cs (662 keV)
Thyroid	6.39±0.11	2.65±0.15	1.59±0.15
Lung	3.25±0.04	2.16±0.21	1.30±0.04
Heart	1.19±0.06	1.36±0.08	1.05±0.09
Liver	2.34±0.17	2.20±0.06	1.13±0.06
Spleen	0.39±0.18	0.55±0.03	0.68±0.12
Kidney	0.24±0.08	0.40±0.02	0.55±0.10
Uterus	2.84±0.10	1.58±0.13	1.37±0.11
Ovaries	5.57±0.32	2.25±0.12	1.67±0.02
Testes	7.37±0.03	2.35±0.09	1.52±0.08

7.4   DISCUSSION

The deer phantom, developed from the red deer CT scan images and by adapting a human dosimetry phantom, can be used as a unique method to enable organ dose estimates of large terrestrial mammals, including red deer (a species falling into the definition of the ICRP Reference Deer) from external exposure sources. The need of organ dosimetry assessment is the advance understanding of radiation interaction in animal species which is also used to assess dose effects for endangered species. Whilst an animal phantom (similar to the human phantom used here) made from tissue equivalent materials has been made for a mouse (Welch et al., 2015) and voxel phantoms for various animal species have been constructed from CT scans (e.g. Caffrey & Higley, 2013; Martinez et al., 2014; Mohammadi et al., 2012; Ruedig et al., 2015; Ruedig et al., 2014), to date there has been no development of a large wild mammal phantom with defined internal organs. The deer phantom in this study was developed using an adult human phantom which will have uncertainties associated with compromises which had to be made regarding the comparative sizes of the human phantom and body of the adult red deer considered and the definition of deer organ sizes. The red deer CT scanned images show appropriate detail to enable deer organs to be incorporated into the adult human phantom based on the ratios of both body sizes. The pre-set organ holes for placing TLDs were also used as the starting points to estimate deer organ location in the phantom using the body ratios between the phantom and the red deer images. The actual sizes of deer organs were not considered to be mapped onto the phantom which may cause an uncertainty of dose estimates. Therefore, the doses to organs which could not be fully located inside of the deer phantom geometry are estimated; in terms of dose rate they will tend to overestimate as the organ which could not be modelled is further from the source and would consequently have a lower dose rates than the portion of the organ which was modelled. However, the deer phantom was compensated using ratios of both bodies and contained tissue equivalent materials which was a suitable study on this first laboratory experiments for determining deer dose organs from external exposure.

The external dose recorded by the TLDs in the aluminium box could be used to estimate the external whole-body dose of the deer phantom by converting from air kerma using conversion coefficients for specific sources. The TLDs of the phantom organ could also be used to estimate mean organ doses. The ratios between the whole-body dose and the organ doses were calculated as conversion factors at the given kVp x-ray or ^{137}Cs. These conversion factors could be used to estimate the contribution of external exposure to specific organs based upon modelled whole-body dose rates or estimates from the attachment of dosimeters to animals. Whilst the conversion factors determined here may only be applicable to the energies used in this study some comments on wider implications can be given. The greatest difference between estimated whole body and organ doses will be for lower energy emissions. The organs nearest to the source and close to phantom surface for lower energy emissions (e.g. <100 keV) have significantly higher conversion factors than those for higher energy emissions (e.g. ^{137}Cs = 662 keV). This is likely explained by ^{137}Cs having a lower absorbed fraction than the x-rays due to its higher energy (Vives i Batlle et al., 2007). There was also less variation between the dose received by the different organs than observed for the x-rays, again this is likely due to the higher energy of the ^{137}Cs emissions. Whilst some organs will still have lower doses for higher energy emissions the difference of those organs dose and the whole-body dose will decrease. (e.g. for the ^{137}Cs example presented here with the exception of kidney and spleen the dose to all organs is between 5% and 60% of the whole-body dose). Although these conversion factors are estimated for specific sources, the values may be considered to be used to initially estimate organ dose of large mammal species from external exposure for sources occurring in the environment giving energies similar to those sources (e.g. Amerisium-241 (^{241}Am) = 60 keV).

The CT images obtained in this study could also be used to develop a voxel phantom. The resultant voxel phantom could then be used to explore the uncertainties associated with the 'deer phantom' created in this study due to compromises that had to be made associated with the size of the human phantom and positioning of the TLD holes on which it was based. The advantage the approach used here has over the voxel phantom is that it used actual measurements made in a phantom

comprising tissue equivalent material. Therefore, whilst the voxel phantom could be used to investigate uncertainties, the results of this study could also be used to validate the voxel phantom.

CHAPTER 8   CONCLUSION AND RECOMMENDATION

This study has incorporated critical review, laboratory experimentation, field testing and computer modelling to develop appropriate methods for directly measuring external radiation exposure of free-ranging terrestrial animals using passive dosimeters. The conclusions related to each of the five study objectives (Section 1.2) are presented in the sub-sections below.

8.1   CRITICAL EVALUATION OF THE EFFECTIVENESS OF THE SELECTED PASSIVE DOSIMETERS FOR DIRECT TERRESTRIAL WILDLIFE DOSIMETRY MEASUREMENT UNDER FIELD CONDITIONS

A comprehensive evaluation of different dosimetry technologies for measuring the external exposure of wildlife was undertaken. This review focused on four main passive dosimetry technologies (TLD, OSLD, RPLD and DIS (Instadose+)) and evaluated dosimeter properties in relation to studied organism and environment characteristics. It was concluded that LiF and Al_2O_3:C TLDs, OSLD and RPLD could all be used to estimate doses to wildlife. Whilst DIS units have the advantage that they can record temporal variations in dose, the mass of these units means that are only suitable for comparatively large species (e.g. medium to large mammals). Irrespective of the dosimeter selected, calibration is required to ensure that the dose measurements reported can be interpreted appropriately for the organisms of interest. Based on this evaluation and the conclusions drawn, guidance was developed to inform selection of appropriate passive dosimeters for external exposure measurement of terrestrial wildlife under field conditions.

8.2   SELECTION OF SUITABLE PASSIVE DOSIMETERS FOR LONG TERM LARGE MAMMAL DOSIMETRY MEASUREMENTS UNDER FIELD CONDITIONS

Selected passive dosimeters (i.e. TLD, OSLD, RPLD and DIS) were assembled within an aluminium box (i.e. dosimeter box) for measuring large mammal species external exposure under field conditions. The dose responses of the dosimeter box were tested in laboratory by attaching on a phantom representing the deer's neck. The dose responses include dose linearity, dose response at different angles and energies, dose response to beta radiation and contribution of ^{137}Cs activity concentration from an animal's body to dosimeters fixed in the dosimeter box on the outside of the body. It was concluded that the dosimeter box showed linear dose response and flat angle dependence of response for the angles tested (45° - 135°) and flat energy response for the radionuclides tested (^{137}Cs, ^{60}Co and ^{226}Ra). The dosimeters in the aluminium box did not respond to beta radiation absorbed dose therefore making the assembly suitable for measuring external dose from radionuclides emitting gamma radiation. However, doses contributed by internal activity concentration (i.e. ^{137}Cs) within the large mammals need to be taken into account when attaching the dosimeter box to the large mammals for field studies. This is because the mean dose rate per activity concentration for ^{137}Cs at 1 Bq kg^{-1} is 0.028 nGy h^{-1} Bq^{-1} determined when the dosimeter box was placed on an active phantom containing 60 kBq of ^{137}Cs. Therefore, the dosimeter types tested for this study can be used to measure external doses of large mammals by placement in the dosimeter box

8.3 THE USE OF COLLAR-MOUNTED DOSIMETERS FOR LONG TERM MEASUREMENTS OF EXTERNAL ABSORBED DOSES USING FREE-RANGING LARGE MAMMALS IN AN AREA CONTAMINATED BY THE CHERNOBYL ACCIDENT

External absorbed doses of reindeer in Vågå, Norway, which live in an area contaminated by the Chernobyl accident, were measured over 11 months using a purpose-built dosimeter box containing TLD, OSLD, RPLD and DIS. Between early January and early December 2016, the dosimeter boxes were attached on collars with Global Positioning System (GPS) units and fitted to 15 reindeer. The external absorbed doses of reindeer recorded by four selected dosimeter types were between 480 and 825 µGy over study period. These absorbed doses were corrected for contributions from the transit dose (330-450 µGy) and internally incorporated ^{137}Cs (100-202 µGy). Whilst there was a significant difference between the estimates of dosimeters, the difference of the mean doses between maximum and minimum values was <14 %. Therefore, it is likely that all four dosimeters will give similar results of integrated dose for relatively long-term (i.e. 1 year) dose measurements of large mammal species under field conditions. However, the performance of the Instadose+ was found to be compromised by extreme cold (< -10 °C). This prevented Instadose+ units from providing temporal measurements over the study period, but nine of the twelve units were able to provide accumulated dose measurements.

8.4 EVALUATION OF MODEL PERFORMANCE BY COMPARING MODEL PREDICTION OF EXTERNAL DOSES OF TARGET ORGANISMS WITH DIRECT DOSE MEASUREMENTS OBTAINED FROM THE FIELD STUDY

External dose measurements by the four dosimeter types in the GPS collar-mounted dosimeter boxes were compared with model predictions. Two approaches for

deriving model predictions were used: (i) external dose to reindeer predicted from average radionuclide activity concentrations in soil across the ranging area of the herd; and (ii) external absorbed doses of individual reindeer using GPS tracking data to determine appropriate average soil radionuclide activity concentrations for each reindeer based on their actual movement within the herding area.

Predicted external doses using individual GPS tracking data (the second approach) were between 582 and 630 µGy. These predicted doses included the contributions from ^{137}Cs, natural series radionuclides and cosmic radiation. The mean predicted doses using the GPS tracking data were not significantly different to RPLD and DIS. However, the TLD and OSLD results were 18% higher than the mean dose estimated using the GPS tracking data.

The average external dose (i.e. 471 µGy) predicted across the herd area (without using GPS data) was significantly lower than doses from all dosimeter types and the mean dose predicted using the GPS data. This is because the animals favoured the more contaminated area of the study site which were good grazing in several seasons for those reindeer. For ^{137}Cs the average external absorbed dose predicted using the GPS tracking data was about twice that predicted across all the herd area suggesting that, in some circumstances, the assumption of averaging contamination over an assumed home range within assessments (a typical assumption) may be inadequate.

8.5 QUANTIFICATION OF THE RELATIONSHIP BETWEEN EXTERNAL RADIATION EXPOSURE AND ORGAN DOSES FOR A LARGE MAMMAL SPECIES

A deer dosimetry phantom was created from red deer CT images and a human adult dosimetry phantom. Deer organ doses from external radiation exposure were measured using the developed deer phantom. The deer dosimetry phantom was loaded with thermoluminescent dosimeters (TLD-100H). An aluminium box containing TLD-100H was attached to an animal collar, which was then fitted to the phantom. The dosimetry deer phantom was irradiated using an x-ray source at 50

and 100 kVp; the procedure was then repeated using ^{137}Cs (662 keV). The data of whole-body and organ doses from x-ray and ^{137}Cs were used to calculate conversion factors that can be used to convert external whole-organism doses of deer species to individual organ doses from external exposure.

8.6 TRANSLATING RESEARCH INTO IMPACT

The research presented in this thesis has already been communicated to the scientific community through journal publications (one published and three submitted) and presentations at national and international conferences. This research is also being used to underpin activity within the International Atomic Energy Agency's (IAEA) Modelling and Data for Radiological Impact Assessments (MODARIA II) programme. In recognition of the scientific excellence of the research presented in this thesis, I was awarded, the best oral presentation in Glasgow (April 2015), the *International Union of Radioecology (IUR) Young Investigator's Award* in Berlin (September 2017) and the Anglo-Thai Society Educational Award in London (December 2017). The research was also selected to receive additional funding from the CONCERT-European Joint Programme for the Integration of Radiation Protection Research.

8.7 RECOMMENDATIONS

The use of different passive dosimetry technologies for long-term external exposure measurement of terrestrial wildlife has been demonstrated within this thesis, comprehensively addressing both the aim and objectives of this PhD. Based on the research presented in this thesis, the following recommendations are made:

- To further advance the use of various types of passive dosimetry technologies within radioecological research, it is recommended that the use of these technologies is tested for other types of terrestrial organisms and also for aquatic organisms (e.g. the RAP species suggested by ICRP).
- The applicability to aquatic organisms of the guidance for selecting suitable dosimetry technologies should be evaluated and amended guidance

developed as appropriate to support future deployment of dosimeters within aquatic systems.

- The utility of dosimeters for wildlife dose measurement during short term field studies (i.e. days to 1 month) should be evaluated.

- To address the challenges identified in measuring temporal changes in reindeer dose due to low temperature effects on the DIS, further development of DIS technology should be undertaken in collaboration with the manufacturer.

- The deer CT images obtained in this PhD should be used to develop a voxel phantom. This would allow uncertainties associated with the 'deer phantom' created in this research to be further investigated and provide a model that could be used to further inform the developing ICRP RAP approach.

Addressing these recommendations would further increase the development of direct dose measurement technologies for quantifying the external radiation exposure of both terrestrial and aquatic species under field conditions. This would significantly improve the value of field-based research on dose-effect relationships and also allow for further validation of dose assessment model predictions.

REFERENCE

AGC Techno Glass. 2012. *Glass Dosimeter GD-300 series Instruction Manual*. Shizuoka, Japan: AGC TECHNO GLASS CO., LTD.

Agüero, A., Alonzo, F., Björk, M., Ciffroy, P., Copplestone, D., Garnier-Laplace, J., Gilbin, R., Gilek, M., Hertel-Aas, T., Jaworska, A., Larsson, C.-M., Oughton, D., & Zinger, I. 2006. ERICA DELIVERABLE 5: Derivation of Predicted-No-Effect-Dose-Rate values for ecosystems (and their sub-organisational levels) exposed to radioactive substances. European Commission: Community research.

Akselrod, M., Kortov, V., Kravetsky, D., & Gotlib, V. 1990. Highly sensitive thermoluminescent anion-defect alpha-Al2O3: C single crystal detectors. *Radiation Protection Dosimetry, 33*(1-4), 119-122.

Andersson, P., Garnier-Laplace, J., Beresford, N. A., Copplestone, D., Howard, B. J., Howe, P., Oughton, D., & Whitehouse, P. 2009. Protection of the environment from ionising radiation in a regulatory context (protect): proposed numerical benchmark values. *Journal of Environmental Radioactivity, 100*(12), 1100-1108. doi: http://dx.doi.org/10.1016/j.jenvrad.2009.05.010

Annalakshmi, O., Jose, M., & Amarendra, G. 2011. Dosimetric characteristics of manganese doped lithium tetraborate–An improved TL phosphor. *Radiation Measurements, 46*(8), 669-675.

Antonio, E. J., Poston, T. M., & Rathbone, B. A. 2010. Thermoluminescent Dosimeter Use for Environmental Surveillance at the Hanford Site, 1971–2005. *PNNL-19207, Richland, WA (US)*.

Aramrun, P., Beresford, N. A., & Wood, M. D. 2018. Selecting passive dosimetry technologies for measuring the external dose of terrestrial wildlife. *Journal of Environmental Radioactivity, 182*, 128-137. doi: https://doi.org/10.1016/j.jenvrad.2017.12.001

Arshak, K., & Korostynska, O. 2006. *Advanced materials and techniques for radiation dosimetry*: Artech House Boston.

Avila, R., Beresford, N. A., Agüero, A., Broed, R., Brown, J., Iospje, M., Robles, B., & Suañez, A. 2004. Study of the uncertainty in estimation of the exposure of non-human biota to ionising radiation. *Journal of Radiological Protection, 24*(4A), A105-A122. doi: 10.1088/0952-4746/24/4a/007

Backe, S., Bjerke, H., Rudjord, A. L., & Ugletveit, F. 1986. Cesium fallout in Norway after the Chernobyl accident: Statens Inst. for Straalehygiene.

Baranwal, V. C., Ofstad, F., Rønning, J. S., Watson, R. J., Lom, V., Sel, N.-F., & og Lillehammer, Å. 2011. Mapping of caesium fallout from the Chernobyl accident in the Jotunheimen area. *Geological Survey of Norway (NGU), Trondheim, Norway. Report*.

Bartlett, D. T., & Tanner, R. J. 2005. Adequacy of external dosimetry methods and suitability of personal dosemeters for workplace radiation fields *RESEARCH REPORT 385*. Health Protection Agency.

Beaugelin-Seiller, K., Garnier-Laplace, J., & Beresford, N. A. submitted. Estimating radiological exposure of wildlife in the field. *Journal of Environmental Radioactivity*.

Beresford, N. A., Balonov, M., Beaugelin-Seiller, K., Brown, J., Copplestone, D., Hingston, J. L., Horyna, J., Hosseini, A., Howard, B. J., Kamboj, S., Nedveckaite, T., Olyslaegers, G., Sazykina, T., Vives, I. B. J., Yankovich, T. L., & Yu, C. 2008a. An international comparison of models and approaches for the estimation of the radiological exposure of non-human biota. *Appl Radiat Isot, 66*(11), 1745-1749. doi: 10.1016/j.apradiso.2008.04.009

Beresford, N. A., Barnett, C. L., Beaugelin-Seiller, K., Brown, J. E., Cheng, J. J., Copplestone, D., Gaschak, S., Hingston, J. L., Horyna, J., Hosseini, A., Howard, B. J., Kamboj, S., Kryshev, A., Nedveckaite, T., Olyslaegers, G., Sazykina, T., Smith, J. T., Telleria, D., Vives i Batlle, J., Yankovich, T. L., Heling, R., Wood, M. D., & Yu, C. 2009. Findings and recommendations from an international comparison of models and approaches for the estimation of radiological exposure to non-human biota. *Radioprotection, 44*(5), 565-570. doi: 10.1051/radiopro/20095104

Beresford, N. A., Barnett, C. L., Brown, J. E., Cheng, J.-J., Copplestone, D., Gaschak, S., Hosseini, A., Howard, B. J., Kamboj, S., Nedveckaite, T., Olyslaegers, G., Smith, J. T., Vives i Batlle, J., Vives-Lynch, S., & Yu, C. 2010. Predicting the radiation exposure of terrestrial wildlife in the Chernobyl exclusion zone: an international comparison of approaches. *Journal of Radiological Protection, 30*(2), 341.

Beresford, N. A., Barnett, C. L., Brown, J. E., Cheng, J. J., Copplestone, D., Filistovic, V., Hosseini, A., Howard, B. J., Jones, S. R., Kamboj, S., Kryshev, A., Nedveckaite, T., Olyslaegers, G., Saxén, R., Sazykina, T., Vives i Batlle, J., Vives-Lynch, S., Yankovich, T., & Yu, C. 2008b. Inter-comparison of models to estimate radionuclide activity concentrations in non-human biota. *Radiation and Environmental Biophysics, 47*(4), 491-514. doi: 10.1007/s00411-008-0186-8

Beresford, N. A., Barnett, C. L., Jones, D. G., Wood, M. D., Appleton, J. D., Breward, N., & Copplestone, D. 2008c. Background exposure rates of terrestrial wildlife in England and Wales. *Journal of Environmental Radioactivity, 99*(9), 1430-1439.

Beresford, N. A., & Copplestone, D. 2011. Effects of ionizing radiation on wildlife: what knowledge have we gained between the Chernobyl and Fukushima accidents? *Integrated environmental assessment and management, 7*(3), 371-373.

Beresford, N. A., Gaschak, S., Barnett, C. L., Howard, B. J., Chizhevsky, I., Strømman, G., Oughton, D. H., Wright, S. M., Maksimenko, A., & Copplestone, D. 2008d. Estimating the exposure of small mammals at three sites within the Chernobyl exclusion zone – a test application of the ERICA Tool. *Journal of Environmental Radioactivity, 99*(9), 1496-1502. doi: http://dx.doi.org/10.1016/j.jenvrad.2008.03.002

Beresford, N. A., Scott, M., & Copplestone, D. in press 2018. Field effects studies in the Chernobyl Exclusion Zone: Lessons to be learnt. *Journal of Environmental Radioactivity*.

Beresford, N. A., Wright, S. M., Barnett, C. L., Wood, M. D., Gaschak, S., Arkhipov, A., Sazykina, T. G., & Howard, B. J. 2005. Predicting radionuclide transfer to wild animals: an application of a proposed environmental impact assessment framework to the Chernobyl exclusion zone. *Radiation and Environmental Biophysics, 44*(3), 161-168.

Bhatt, B. C. 2011. Thermoluminescence, optically stimulated luminescence and radiophotoluminescence dosimetry: An overall perspective. *Radiation Protection and Environment, 34*(1), 6-16.

Bilski, P., Berger, T., Hajek, M., Twardak, A., Koerner, C., & Reitz, G. 2013. Thermoluminescence fading studies: Implications for long-duration space measurements in Low Earth Orbit. *Radiation Measurements, 56*, 303-306. doi: http://dx.doi.org/10.1016/j.radmeas.2013.01.045

Bonisoli-Alquati, A., Koyama, K., Tedeschi, D. J., Kitamura, W., Sukuzi, H., Ostermiller, S., Arai, E., Møller, A. P., & Mousseau, T. A. 2015. Abundance and genetic damage of barn swallows from Fukushima. *Scientific Reports, 5*, 9432. doi: 10.1038/srep09432

Bonzom, J.-M., Hättenschwiler, S., Lecomte-Pradines, C., Chauvet, E., Gaschak, S., Beaugelin-Seiller, K., Della-Vedova, C., Dubourg, N., Maksimenko, A., Garnier-Laplace, J., & Adam-Guillermin, C. 2016. Effects of radionuclide contamination on leaf litter decomposition in the Chernobyl exclusion zone. *Science of The Total Environment, 562*, 596-603. doi: http://dx.doi.org/10.1016/j.scitotenv.2016.04.006

Bordy, J., Gualdrini, G., Daures, J., & Mariotti, F. 2011. Principles for the design and calibration of radiation protection dosemeters for operational and protection quantities for eye lens dosimetry. *Radiation Protection Dosimetry, 144*(1-4), 257-261.

Botter-Jensen, L., Agersnap Larsen, N., Markey, B. G., & McKeever, S. W. S. 1997. Al$_2$O$_3$:C AS A sensative OSL dosimeter for rapid assessment of environmental photon dose rates. *Radiation Measurements, 27*(2), 295-298.

Brown, J. E., Alfonso, B., Avila, R., Beresford, N. A., Copplestone, D., & Hosseini, A. 2016. A new version of the ERICA tool to facilitate impact assessments of radioactivity on wild plants and animals. *Journal of Environmental Radioactivity, 153*, 141-148. doi: http://dx.doi.org/10.1016/j.jenvrad.2015.12.011

Brown, J. E., Alfonso, B., Avila, R., Beresford, N. A., Copplestone, D., Pröhl, G., & Ulanovsky, A. 2008. The ERICA Tool. *Journal of Environmental Radioactivity, 99*(9), 1371-1383. doi: http://dx.doi.org/10.1016/j.jenvrad.2008.01.008

Buisset-Goussen, A., Goussen, B., Della-Vedova, C., Galas, S., Adam-Guillermin, C., & Lecomte-Pradines, C. 2014. Effects of chronic gamma irradiation: a multigenerational study using Caenorhabditis elegans. *Journal of Environmental Radioactivity, 137*, 190-197. doi: http://dx.doi.org/10.1016/j.jenvrad.2014.07.014

Caffrey, E., Johansen, M., & Higley, K. 2016. Voxel modeling of rabbits for use in radiological dose rate calculations. *Journal of Environmental Radioactivity, 151*, 480-486.

Caffrey, E. A., & Higley, K. A. 2013. Creation of a voxel phantom of the ICRP reference crab. *Journal of Environmental Radioactivity, 120*, 14-18. doi: https://doi.org/10.1016/j.jenvrad.2013.01.006

Černe, M., Smodiš, B., Štrok, M., & Benedik, L. 2012. Radiation impact assessment on wildlife from an uranium mine area. *Nuclear Engineering and Design, 246*, 203-209. doi: 10.1016/j.nucengdes.2011.07.012

Chesser, R. K., Sugg, D. W., Lomakin, M. D., Bussche, R. A. V. D., DeWoody, A. J., Jagoe, C. H., Dallas, C. E., Whicker, F. W., Smith, M. H., Gaschak, S. P., Chizhevsky, I. V., Lyabik, V. V., Buntova, E. G., Holloman, K., & Baker, R. J. 2000. Concentrations and dose rate estimates of 134, 137 Cesium and 90 Strontium in small mammals at Chornobyl, Ukraine. *Environmental Toxicology and Chemistry, 19*(2), 305-312. doi: 10.1897/1551-5028(2000)019<0305:CADREO>2.3.CO;2

Chiriotti, S., Ginjaume, M., Vano, E., Sanchez, R., Fernandez, J. M., Duch, M. A., & Sempau, J. 2011. Performance of several active personal dosemeters in interventional radiology and cardiology. *Radiation Measurements, 46*(11), 1266-1270. doi: http://dx.doi.org/10.1016/j.radmeas.2011.05.073

Chisté, V., Bé, M.-M., & Dulieu, C. 2007. *Evaluation of decay data of radium-226 and its daughters.* Paper presented at the International Conference on Nuclear Data for Science and Technology.

Cinelli, G., Gruber, V., De Felice, L., Bossew, P., Hernandez-Ceballos, M. A., Tollefsen, T., Mundigl, S., & De Cort, M. 2017. European annual cosmic-ray dose: estimation of population exposure. *Journal of Maps, 13*(2), 812-821. doi: 10.1080/17445647.2017.1384934

Copplestone, D. 2012. Application of radiological protection measures to meet different environmental protection criteria. *Ann ICRP, 41*(3-4), 263-274. doi: 10.1016/j.icrp.2012.06.007

Copplestone, D., Andersson, P., Beresford, N., Brown, J., Dysvik, S., Garnier-Laplace, J., Hingston, J., Howard, B., Oughton, D., & Whitehouse, P. 2009. Protection of the environment from ionising radiation in a regulatory context (PROTECT): Review of current regulatory approaches to both chemicals and radioactive substances. *Radioprotection, 44*(5), 881-886.

Copplestone, D., Beresford, N., & Howard, B. 2010. Protection of the environment from ionising radiation: Developing criteria and evaluating approaches for use in regulation. *Journal of Radiological Protection, 30*(2), 191.

Copplestone, D., Bielby, S., Jones, S., Patton, D., Daniel, P., & Gize, I. 2001. Impact Assessment of Ionising Radiation on Wildlife (R&D Puclication 128). UK: Environment Agency.

Copplestone, D., Hingston, J., & Real, A. 2008. The development and purpose of the FREDERICA radiation effects database. *Journal of Environmental Radioactivity, 99*(9), 1456-1463. doi: http://dx.doi.org/10.1016/j.jenvrad.2008.01.006

David, Y. C. H., & Shih-Ming, H. 2011. *Radio-Photoluminescence Glass Dosimeter (RPLGD)*. Rijeka, Croatia: InTech.

Duggan, L., Budzanowski, M., Przegietka, K., Reitsema, N., Wong, J., & Kron, T. 2000. The light sensitivity of thermoluminescent materials: LiF:Mg,Cu,P, LiF:Mg,Ti

and Al2O3:C. *Radiation Measurements, 32*(4), 335-342. doi: http://dx.doi.org/10.1016/S1350-4487(00)00048-2

El-Faramawy, N. A., El-Kameesy, S. U., El-Agramy, A., & Metwally, G. 2000. The dosimetric properties of in-house prepared copper doped lithium borate examined using the TL-technique. *Radiation Physics and Chemistry, 58*(1), 9-13. doi: http://dx.doi.org/10.1016/S0969-806X(99)00361-8

French, N. R., Maza, B. G., & Aschwanden, A. P. 1966. Periodicity of desert rodent activity. *Science, 154*(3753), 1194-1195.

Fuma, S., Ihara, S., Kawaguchi, I., Ishikawa, T., Watanabe, Y., Kubota, Y., Sato, Y., Takahashi, H., Aono, T., & Ishii, N. 2015. Dose rate estimation of the Tohoku hynobiid salamander, Hynobius lichenatus, in Fukushima. *Journal of Environmental Radioactivity, 143*, 123-134.

Furetta, C., Prokic, M., Salamon, R., Prokic, V., & Kitis, G. 2001. Dosimetric characteristics of tissue equivalent thermoluminescent solid TL detectors based on lithium borate. *Nuclear Instruments and Methods in Physics Research Section A: Accelerators, Spectrometers, Detectors and Associated Equipment, 456*(3), 411-417.

Furetta, C., & World, S. 2010. *Handbook of Thermoluminescence* (Vol. 2nd ed). Singapore: World Scientific Publishing Company.

Gano, K. 1979. Analysis of small mammal populations inhabiting the environs of a low-level radioactive waste pond: Battelle Pacific Northwest Labs., Richland, WA (USA).

Gilvin, P., Baker, S., Daniels, T., Eakins, J., McClure, D., Bartlett, D., & Boucher, C. 2007. Type testing of a new TLD for the UK Health Protection Agency. *Radiation Protection Dosimetry, 128*(1), 36-42.

Guthrie, J., & Scott, A. 1969. Measurement of radiation dose distribution in a pond habitat by lithium fluoride dosimetry. *Canadian journal of zoology, 47*(1), 17-20.

Halford, D. K., & Markham, O. D. 1978. Radiation Dosimetry of Small Mammals Inhabiting a Liquid Radioactive Waste Disposal Area. *Ecology, 59*(5), 1047-1054. doi: 10.2307/1938557

Hashim, S., Alajerami, Y. S. M., Ramli, A. T., Ghoshal, S. K., Saleh, M. A., Abdul Kadir, A. B., Saripan, M. I., Alzimami, K., Bradley, D. A., & Mhareb, M. H. A. 2014. Thermoluminescence dosimetry properties and kinetic parameters of lithium potassium borate glass co-doped with titanium and magnesium oxides. *Applied Radiation and Isotopes, 91*, 126-130. doi: https://doi.org/10.1016/j.apradiso.2014.05.023

Hidehito, N., Yoshinori, T., & Yuka, M. 2011. *Environmental Background Radiation Monitoring Utilizing Passive Solid Sate Dosimeters, Environmental Monitoring*. Rijeka, Croatia: InTech.

Hinton, T. G., Byrne, M. E., Webster, S., & Beasley, J. C. 2015. Quantifying the spatial and temporal variation in dose from external exposure to radiation: a new tool for use on free-ranging wildlife. *Journal of Environmental Radioactivity, 145*(0), 58-65. doi: http://dx.doi.org/10.1016/j.jenvrad.2015.03.027

Hinton, T. G., Garnier-Laplace, J., Vandenhove, H., Dowdall, M., Adam-Guillermin, C., Alonzo, F., Barnett, C., Beaugelin-Seiller, K., Beresford, N. A., Bradshaw, C., Brown, J., Eyrolle, F., Fevrier, L., Gariel, J. C., Gilbin, R., Hertel-Aas, T.,

Horemans, N., Howard, B. J., Ikäheimonen, T., Mora, J. C., Oughton, D., Real, A., Salbu, B., Simon-Cornu, M., Steiner, M., Sweeck, L., & Vives i Batlle, J. 2013. An invitation to contribute to a strategic research agenda in radioecology. *Journal of Environmental Radioactivity, 115*, 73-82. doi: http://dx.doi.org/10.1016/j.jenvrad.2012.07.011

Howard, B. J., Beresford, N. A., Andersson, P., Brown, J. E., Copplestone, D., Beaugelin-Seiller, K., Garnier-Laplace, J., Howe, P. D., Oughton, D., & Whitehouse, P. 2010. Protection of the environment from ionising radiation in a regulatory context—an overview of the PROTECT coordinated action project. *Journal of Radiological Protection, 30*(2), 195.

Hsu, S. M., Yeh, S. H., Lin, M. S., & Chen, W. L. 2006. Comparison on characteristics of radiophotoluminescent glass dosemeters and thermoluminescent dosemeters. *Radiat Prot Dosimetry, 119*(1-4), 327-331. doi: 10.1093/rpd/nci510

IAEA. 2010. *Modelling Radiation Exposure and Radionuclide Transfer for Non-human Species Report of the Biota Working Group of EMRAS Theme 3*. Vienna, Austria: International Atomic Energy Agency.

IAEA, F. S. P. 2006. Safety Fundamentals No SF-1. *Vienna: International Atomic Energy Agency*.

ICRP. 1977. Recommendations of the ICRP. *ICRP Publication 26, 1*(3).

ICRP. 1991. Recommendations of the International Commission on Radiological Protection. *ICRP Publication 60, 21*(1-3).

ICRP. 1996. Conversion Coefficients for use in Radiological Protection against External Radiation (Vol. Ann. ICRP 26 (3-4)).

ICRP. 2003. A Framework for Assessing the Impact of Ionising Radiation on Non-human Species. *ICRP Publication 91, 33*(3).

ICRP. 2007. The 2007 Recommendations of the International Commission on Radiological Protection. *ICRP Publication 103, 37*((2-4)).

ICRP. 2008. Environmental Protection - the Concept and Use of Reference Animals and Plants. *ICRP Publication 108, 38*(4-6).

ICRP. 2009. Environmental Protection: Transfer Parameters for Reference Animals and Plants. *ICRP Publication 114, 39*(16).

ICRP. 2010. Conversion Coefficients for Radiological Protection Quantities for External Radiation Exposures (Vol. Ann. ICRP 40(2-5).).

ICRU. 1993. Quantities and Units in Radiation Protection Dosimetry. ICRU Report 51.

ICRU. 1998. Conversion coefficients for use in radiological protection against external radiation. *Journal of the International Commission on Radiation Units and Measurements, os29*(2), NP-NP. doi: 10.1093/jicru/os29.2.Report57

ISO. 1999. X and gamma reference radiation for calibrating dosemeters and doserate meters and for determing their response as a function of photon energy - Part 3: Calibration of area and personal dosemeters and the measurement of their response as a function of energy and angle of incidence *ISO 4037-3*. Geneve, switzerland.

Jakobsen, S. E. 2014, October 8, 2014. Surprisingly high levels of radioactivity in Norwegian reindeer and sheep. from http://sciencenordic.com/surprisingly-high-levels-radioactivity-norwegian-reindeer-and-sheep

Johansen, M. P., Barnett, C. L., Beresford, N. A., Brown, J. E., Černe, M., Howard, B. J., Kamboj, S., Keum, D. K., Smodiš, B., Twining, J. R., Vandenhove, H., Vives i Batlle, J., Wood, M. D., & Yu, C. 2012. Assessing doses to terrestrial wildlife at a radioactive waste disposal site: Inter-comparison of modelling approaches. *Science of The Total Environment, 427–428*, 238-246. doi: http://dx.doi.org/10.1016/j.scitotenv.2012.04.031

Jursinic, P. A. 2007. Characterization of optically stimulated luminescent dosimeters, OSLDs, for clinical dosimetric measurements. *Medical physics, 34*(12), 4594-4604.

Kamal, S. M., Gerges, A., & Al-Said, M. 2004. *Thermoluminescence properties of home-made CaSO 4: Dy For Dosimetry Purposes*. Paper presented at the 4th Conference on Nuclear and Particle Physics, Fayoum, Egypt. http://www.iaea.org/inis/collection/NCLCollectionStore/_Public/37/121/37121599.pdf

Kathren, R. L. 1984. Radioactivity in the environment: Sources, distribution and surveillance.

Kelly, M., & Thorne, M. 2003. Radionuclides handbook *R&D Technical Report P3-101/SP1b*. Bristol, UK: Environmental Agency.

Kinase, S. 2008. Voxel-Based Frog Phantom for Internal Dose Evaluation. *Journal of Nuclear Science and Technology, 45*(10), 1049-1052. doi: 10.1080/18811248.2008.9711891

Knežević, Ž., Stolarczyk, L., Bessieres, I., Bordy, J. M., Miljanić, S., & Olko, P. 2013. Photon dosimetry methods outside the target volume in radiation therapy: Optically stimulated luminescence (OSL), thermoluminescence (TL) and radiophotoluminescence (RPL) dosimetry. *Radiation Measurements, 57*, 9-18. doi: http://dx.doi.org/10.1016/j.radmeas.2013.03.004

Kortov, V. 2007. Materials for thermoluminescent dosimetry: Current status and future trends. *Radiation Measurements, 42*(4–5), 576-581. doi: http://dx.doi.org/10.1016/j.radmeas.2007.02.067

Kubota, Y., Takahashi, H., Watanabe, Y., Fuma, S., Kawaguchi, I., Aoki, M., Kubota, M., Furuhata, Y., Shigemura, Y., Yamada, F., Ishikawa, T., Obara, S., & Yoshida, S. 2015. Estimation of absorbed radiation dose rates in wild rodents inhabiting a site severely contaminated by the Fukushima Dai-ichi nuclear power plant accident. *J Environ Radioact, 142C*, 124-131. doi: 10.1016/j.jenvrad.2015.01.014

Lake Mary, F. 2014. Recent Developments in Direct Ion Storage Dosimeters. Retrieved 30, 2014, from http://hpschapters.org/florida/11PPT.pdf

Landauer. 2015, August 1, 2016. Whole body dosimetry. Retrieved August 1, 2016, from http://www.landauer.co.uk/whole_body.html

Larsson, C.-M. 2004. The FASSET Framework for assessment of environmental impact of ionising radiation in European ecosystems—an overview. *Journal of Radiological Protection, 24*(4A), A1.

Lee, M.-S., Liao, Y.-J., Huang, Y.-H., Lee, J.-H., Hung, S.-K., Chen, T.-R., & Hsu, S.-M. 2011. Radiation characteristics of homemade radiophotoluminescent glass dosimeter. *Radiation Measurements, 46*(12), 1477-1479. doi: 10.1016/j.radmeas.2011.02.010

Lilley, J. S. 2001. *Nuclear Physic (Principles and Applications)*. West Sussex, UK: John Wiley & Sons Ltd.

Lowe, V. P. W. 2014. *Scottish Red Deer and their Conservation*: Hayloft Publishing Ltd.

Martinez, N. E., Johnson, T. E., Capello, K., & Pinder, J. E. 2014. Development and comparison of computational models for estimation of absorbed organ radiation dose in rainbow trout (Oncorhynchus mykiss) from uptake of iodine-131. *Journal of Environmental Radioactivity, 138*, 50-59. doi: https://doi.org/10.1016/j.jenvrad.2014.08.001

Mathur, V. K. 2001. Ion stoeage dosimetry. *Nuclear Instruments and Methods in Physics Research, B*(184), 190-206.

McKeever, S. W., Moscovitch, M., & Townsend, P. D. 1995. Thermoluminescence dosimetry materials: properties and uses.

Mckinlay, A. F. 1981. *Thermoluminescence Dosimetry (Medical Physic Handbook; 5)* Norwich, UK: Adam Hilger Ltd,.

Mhareb, M., Hashim, S., Ghoshal, S., Alajerami, Y., Saleh, M., Razak, N., & Azizan, S. 2015. Thermoluminescence properties of lithium magnesium borate glasses system doped with dysprosium oxide. *Luminescence, 30*(8), 1330-1335.

Ministry of Environment, & Lands and Parks Resources Inventory Branch for the Terrestrial Ecosystems Task Fource Resources Inventory Committee. 1998. Wildlife Radio-telemetry *Standards for Components of British Columbia's Biodiversity No.5*: Ministry of Environment, Lands and Parks Resources Inventory Branch for the Terrestrial Ecosystems Task Fource Resources Inventory Committee.

Mohammadi, A., Kinase, S., & Saito, K. 2012. Evaluation of absorbed doses in voxel-based and simplified models for small animals. *Radiation Protection Dosimetry, 150*(3), 283-291. doi: 10.1093/rpd/ncr419

Moon, Y. M., Rhee, D. J., Kim, J. K., Kang, Y.-R., Lee, M. W., Lim, H., & Jeong, D. H. 2013. Reference dosimetry and calibration of glass dosimeters for Cs-137 gamma-rays. *Progress in Medical Physics, 24*(3), 140-144.

Nanto, H., Takei, Y., & Miyamoto, Y. 2011. *Environmental background radiation monitoring utilizing passive solid sate dosimeters*: INTECH Open Access Publisher.

Nowegian Radiation Protection Authority. 2006. Radioactive contamination of Norwegian foodstuffs after the Chernobyl accident.   Retrieved 22 June, 2016, from http://www.nrpa.no/dav/8261e12842.pdf

NuclearDataCenter. 2014. Tables of Nuclear Data.   Retrieved 22, 2015, from http://wwwndc.jaea.go.jp/NuC/index.html

Oatway, W., Jones, A., Holmes, S., Watson, S., & Cabianca, T. 2010. *Ionising Radiation Exposure of the UK Population: 2010 Review*: Health Protection Agency Dixcot.

Offenbacher, E. L., & Colbeck, S. C. 1991. Remote sensing of snow covers using the gamma-ray technique: COLD REGIONS RESEARCH AND ENGINEERING LAB HANOVER NH.

Olko, P. 2010. Advantages and disadvantages of luminescence dosimetry. *Radiation Measurements, 45*(3-6), 506-511. doi: 10.1016/j.radmeas.2010.01.016

Oughton, D. H., Aguero, A., Avila, R., Brown, J. E., Copplestone, D., & Gilek, M. 2008. Addressing uncertainties in the ERICA Integrated Approach. *J Environ Radioact, 99*(9), 1384-1392. doi: 10.1016/j.jenvrad.2008.03.005

Pekpak, E., Yılmaz, A., & Özbayoglu, G. 2010. An Overview on Preparation and TL Characterization of Lithium Borates for Dosimetric Use. *The Open Mineral Processing, 3*, 14-24.

Pelowitz, D. B. e. 2013. MCNP6TM USER'S MANUAL Version 1.0. *LA-CP-13-00634*.

Pentreath, R. J. 2009. Radioecology, radiobiology, and radiological protection: frameworks and fractures. *Journal of Environmental Radioactivity, 100*(12), 1019-1026. doi: http://dx.doi.org/10.1016/j.jenvrad.2009.06.004

Pentreath, R. J. 2012a. Clarifying and simplifying the management of environmental exposures under different exposure situations. *Ann ICRP, 41*(3-4), 246-255. doi: 10.1016/j.icrp.2012.06.027

Pentreath, R. J. 2012b. Radiation and protection of the environment: the work of Committee 5. *Ann ICRP, 41*(3-4), 45-56. doi: 10.1016/j.icrp.2012.07.002

Petoussi-Henss, N., Bolch, W., Eckerman, K., Endo, A., Hertel, N., Hunt, J., Pelliccioni, M., Schlattl, H., & Zankl, M. 2010. Conversion coefficients for radiological protection quantities for external radiation exposures. *Ann ICRP, 40*(2), 1-257.

Proki, M. 2002. Dosimetric characteristics of Li2B4O7: Cu, Ag, P solid TL detectors. *Radiation Protection Dosimetry, 100*(1-4), 265-268.

Prokic, M. 2001. Lithium borate solid TL detectors. *Radiation Measurements, 33*(4), 393-396.

Ranogajec-Komor, M. 2008. Passive solid state dosimeters in environmental monitoring *New Techniques for the Detection Agents* (pp. 97-112). Springer Science.

Ranogajec-Komor, M. 2009. Passive Solid State Dosimeters In Environmental Monitoring. In G. A. Aycik (Ed.), *New Techniques for the Detection of Nuclear and Radioactive Agents* (pp. 97-111). Dordrecht: Springer Netherlands.

Ranogajec-Komor, M., Knežević, Ž., Miljanić, S., & Vekić, B. 2008. Characterisation of radiophotoluminescent dosimeters for environmental monitoring. *Radiation Measurements, 43*(2–6), 392-396. doi: http://dx.doi.org/10.1016/j.radmeas.2007.11.020

Røed, K. H., & Jacobsen, M. 1995. Chromosome aberrations in Norwegian reindeer following the Chernobyl accident. *Mutation Research Letters, 346*(3), 159-165.

Ruedig, E., Beresford, N. A., Gomez Fernandez, M. E., & Higley, K. 2015. A comparison of the ellipsoidal and voxelized dosimetric methodologies for internal, heterogeneous radionuclide sources. *Journal of Environmental Radioactivity, 140*, 70-77. doi: https://doi.org/10.1016/j.jenvrad.2014.11.004

Ruedig, E., Caffrey, E., Hess, C., & Higley, K. 2014. Monte Carlo derived absorbed fractions for a voxelized model of Oncorhynchus mykiss, a rainbow trout. *Radiation and Environmental Biophysics, 53*(3), 581-587.

Rumble, M. A., & Denison, S. A. 1986. An Alternative Technique for Attaching Thermoluminescent Dosimeters to Small mammals. *Health Physic Society, 51*(2), 245-248.

Sa´ez-Vergara, J. C. 2000. Recent Developments of Passive and Active Detectors used in the Monitoring of External Environmental Radiation. *Radiation Protection Dosimetry, 92*(2-3), 83-88.

Sarai, S., Kuruta, N., Kamijo, K., Kubota, N., Take, Y., Nanto, H., Kobayashi, I., Komiri, H., & Komura, K. 2004. Detection of self-dose from an OSL dosimeter and a DIS dosimeter for environmental radiation monitoring. *Journal of Nuclear Science and Technology, 41*(sup4), 474-477. doi: 10.1080/00223131.2004.10875750

Schlosser, R. W., Wendt, O., Bhavnani, S., & Nail-Chiwetalu, B. 2006. Use of information-seeking strategies for developing systematic reviews and engaging in evidence-based practice: the application of traditional and comprehensive Pearl Growing. A review. *International Journal of Language & Communication Disorders, 41*(5), 567-582.

Scientific, T. F. 2016, August 1, 2016. Thermo Scientific Harshaw TLD Materials and Dosimeters.   Retrieved August 1, 2016, from https://tools.thermofisher.com/content/sfs/brochures/Dosimetry-Materials-Brochure.pdf

Sirtrack Limitted. 2016, August 1, 2016. VHF: Collar. *Device weight ranges.* Retrieved 26 May, 2016, from http://www.sirtrack.co.nz/index.php/terrestrialmain/vhf/collar

Skuterud, L. 2012. *Living with an existing exposure situation due to accidental contamination: The need for long-term management and involvement-for how long.* Paper presented at the Proceedings of the IRPA13 congress Living with Radiation-Engaging with Society, Glasgow, 13–18 May 2012.

Skuterud, L. 2017, 23 May 2017. Dynamic reindeer: GPS and Chernobyl consequences.   Retrieved 5 May, 2017, from https://www.nmbu.no/en/services/centers/cerad/news/node/31404

Skuterud, L., Gaare, E., Eikelmann, I. M., Hove, K., & Steinnes, E. 2005. Chernobyl radioactivity persists in reindeer. *Journal of Environmental Radioactivity, 83*(2), 231-252.

Skuterud, L., Ytre-Eide, M. A., Hevrøy, T. H., & Thørring, H. 2016. *Caesium-137 in Norwegian reindeer and Sámi herders –50 years of studies*. Paper presented at the Second International Conference on Radioecological Concentration Processes, Seville, Spain.

Smith, J. T., & Beresford, N. A. 2005. *Chernobyl: catastrophe and consequences*: Springer.

Stabin, M. G., Peterson, T. E., Holburn, G. E., & Emmons, M. A. 2006. Voxel-based mouse and rat models for internal dose calculations. *Journal of Nuclear Medicine, 47*(4), 655-659.

Stark, K., Andersson, P., Beresford, N. A., Yankovich, T. L., Wood, M. D., Johansen, M. P., Vives i Batlle, J., Twining, J., Keum, D. K., Bollhöfer, A., Doering, C., Ryan, B., Grzechnik, M., & Vandenhove, H. 2015. Predicting exposure of wildlife in radionuclide contaminated wetland ecosystems. *Environmental Pollution, 196*, 201-213. doi: http://dx.doi.org/10.1016/j.envpol.2014.10.012

Stark, K., Goméz-Ros, J. M., i Batlle, J. V., Hansen, E. L., Beaugelin-Seiller, K., Kapustka, L. A., Wood, M. D., Bradshaw, C., Real, A., & McGuire, C. 2017.

Dose assessment in environmental radiological protection: State of the art and perspectives. *Journal of Environmental Radioactivity, 175*, 105-114.

Stark, K., & Pettersson, H. B. L. 2008. External radiation doses from 137Cs to frog phantoms in a wetland area: in situ measurements and dose model calculations. *Radiation and Environmental Biophysics, 47*(4), 481-489. doi: 10.1007/s00411-008-0185-9

Takenaga, M., Yamamoto, O., & Yamashita, T. 1980. Preparation and characteristics of Li2B4O7 : Cu phosphor. *Nuclear Instruments and Methods, 175*(1), 77-78. doi: http://dx.doi.org/10.1016/0029-554X(80)90259-1

The American Society of Mammologists. 1987. Acceptable Field Methods of Mammalogy, Preliminary guidelines prepared by the American Society of Mammalogists. *Journal of Mammalogy Supp., 68*(6), 13.

Thompson, I. M. G., Botter-Jensen, L., Deme, S., Pernicka, F., & Saez-Vergara, J. C. 1999. Radiation Protection 106: Technical recommendation on measurements of external environmental gamma radiation doses. Luxambourg: European Communities.

Trousil, J., & Spurn, F. 1999. Passive dosimeter characteristics and new developments.

Turner, F. B., & Lannom, J. R. 1968. Radiation doses sustained by lizards in a continuously irradiated natural enclosure. *Ecology, 49*(3), 548-551.

Ulanovsky, A. 2014. Absorbed doses in tissue-equivalent spheres above radioactive sources in soil. *Radiation and Environmental Biophysics, 53*(4), 729-737.

Ulanovsky, A., & Pröhl, G. 2008. Tables of dose conversion coefficients for estimating internal and external radiation exposures to terrestrial and aquatic biota. *Radiat Environ Biophys, 47*(2), 195-203.

Ulanovsky, A., & Pröhl, G. 2012. Dosimetry for Reference Animals and Plants: current state and prospects. *Annals of the ICRP, 41*(3-4), 218-232.

USDoE. 2004. *RESRAD-BIOTA: A Tool for Implementing a Graded Approach to Biota Dose Evaluation*. Washington D.C.: United States Department of the Environment.

Vives i Batlle, J., Balonov, M., Beaugelin-Seiller, K., Beresford, N. A., Brown, J., Cheng, J. J., Copplestone, D., Doi, M., Filistovic, V., Golikov, V., Horyna, J., Hosseini, A., Howard, B. J., Jones, S. R., Kamboj, S., Kryshev, A., Nedveckaite, T., Olyslaegers, G., Prohl, G., Sazykina, T., Ulanovsky, A., Vives Lynch, S., Yankovich, T., & Yu, C. 2007. Inter-comparison of absorbed dose rates for non-human biota. *Radiation and Environmental Biophysics, 46*(4), 349-373. doi: 10.1007/s00411-007-0124-1

Vives i Batlle, J., Beaugelin-Seiller, K., Beresford, N. A., Copplestone, D., Horyna, J., Hosseini, A., Johansen, M., Kamboj, S., Keum, D.-K., Kurosawa, N., Newsome, L., Olyslaegers, G., Vandenhove, H., Ryufuku, S., Vives Lynch, S., Wood, M. D., & Yu, C. 2011. The estimation of absorbed dose rates for non-human biota: an extended intercomparison. *Radiation and Environmental Biophysics, 50*(2), 231-251. doi: 10.1007/s00411-010-0346-5

Vives i Batlle, J., Beresford, N. A., Beaugelin-Seiller, K., Bezhenar, R., Brown, J., Cheng, J. J., Ćujić, M., Dragović, S., Duffa, C., Fiévet, B., Hosseini, A., Jung, K. T., Kamboj, S., Keum, D. K., Kryshev, A., LePoire, D., Maderich, V., Min, B. I., Periáñez, R., Sazykina, T., Suh, K. S., Yu, C., Wang, C., & Heling, R. 2016. Inter-

comparison of dynamic models for radionuclide transfer to marine biota in a Fukushima accident scenario. *Journal of Environmental Radioactivity, 153*, 31-50. doi: http://dx.doi.org/10.1016/j.jenvrad.2015.12.006

Weinstein, B. B.-S. M., & German, U. THE MINIMUM MEASURABLE DOSE (MMD) OF CaF2: Dy MEASURED VIA AN IMPROVED HEATING PROFILE WITH AN AUTOMATIC 6600 THERMOLUMINESCENT DETECTOR.

Wernli, C. 1996. Dosimetric characteristics of a novel personal dosemeter based on direct ion storage (DIS). *Radiation Protection Dosimetry, 66*(1-4), 23-28.

Whicker, F. W., & Schultz, V. 1982. *Radioecology: Nuclear Energy and the environment* (Vol. 1). Florida, USA: CRC Press, Inc.

Wood, M. D. 2010. *Assessing the impact of ionising radiation in temparate coastal sand dune ecosystems: measurement and modelling.* (Doctor in Philosophy), University of Liverpool, Liverpool.

Wood, M. D., Beresford, N. A., Barnett, C. L., Copplestone, D., & Leah, R. T. 2009. Assessing radiation impact at a protected coastal sand dune site: an intercomparison of models for estimating the radiological exposure of non-human biota. *Journal of Environmental Radioactivity, 100*(12), 1034-1052. doi: http://dx.doi.org/10.1016/j.jenvrad.2009.04.010

Woodhead, D. S. 1973. The radiation dose received by plaice *(pleuronectes platessa)* from the waste discharged into the north-east Irish Sea from the fule reprocessing plant at windscale. *Helath Physics, 25*, 115-121.

Xi Shen, Z., Jin-Xiang, Z., Guang-Xiang, T., & Wei-Ji, M. 1996. $CaSo_4$ and LiF:Mg, Cu, P Thermoluminescent Dosimeters for Environmental Monitoring in Ambient Areas of a Nuclear Power Plant *Health Physic Society, 70*(3), 367-371.

Yankovich, T. L., Batlle, J. V. i., Vives-Lynch, S., Beresford, N. A., Barnett, C. L., Beaugelin-Seiller, K., Brown, J. E., Cheng, J. J., Copplestone, D., Heling, R., Hosseini, A., Howard, B. J., Kamboj, S., Kryshev, A. I., Nedveckaite, T., Smith, J. T., & Wood, M. D. 2010. An international model validation exercise on radionuclide transfer and doses to freshwater biota. *Journal of Radiological Protection, 30*(2), 299.

Youngman, M. J. 2003. Calibration and evaluation of a transportable in vivo monitoring system for accident monitoring of internal contamination. *Radiation Protection Dosimetry, 107*(4), 259-267.

APPENDIX 1 DATA OF PREDICTED DOSES OF THE REINDEER HERD

Table A-1: Estimated absorbed doses to dosimeters over 11 months from internal ^{137}Cs concentration of the reindeer

Reindeer Name	^{137}Cs concentration in muscle* (Bq kg^{-1})	Dose rate (nGy hr^{-1})	Dose for 11 months (µGy)
Linn	437	12	100
Ragnhild	636	18	145
Trinerein	625	17	143
Prikka	762	21	174
Sigrid Mathilda	723	20	165
Rinda	659	18	150
Krone	658	18	150
Guri	884	25	202
Frigg	586	16	134
Martine EK	777	22	177
Kari	675	19	154
Torild	828	23	189
Mean	**687**	**21**	**157**
SD	**179**	**5**	**27**

*Average of January and December 2016 live-monitoring results

Table A-2: ^{137}Cs mean predicted external absorbed dose for the reindeer herd

List	Ceasium Deposition (Bq m^{-2})	Soil depth [m]	Avg soil density (kg m^{-3})	Activity conc. (Bq kg^{-1})	DCC (µGy hr^{-1} Bq kg^{-1})	External dose (µGy hr^{-1})	measuring time (hours)	Total dose during the measuring time (µGy)
^{137}Cs	22037	0.06	1600	230	0.0000560	0.012855	8016	**103**
SD of ^{137}Cs	42001	0.06	1600	438	0.0000560	0.024501	8016	196
							SD of ^{137}Cs	**93**

Table A-3: ^{40}K mean predicted external absorbed dose for the reindeer herd

List	K in weight %	Ac in 1% of k-40 (bq kg^{-1})	Activity conc. (bq kg^{-1})	DCC (µGy hr^{-1} Bq kg^{-1})	External dose rate (µGy hr^{-1})	measuring time (hours)	Total dose during the measuring time (µGy)
^{40}K	1.14	313	357.45	1.63E-05	5.83E-03	8016	**47**
SD of ^{40}K	1.61	313	503.93	1.63E-05	8.21E-03	8016	66
						SD of ^{40}K	**19**

Table A-4: ^{232}Th series mean predicted external absorbed dose for the reindeer herd

List	Mean in ppm	Mean in ppb	Conc. at 1 bq kg^{-1}	Activity conc. (bq kg^{-1})	DCC (µGy hr^{-1} Bq kg^{-1})	External dose rate (µGy hr^{-1})	measuring time (hours)	Total dose during the measuring time (µGy)
^{232}Th*	1.838	1838	246	7.47	1.30E-08	9.71E-08	8016	0.0008
SD of ^{232}Th	3.323	3323	246	13.51	1.30E-08	1.76E-07	8016	0.0014
							SD of ^{232}Th	0.0006
^{228}Ra				7.47	9.70E-05	7.25E-04	8016	5.8
SD of ^{228}Ra				13.51	9.70E-05	1.31E-03	8016	10.5
							SD of ^{228}Ra	4.7
^{228}Th				7.47	1.60E-04	1.20E-03	8016	9.6
SD of ^{228}Th				13.51	1.60E-04	2.16E-03	8016	17.3
							SD of ^{228}Th	7.7
							Total dose of ^{232}Th series	**15.4**
							SD of ^{232}Th series	**9.1**

*^{232}Th series radionuclides with physical half-lives greater than ten days were assumed to be in equilibrium with the series parent; daughter radionuclides with a half-life of less than ten days are included in their immediate parents for dose conversion coefficient

Table A-5: ^{238}U series mean predicted external absorbed dose for the reindeer herd

List	Mean in ppm	Mean in ppb	Conc. at 1 bq kg^{-1}	Activity conc. (bq kg^{-1})	DCC (μGy hr^{-1} Bq kg^{-1})	External dose rate (μGy hr^{-1})	measuring time (hours)	Total dose during the measuring time (μGy)
^{238}U	0.481	481.00	81	5.94	1.00E-08	5.94E-08	8016	0.0005
	0.843	843.00	81	10.41	1.00E-08	1.04E-07	8016	0.0008
							SD of ^{238}U	0.0004
^{234}Th				5.94	2.20E-06	1.31E-05	8016	0.1
				10.41	2.20E-06	2.29E-05	8016	0.2
							SD of ^{234}Th	0.1
^{234}U				5.94	1.70E-08	1.01E-07	8016	0.0008
				10.41	1.70E-08	1.77E-07	8016	0.0014
							SD of ^{234}U	0.0006
^{230}Th				5.94	2.50E-08	1.48E-07	8016	0.001
				10.41	2.50E-08	2.60E-07	8016	0.002
							SD of ^{230}Th	0.001
^{226}Ra				5.94	1.80E-04	1.07E-03	8016	8.6
				10.41	1.80E-04	1.87E-03	8016	15.0
							SD of ^{226}Ra	6.4
^{210}Pb				5.94	7.70E-08	4.57E-07	8016	0.004
				10.41	7.70E-08	8.01E-07	8016	0.006
							SD of ^{210}Pb	0.003
^{210}Po				5.94	8.60E-10	5.11E-09	8016	0.00004
				10.41	8.60E-10	8.95E-09	8016	0.00007
							SD of ^{210}Po	0.00003
							Total dose of ^{238}U series	**8.7**
							SD of ^{238}U series	**6.4**

*^{238}U series radionuclides with physical half-lives greater than ten days were assumed to be in equilibrium with the series parent; daughter radionuclides with a half-life of less than ten days are included in their immediate parents for dose conversion coefficient

APPENDIX 2   ETHIC APPROVAL LETTER